Shimane University
島根大学大学院総合理工学研究科博士後期課程総合理工学専攻地球科学・地球環境コース

Doctoral Dissertation

GEOCHEMICAL EVALUATION OF MATURITY OF POCKET BEACH SANDS IN SOUTHWEST JAPAN

(西南日本のポケットビーチの砂の成熟度の地球化学的検討)

BY

BAH MAMADOU LAMINE MALICK

Submitted in partial fulfillment of the requirements for the degree of Doctor of Science in Earth Science and Geoenvironmental Science in the Interdisciplinary Graduate School of Science and Engineering of Shimane University

MARCH, 2017

DOCTORAL COMMITTEE

Hiroaki ISHIGA Professor Dr. Sci. (Dept. of Geoscience)
Toshiaki IRIZUKI Professor Dr. Sci. (Dept. of Geoscience)
Yasushi SEIKE Professor Dr. Agr. (Dept. of Material Science)
Tetsuya SAKAI Associate Professor Ph.D. (Dept. of Geoscience)
Hiroki HAYASHI Associate Professor Ph.D. (Dept. of Geoscience)
Andreas AUER Associate Professor Ph.D. (Dept. of Geoscience)

Name: Bah Mamadou Lamine Malick
Date of Degree: March, 2017
Title of Study: Earth Science and Geoenvironmental Science
Major Field: Geoscience
Supervisor: Hiroaki ISHIGA Professor Dr. Sci. (Dept. of Geoscience)

ABSTRACT

The geochemical maturity of pocket beach sand was evaluated using major and trace element compositions of sample sets from nine Prefectures in South West Japan. These included northern Kyushu (n=30), Yamaguchi Prefecture (n=27), Shimane Prefecture (n=50), Tottori Prefecture (n=15), Tango Peninsula (n=38) and Noto Peninsula (n=30). The geochemical data obtained by X-ray fluorescence (XRF) analysis were compared to the content of beach sands from Kotobikihama and Kotogahama, which were assumed to be representative of matured sands. Data were also compared with the geochemical compositions of 15 local river sediments from the Geological Survey of Japan and National Institute of Advanced Industrial Science and Technology and with 15 near-shore marine sediments around Yamaguchi. Furthermore, comparison with average Upper Continental Crust of the Japanese Archipelago, and average Upper Continental Crust was performed. The relatively high concentration of quartz in the silica-rich sands from Kotogahama, Kotobikihama, Shimane and Yamaguchi was reflected in the geochemical analysis of those sands, the major and trace element compositions being characterized by high SiO_2 contents. The Tango Peninsula and Wakasa Bay were very similar, showing a moderate geochemical maturation. Beach sands from Tottori and Noto Peninsula had lower SiO_2 and Al_2O_3 values, which reflected the abundance of feldspar, suggesting geochemical immaturity, and relatively high K_2O and Na_2O associated with feldspars. CaO contents were generally low, although enrichments occurred in a few samples due to presence of shell material. Following geochemical classification of the coastal beach sands from the six regions of South West Japan, a growing abundance of both quartz and feldspar was indicated by the sands being bracketed by arkose and subarkose, with a diminishing trend towards sub-litharenite. The relatively low-to-moderate values of weathering indices of Chemical Index of Alteration (CIA), Plagioclase Index of Alteration (PIA) and Chemical Index of Weathering (CIW), indicated that the beach sands from the sites in the source area have undergone low to moderate degree of chemical weathering. A-CN-K and A-CNK-FM plots, which suggest a granitic source composition, also confirmed that the sand samples from these sites have undergone a low to moderate degree of chemical weathering in consistent with CIA, PIA and CIW values. Investigated beach sands from the six coastal regions of South West Japan comprised variable mixtures of terrigenous detritus (represented by Al_2O_3 and SiO_2) and biogenous material (represented by CaO). The primary component of beach sands from Shimane was quartz, or silica (SiO_2), Sands from Tottori were composed largely of weathered feldspar particles, while, in contrast, components of biogenic and quartz-rich sands from Yamaguchi were primarily shell fragments, quartz, and igneous rock. The sands of northern Kyushu might have been expected to exhibit a relatively high carbonate content, not least on account of the warm-water currents there. However, the water quality is poor (type B), which is likely to explain the low carbonate contents measured. Plentiful warm-water species and high-quality (type AA) water in the Yamaguchi area were reflected in the high to moderately low carbonate content of the beach sands from that location. Contents of local river and near-shore marine sediments differed distinctly from those at Yamaguchi, suggesting that inputs of existing river or marine sediment to the beach from currents or storm events are minimal.

Key words: Pocket beach, beach sand, foreshore, geochemistry, silica, biogenic, southwest Japan

ACKNOWLEDGEMENTS

This study was largely supported by Shimane University. I should like to express my sincere gratitude to Professor Hiroaki ISHIGA Dr. Sci. (Dept. of Geoscience) for supervising this study and related research, for his patience, motivation and immense knowledge. His guidance helped me throughout my research and the writing of this thesis.

Professor Toshiaki IRIZUKI Dr. Sci. (Dept. of Geoscience) for microscopic sands photography, and Tetsuya SAKAI Associate Professor Ph.D. (Dept. of Geoscience) for Sands Grain Size Analysis.

I should like to thank the rest of my thesis committee: Hiroaki ISHIGA Professor Dr. Sci. (Dept. of Geoscience), Toshiaki IRIZUKI Professor Dr. Sci. (Dept. of Geoscience), Yasushi SEIKE Professor Dr. Agr. (Dept. of Material Science) , Tetsuya SAKAI Associate Professor Ph.D. (Dept. of Geoscience), Hiroki HAYASHI Associate Professor Ph.D. (Dept. of Geoscience), and Andreas AUER Associate Professor Ph.D. (Dept. of Geoscience), for their insightful comments and encouragement, but also for the challenging question which stimulated me to widen my research from various perspectives.

I gratefully acknowledge the assistance of Erika Sano and Dr. Sansfica Marlyn Young's sampling and analysis.

TABLE OF CONTENTS

List of tables x
List of figures xi
Chapter One 15
1. Introduction 15
1. 1. Study area 18
1. 2. Pocket beach characteristics 21
Chapter Two 29
2. Materials and methods 29
2. 1. Sample collection at foreshore 29
2. 2. Sample preparation and analysis 30
Chapter Three 33
3. Results 33
3. 1. Major and Trace Elements Geochemistry 33
3. 1. 1. Northern Kyushu 34
3. 1. 2. Yamaguchi Prefecture 35
3. 1. 3. Shimane Prefecture 36
3. 1. 4. Tottori Prefecture 37
3. 1. 5. Tango Peninsula 38
3. 1. 6. Noto peninsula 39
3. 2. UCJA and UCC – Normalized compositions.............40
3. 3. Inter-Element Relationship 49
Chapter Four 59
4. Discussion 59
4. 1. Evaluation of biogenic productivity 59
4. 2. Geochemical Maturity 60
4. 3. Geochemical classification 65
4. 4. Weathering process 72
4. 5. Palaeoweathering indices in A-CN-K and A-C-M diagrams 76
Chapter Five 81
5. Conclusions 81
References 84

LIST OF TABLES

Table 1. Shape and characteristics of beaches on the coastline of Yamaguchi, Shimane and Tottori, South West Japan. (L= length of beach, and l = arc length of beach). 27

Table 2. XRF major (wt%) and trace (ppm) element analyses of beach sands from northern Kyushu, Japan. LOI, oven-dried loss on ignition; and indices of Chemical Index of Alteration (CIA), Plagioclase Index of Alteration (PIA) and Chemical Index of Weathering (CIW). 40

Table 3. XRF major (wt%) and trace (ppm) element analyses of beach sands from Yamaguchi Prefecture, Japan. LOI, oven-dried loss on ignition; and indices of CIA, PIA and CIW. 41

Table 4. XRF major (wt%) and trace (ppm) element analyses of beach sands from Shimane Prefecture, Japan. LOI, oven-dried loss on ignition; and CIA, PIA and CIW. 42

Table 5. XRF major (wt%) and trace (ppm) element analyses of beach sands from Tottori Prefecture, Japan. LOI, oven-dried loss on ignition; and CIA, PIA and CIW. 43

Table 6. XRF major (wt%) and trace (ppm) element analyses of beach sands from the Eastern San'in coast, Tango Peninsula and Wakasa Bay, Japan. LOI, oven-dried loss on ignition; and CIA, PIA and CIW. 44

Table 7. XRF major (wt%) and trace (ppm) element analyses of beach sands from Noto Peninsula, Japan. LOI, oven-dried loss on ignition; and CIA, PIA and CIW. 45

Table 8. Summary statistics of major element abundances in beach sands from the coasts of South West Japan, on the coastline of Northern Kyushu Yamaguchi, Shimane, Tottori, Tango Peninsula, Wakasa Bay, and Noto Peninsula. LOI, oven-dried loss on ignition; and CIA, PIA and CIW. Average geochemical compositions of local river sediments from the Geological Survey of Japan and National Institute of Advanced Industrial Science and Technology (AIST 2013a), near-shore marine sediments around Yamaguchi (AIST 2013b), average Upper Crust of the Japanese Archipelago (UCJA), according to (Togashi *et al.* 2000), and average Upper Continental Crust (UCC) (Rudnick & Gao, 2005). 46

LIST OF FIGURES

Figure 1. Geological map showing water circulation systems of the Sea of Japan, and geotectonic subdivision of the Japanese Island. Modified from the Geological Survey of Japan (GSJ) and National Institute of Advanced Industrial Science and Technology (AIST), 2016. 19

Figure 2. Genesis of beach sand. Siliciclastic rocks supply mostly quartz and feldspar, and rock fragments, biogenic carbonate mostly animal skeletons, forms, shells. 20

Figure 3. Detailed geological map of the coasts of South West Japan, showing the location of beaches sampled on the coastline of Northern Kyushu, Yamaguchi, Shimane, Tottori, Tango Peninsula, Wakasa Bay, and Noto Peninsula. Modified from, the Geological Survey of Japan (GSJ) and National Institute of Advanced Industrial Science and Technology (AIST), 2016. 22

Figure 4. Regular representation of pocket beach, San' in district. 23

Figure 5. Terms describing an ideal beach profile. Note the wave-formed ripples by foreshore tidal flat on the Nijo beach, Fukuoka Prefecture, Japan (2012). 24

Figure 6. Shape of the Makitani and Higashihama pocket beaches in Tottori, Japan: (L) beach length, (l) arc length of the beach, and (r) radius of the approximated circle. 26

Figure 7. Foreshore sampling of beach sands at shoreline, Sands without or less of clay and finer particles. 27

Figure 8. Experimental workflow for the sample preparation and data analysis. 31

Figure 9. Average major and trace elements diagrams of beach sands collected along the coasts of South West Japan, on the coastline of Northern Kyushu, Yamaguchi, Shimane, Tottori, Tango Peninsula, and Noto Peninsula, normalised to average Upper Crust of the Japanese Archipelago (UCJA), according to (Togashi *et al.* 2000), and average Upper Continental Crust (UCC) (Rudnick & Gao, 2005). 48

Figure 10. Harker diagrams for selected major elements of beach sands collected along the coasts of South West Japan, on the coastline of Northern Kyushu, Yamaguchi, Shimane, Tottori, Tango Peninsula, and Noto Peninsula. 51

Figure 11. Geological map of South West Japan, showing the geochemical composition of SiO_2 and Al_2O_3 elements, and location of beaches sampled along the coastline of

Northern Kyushu, Yamaguchi, Shimane, Tottori, Tango Peninsula, Wakasa Bay, and Noto Peninsula. Modified from the Geological Survey of Japan (GSJ) and National Institute of Advanced Industrial Science and Technology (AIST), 2016. 52

Figure 12. Geological map of South West Japan, showing the geochemical composition of SiO_2 and CaO elements, and location of beaches sampled along the coastline of Northern Kyushu, Yamaguchi, Shimane, Tottori, Tango Peninsula, Wakasa Bay, and Noto Peninsula. Modified from the Geological Survey of Japan (GSJ) and National Institute of Advanced Industrial Science and Technology (AIST), 2016. 53

Figure 13. Selected microscopic photographs biogenic carbonate sands from the Tsunoshima, Akada, Hinaka, Arata, and Doigahama Beaches, Yamaguchi Prefecture, South West Japan. The identified species are Foraminifera, ostracod, shells, and sea urchin, made primarily of $CaCO_3$. 54

Figure 14. The variations of ecosystem and geography of marina condition in Hinaka and Arata beaches, Yamaguchi Prefecture, South West Japan. Typical small-scale pocket beach, and inlet of beach shape characteristic. 55

Figure 15a. Rocky points of both sides of the Hinaka beach, *Zostera marina* and other sea weed are exposed on the shore of the Hinaka beach. 55

Figure 15b. Rocky points of both sides of the Hinaka beach, *Zostera marina* and other sea weed are exposed on the shore of the Hinaka beach. 56

Figure 15c. Rocky points of both sides of the Hinaka beach, *Zostera marina* and other sea weed are exposed on the shore of the Hinaka beach. On the left side of the Hinaka beach, *Zostera marina* are found on the shore. 56

Figure 16. The variations of ecosystem and geography of marine condition in Doigahama beach, Yamaguchi Prefecture, South West Japan. 57

Figure 17. Surface water mass temperature; mean 50 m in western Japan for 11th-20th August 2016. In addition, for 11th-20th May, 2016 (Japan Meteorological Agency). 61

Figure 18. Tidal-flat deposits on the foreshore of Arata beach, Yamaguchi Prefecture, South West Japan. 62

Figure 19. Classification based on the chemical oxygen demand (COD) and faecal coliform criteria of levels of water quality in Yamaguchi in contrast to level water quality in northern Kyushu, South West Japan. 63

Figure 20. Ternary diagram of relative proportions of $Al_2O_3 \times 5$, SiO_2, and $CaO \times 2$ (Brumsack, 1989), of beach sand samples from Northern Kyushu, Yamaguchi, Shimane, Tottori, Tango Peninsula, Wakasa Bay, and Noto Peninsula, southwest Japan. An arbitrary multiplier of 5 and 2 are used respectively for Al_2O_3 and CaO in order to better distribute the data points within the graph. 64

Figure 21. Box plots showing the SiO_2/Al_2O_3 and Na_2O/K_2O ratios in the investigated beach sands from the coasts of South West Japan, on the coastline of Northern Kyushu, Yamaguchi, Shimane, Tottori, Tango Peninsula, and Noto Peninsula. 66

Figure 22. Geochemical classification schemes of beach sands along the coastline of Northern Kyushu, Yamaguchi, Shimane, Tottori, Tango Peninsula, Wakasa bay, and Noto Peninsula. Based on: **a)** $\log(SiO_2/Al_2O_3)$ versus $\log(Na_2O/K_2O)$ diagram of Pettijohn *et al*. (1972), and **b)** the log (SiO_2/Al_2O_3) versus log $(Fe_2O_3{}^*/K_2O)$ diagram of Herron (1988). LA. Litharenite and WK. Wacke. 68

Figure 23. Observation of sands holder of the Hashi beach, Shimane Prefecture. Beach sands composed primarily of well-sorted quartz, a durable mineral that is hard and does not weather easily. 69

Figure 24. Grain size distributions of beach sands collected at the shorelines of selected beaches on the western San' in coast. Ishiga *et al*. (2010). 70

Figure 25. a) Bivariate plot of SiO_2 against Al_2O_3, and **b)** plot of SiO_2 (reflective of quartz content) versus $K_2O+Na_2O+Al_2O_3$ (reflective of feldspar content) of beach sand samples from Northern Kyushu, Yamaguchi, Shimane, Tottori, Tango Peninsula, Wakasa bay, and Noto Peninsula, South West Japan. 70

Figure 26. Box-plot diagrams of geochemical weathering indices. **a)** Chemical Index of Alteration (CIA), **b)** Plagioclase Index of Alteration (PIA), **c)** and Chemical Index of Weathering (CIW). 74

Figure 27. (a) A-CN-K and **(b)** A-CNK-FM (after Nesbitt and Young, 1984; Fedo *et al*., 1995) and CIA showing weathering trends for investigated beach sands from the coasts of South West Japan, on the coastline of Northern Kyushu, Yamaguchi, Shimane, Tottori, Tango Peninsula, and Noto Peninsula. Ka= kaolinite; Chl= chlorite; Gi= gibbsite; Sm= smectite; Pl= plagioclase; Ks= K-feldspar; Fel= feldspar; Bi= biotite. Dotted line linking stars is the compositional trend in pristine average Phanerozoic-Cenozoic igneous rocks (Condie, 1993). Stars: BA= basalt, AN= andesite, FV= felsic volcanic rock, GR= granite. A= Al_2O_3; CN= CaO^*+Na_2O; K= K_2O; CNK=$CaO^*+Na_2O+K_2O$; FM= FeO^*+MgO. 79

Chapter One

1. INTRODUCTION

Coastal region can be considered as a place with its own characteristic qualities and features, in which the inhabitants perform activities, both economic and social, that are specific only to that region. Numerous components and processes, including source composition, sorting, climate, relief, long shore drift, and winnowing by wave action, influence its sediments. Sandy beaches are regions of transition from the shore to the sea, and are subjected to significant influences from both ecosystems. These regions are open to significant variations in the length of exposure to the sun, immersion and submersion, the amount of rainfall and concentration of nutrients. Among other factors, beaches are also subject to local processes such as wave and tidal regimes, fluvial discharges, and wind transport (Carranza-Edwards *et al.,* 2009). The geochemical composition of beach sands is influenced by many components and processes. These (components and processes) contain important information regarding the geochemical maturity, composition, weathering conditions and tectonic settings of both the provenance and associated depositional basins. The constituents of beach sands include various materials resistant to abrasion by waves, including silicates such as feldspar and quartz and shells and other derivatives of living organisms and lithic fragments. As described by Pettijohn *et al.* (1987), weathering, degradation and fragmentation of these materials leads to the particles that together form the sands. The geochemistry of clastic sediments can be effectively utilized in both evaluating geochemical maturity and tectonic setting and determining provenance (Bhatia, 1983; Roser & Korsch, 1986; Roser & Korsch,1988; Condie *et al.*, 1992). Pettijohn *et al.* (1972) first discussed the concept of maturity in sediment, suggesting that maturity should be assessed using a QFL diagram. A very mature sand, for example, may primarily comprise quartz. However, this method is limited by there being in excess of 50 sand and sandstone classification systems, laboratory analysis is required with point counting (typically of 500 points) and petrographic thin sections and carbonates are excluded. As an alternative, the X-ray fluorescence (XRF) analyses method was employed to this study.

The sands from six regions on the coasts of South West Japan were examined; these were the coasts of: Northern Kyushu, Shimane, the Noto Peninsula, the Tango Peninsula, Yamaguchi and Tottori. The chemical weathering intensity was investigated through the characterization of sands from each of these locations using three indices commonly used for describing weather profiles – the Chemical Index of Alteration (CIA), the Plagioclase Index of Alteration (PIA) and the Chemical Index of Weathering (CIW). For each sample, these indices combine the bulk of major element oxide chemistry into a single value. For further analysis, a variety of triangular and scatter plots were constructed from the geochemical data obtained. Additionally, the geochemical composition data was compared with that of four other sources. The composition of 15 local river sediments was obtained from the Geological Survey of Japan and the National Institute of Advanced Industrial Science and Technology (GSJ & AIST, 2013a). That of 15 near-shore marine sediments from around Yamaguchi was obtained from the same source

(GSJ & AIST, 2013b). The remaining two sources were both upper crust data – the average upper continental crust (UCC) data (Rudnick & Gao, 2005) and the average upper crust of the Japanese Archipelago (UCJA) (Togashi *et al.*, 2000). By their very nature, local river and near-shore marine sediments broadly reflect the composition of the beach sands present in their drainage basins; studying the geochemical compositions of the sediments provides valuable baseline data for use in many geological and environmental fields. However, the chemical compositions of local river and near-shore marine sediments do not necessarily directly reflect those of their source rocks. Significant differences between the source and sediment compositions may result from factors such as the extent of source area weathering, sorting and average grain size, localized heavy mineral concentration, and alluvial storage or flushing of fine material.

The purpose of this study is to consider foreshore sampling and examine pocket beaches. This is important because the geochemical maturity of sands and biogenic production can be evaluated using silica, aluminium and calcium from major element X-ray fluorescence (XRF) analyses. The objective of this study is to conduct a systematic evaluation of geochemical maturity and weathering and to provide insight into the source area paleo-weathering conditions in beach sands of the six coastlines of interest of South West Japan. These factors are evaluated in this study using elemental abundances, weathering indices and principal ratios in comparison to the mean UCC and mean UCJA, as estimated from the representative surface rocks. In order to evaluate the biogenic productivity in Yamaguchi coast, the climatic conditions and water quality in Yamaguchi and Kyushu is observed. The aims of this study are twofold. The first aim is to present new data that is obtained by XRF. The second is to describe the characteristics of the four series of data previously mentioned – that is, the 15 local river sediments (GSJ & AIST, 2013a), the 15 near-short marine sediments (GSJ & AIST, 2013b), the average UCC (Rudnick & Gao, 2005) and the average UCJA (Togashi *et al.*, 2000) in terms of the general relationships between their geochemical composition and the abundance of elements contained within them.

1. 1. Study area

The Japanese Islands have complex coastal landforms, where mountains and hills meet the sea in composite geometries. Japan has an extensive coastline of approximately 35,000 km in length, which contains a large number of beaches, among which are a significant number of pocket beaches concentrated along the coastline of South West of the country. From a tectonic point of view, South West Japan is generally subdivided into an Inner Zone (Asian Continent side) and an Outer Zone (Pacific Ocean side) that are separated by the Median Tectonic Line (MTL) (Figure 1). The Outer and Inner Zones have broadly similar geological structures, both comprising stacks of flat-lying tectonic layers that become progressively younger with increasing depth from the surface. In contrast to the Outer Zone, the Inner Zone contains Cretaceous to Palaeogene subduction-related, mainly granitic volcanic–plutonic complexes (Takagi, 2003; Nakajima *et al.*, 2004), locally associated with high-temperature, low-pressure "Ryoke" metamorphism (Nakajima 1997; Brown 1998; De-Jong *et al.*, 2008). Pocket beaches are common along the coastline of South West Japan' s Inner Zone. This is broadly coincident with the southwestern mountain arc.

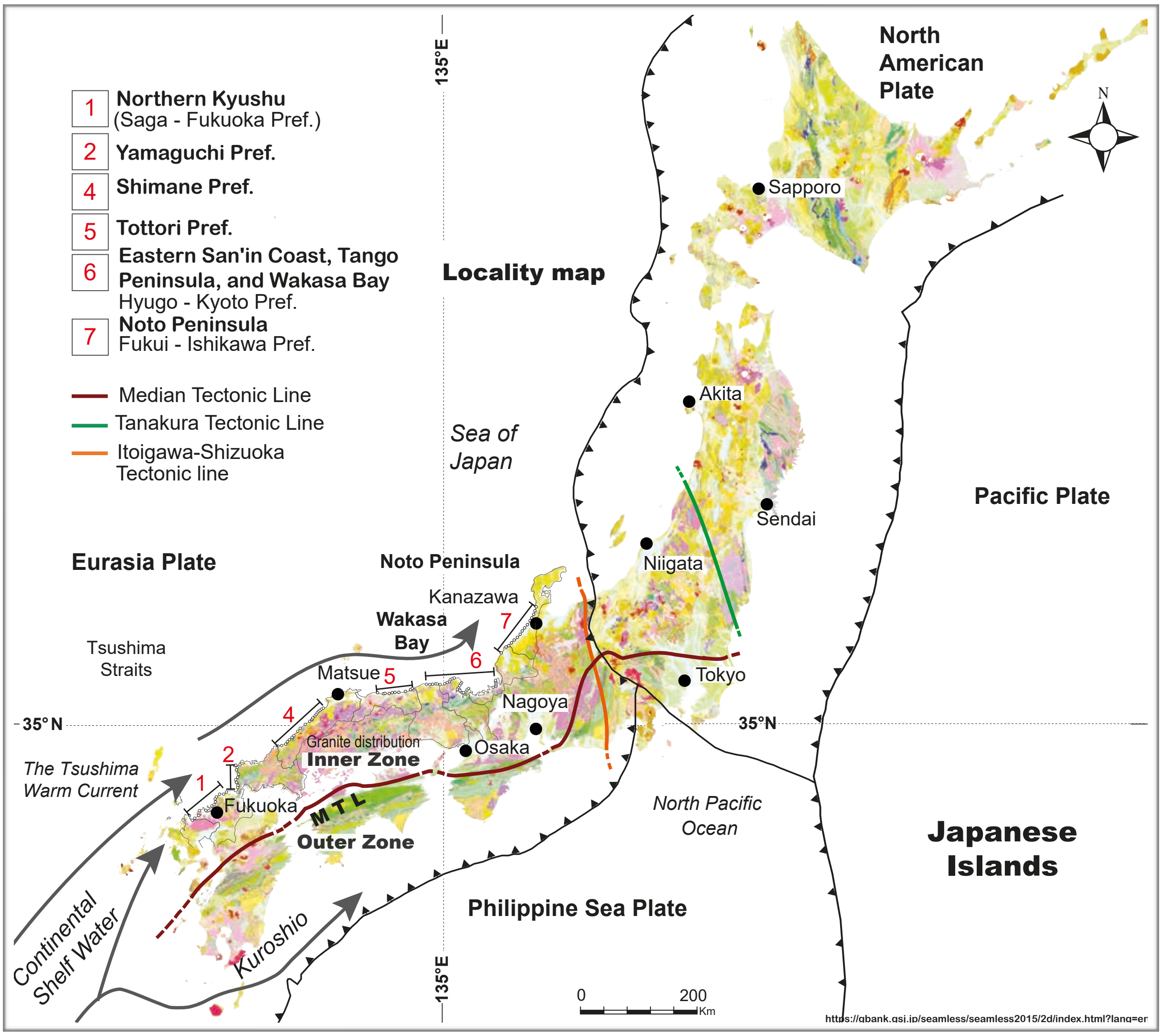

Figure 1. Geological map showing water circulation systems of the Sea of Japan, and geotectonic subdivision of the Japanese Island. Modified from the Geological Survey of Japan (GSJ) and National Institute of Advanced Industrial Science and Technology (AIST), 2016.

It also tends to follow the common pattern of the low- and highlands that curve around towards the Sea of Japan. This is in clear contrast to the beaches on the Outer Zone, which is characterized by an upper crust occupied with the Shimanto accretionary complex, gently dipping northward and with an extremely thin lower crust. The Shimanto and younger accretionary complexes intrude into the inner zone. The Sambagawa metamorphic rocks are distributed along the MTL, traced to a depth of about 20 km. Cretaceous and Paleogene granitoids are widely distributed in the San' in district of South West Japan. Locally, these granitoids are known as the Daito granodiorite, which consists of medium-to-coarse-grained hornblende-biotite granodiorite of the magnetite series (Ishihara, 1977). Tertiary sedimentary and volcanic complexes are distributed in sedimentary basins in the north of the district along the coast of the Japan Sea. Lower Miocene non-marine sediments unconformably overlie the basement granitoids; this may be indicative of Early Miocene paleo-weathering. The Miocene basins mainly developed along the Japan Sea coast during its opening, but small basins also occur sporadically in limited areas in the mountain regions.

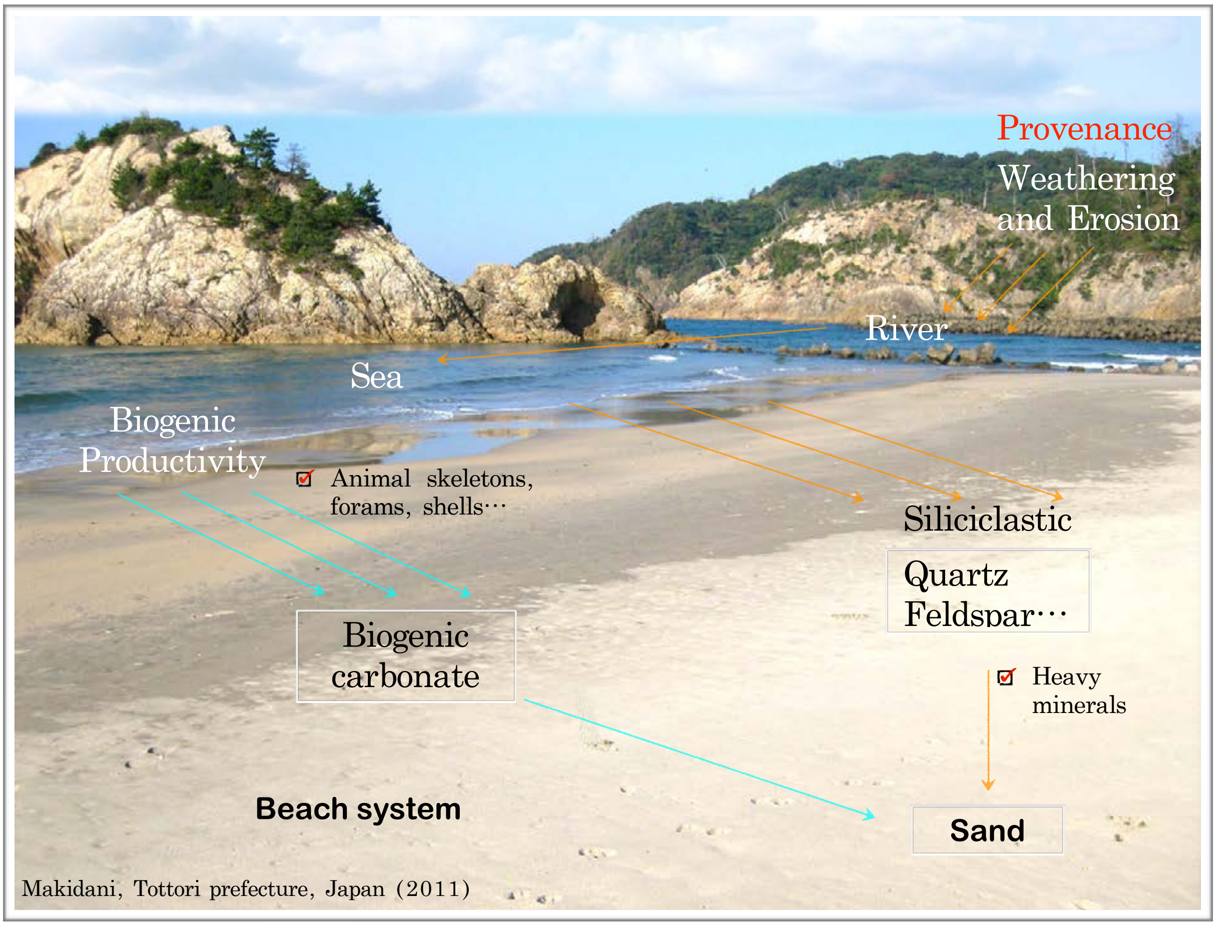

Figure 2. Genesis of beach sands. Siliciclastic rocks supply mostly quartz and feldspar, and rock fragments, biogenic carbonate mostly animal skeletons, forms, shells….

The Sea of Japan, one of the largest marginal seas of the Western Pacific Ocean, is located along the edge of the Eurasian continent and is partially separated from the unclosed ocean by Japan's islands (Gamo & Horibe, 1983; Danchenkov *et al.*, 2006; Talley *et al.*, 2006; Inoue *et al.*, 2007). It is connected to the open Pacific Ocean through the Tsushima strait in the south and the Tsugaru, Soya and Mamiya Straits in the North. The Tsushima current, a warm current providing significant nutrients and heat as well as a means of transportation for marine organisms in the Sea of Japan, comprises three branch currents, one of which travels north-eastwards along the San' in coast (Inoue *et al.*, 2007) towards Yamaguchi. Therefore, is reasonable to expect that not only did the Tsushima current play a significant role shaping the ecosystem, climate and environment of the Sea of Japan and its surrounding coastline within the Quaternary period (Kitamura *et al.*, 1997), but also it continues to contribute to the flourishing biogenic productivity in the Yamauchi coastal region. The annual temperature range is 12-24° C (the average being 14° C), while the total rainfall ranges from 1,200 to 1,500 mm per year, with heaviest falls occurring in June and July.

1. 2. Pocket beach characteristics

Sand originates mainly from the weathering and erosion of land and is transported to the sea by river systems. The most common beach materials are quartz and feldspar (both siliciclastic rocks). Additionally, biogenic materials from the sea such as animal skeletons, Foraminifera and shells also produce sand.

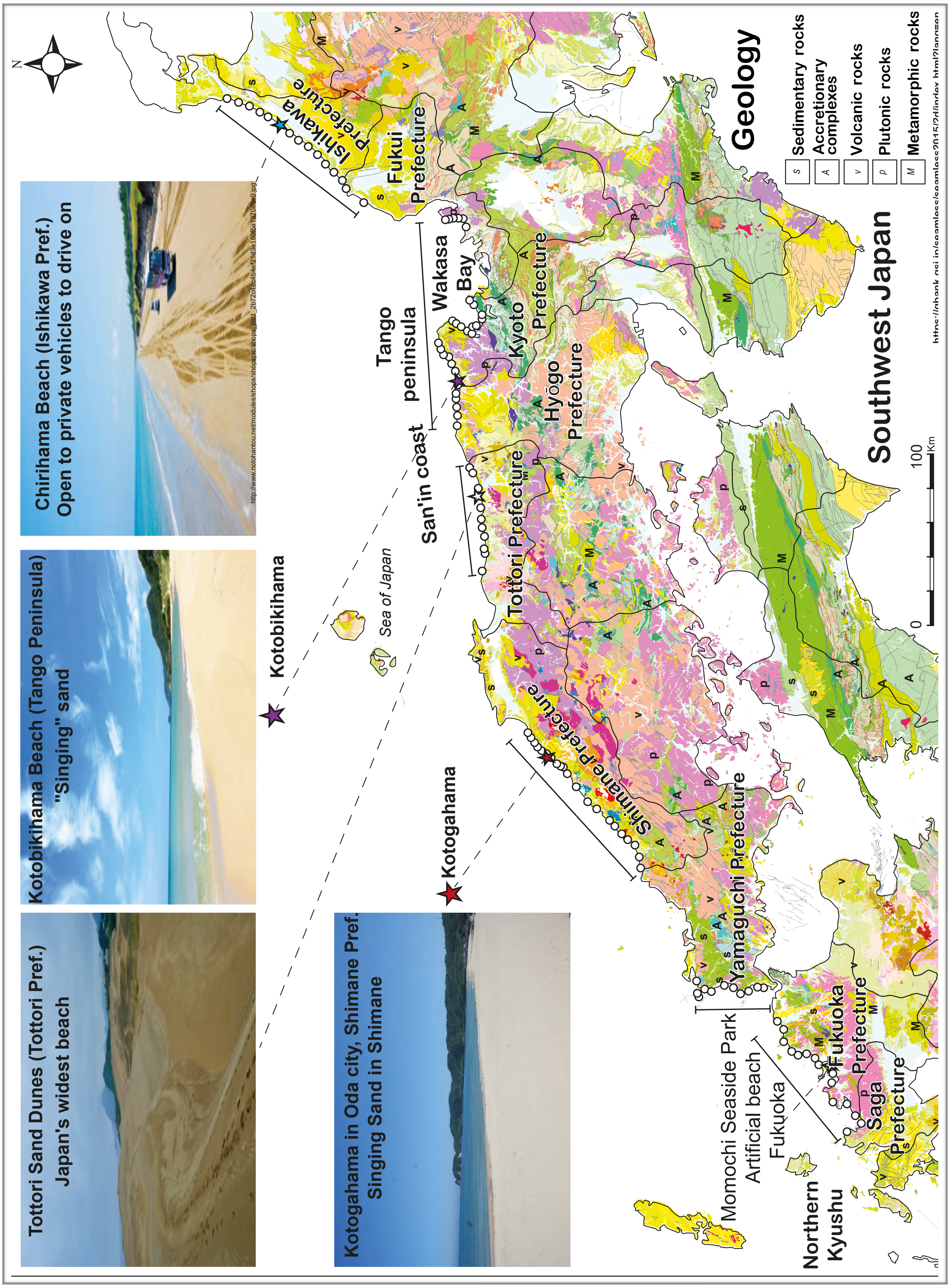

Figure 3. Detailed geological map of the coasts of South West Japan, showing the location of beaches sampled on the coastline of Northern Kyushu, Yamaguchi, Shimane, Tottori, Tango Peninsula, Wakasa Bay, and Noto Peninsula. Modified from, the Geological Survey of Japan (GSJ) and National Institute of Advanced Industrial Science and Technology (AIST), 2016.

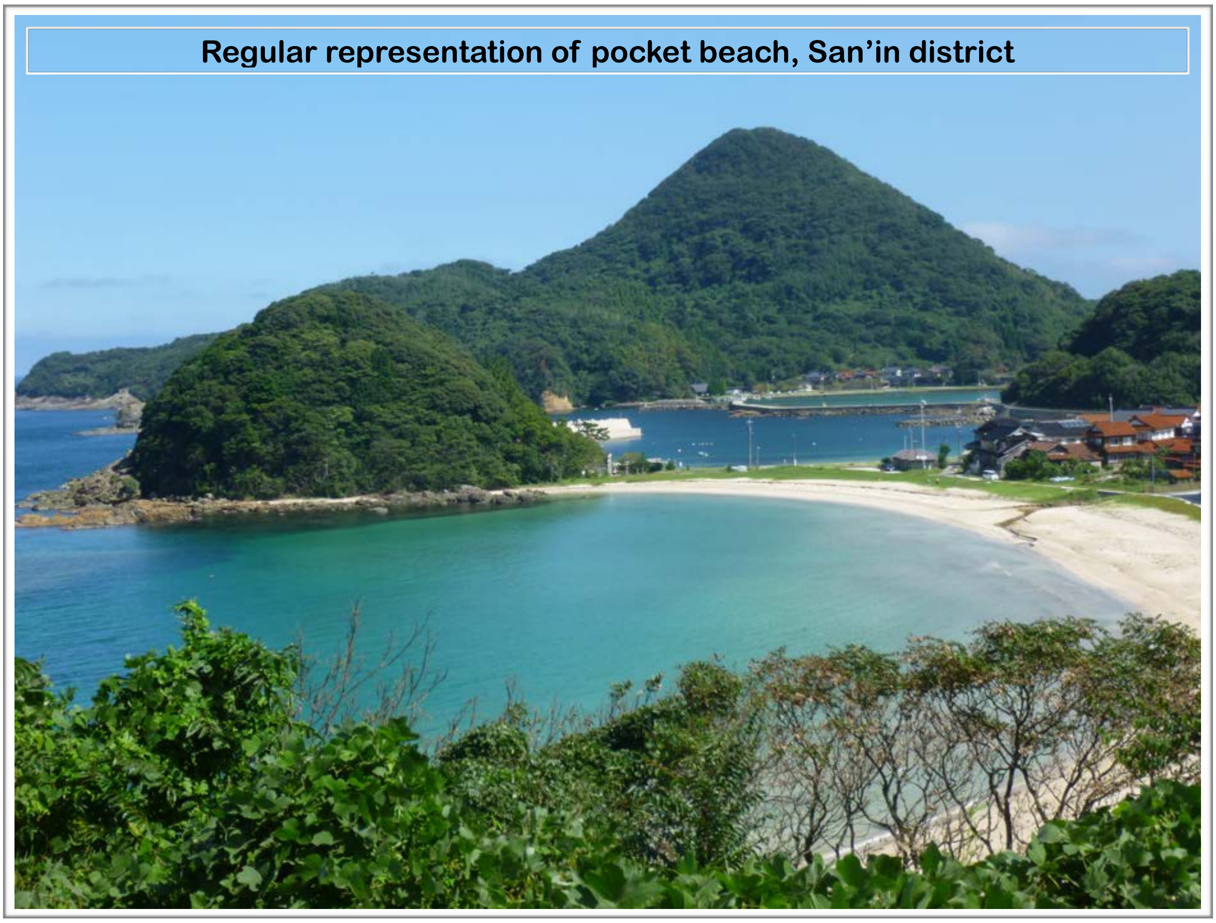

Figure 4. Regular representation of pocket beach, San' in district.

Biogenic carbonates of marine origin become important when the climatic conditions and the seawater qualities are good (Figure 2). It is worthwhile for someone wishing to investigate beach sands to discuss at least one of the locations identified in Figure 3, each of which has an unusual characteristic. For example, Momochi in Fukuoka is a man-made beach developed on reclaimed land. Chirihama beach, in Ishikawa Prefecture, has a driveway 8 km in length and 50 m wide, which is open to private vehicles, while the Tottori Sand Dunes within the San' in Kaigan National Park are a famous tourist attraction on account of being the country' s largest. Finally, three beaches are noted for the curious phenomenon of 'singing sand' ; the name of Kotobikihama Beach (on the Tango

Peninsula) is derived from this, while there is a legend associated with it on Katogahama beach in Oda city.

Figure 5. Terms describing an ideal beach profile. Note the wave-formed ripples by foreshore tidal flat on the Nijo beach, Fukuoka Prefecture, Japan (2012).

Beaches are environments where loose sediments such as sand, gravel and cobbles are regulated by oceanic processes. Figure 4 is a typical representation of a pocket beach, a form of beach particularly common throughout Japan, especially in the southwestern part. Figure 5 shows a typical beach profile from foreshore to backshore; many of the investigated beaches have such profiles. Wave-formed ripples by foreshore tidal flat are observed on the Nijo beach.

The first part is the foreshore, the part of the seashore that slopes from the low tide mark toward the crest of the berm. Next is the backshore bar, which protects beaches from erosion. Finally, sand dunes may form in the backshore environment through wind action. Based on field observations and measurements, the types of beaches present in the area reflect the processes from which the beaches formed and demonstrate characteristics of beach sands.

The beaches investigated can be classified into long beaches or pocket beaches according to the characteristics of their shapes using the length (L) and the arc length (l) (Figure 6). Pocket beaches are small (usually no more than a hundred meters) and are generally found between headlands. Small-pocket beaches are typically composed of sand and floating material such as algae, and provide isolated habitats for a variety of plants and animals. Beaches play an important role in protecting the coast; their loss negatively influences human activities as well as the environment.

The approximate arc lengths of the Makitani and Higashihama pocket beaches (Tottori Prefecture) are 1.48 km and 1.53 km. The Makitani pocket beach and the Hōjō long beach are illustrated in Figure 6. The average length of all the beaches investigated in Yamaguchi Prefecture is 1.13 km (Table 1), indicating they are relatively pocket beaches. The average length of beaches in the Shimane Prefecture is 1.73 km, three significant ones being Tinoza, Hashi 1 and Kuromatsu 3 with elongated seating areas of lengths 4.55 km, 3.80 km and 0.85 km respectively (Table 1). However, on the 82-km section of the Prefecture's coast between Masuda and Ohda, the beaches are essentially indistinguishable. At 12.5 km, the longest is Mochiishi, although this comprises seven 'sub-beaches'. The coastline of Tottori Prefecture is some 129 km in length. The longest of the beaches is that at Houzyou, which stretches some 19.5 km, while the shortest is that at Ishiwaki (0.96 km). The average length of all the beaches investigated is 5.79 km. Among the ten beaches sampled, four are long (Houzyou, Hakuto, Karo and Sakyuuhigashi); three are of medium length (Tomari, Anedomaria, and Hamamura), and two (Makitani and Higashihama) are classical pocket beaches. The tenth beach was Ishiwaki; although this was undoubtedly very small, its characteristics were such that it could not be classified as a pocket beach.

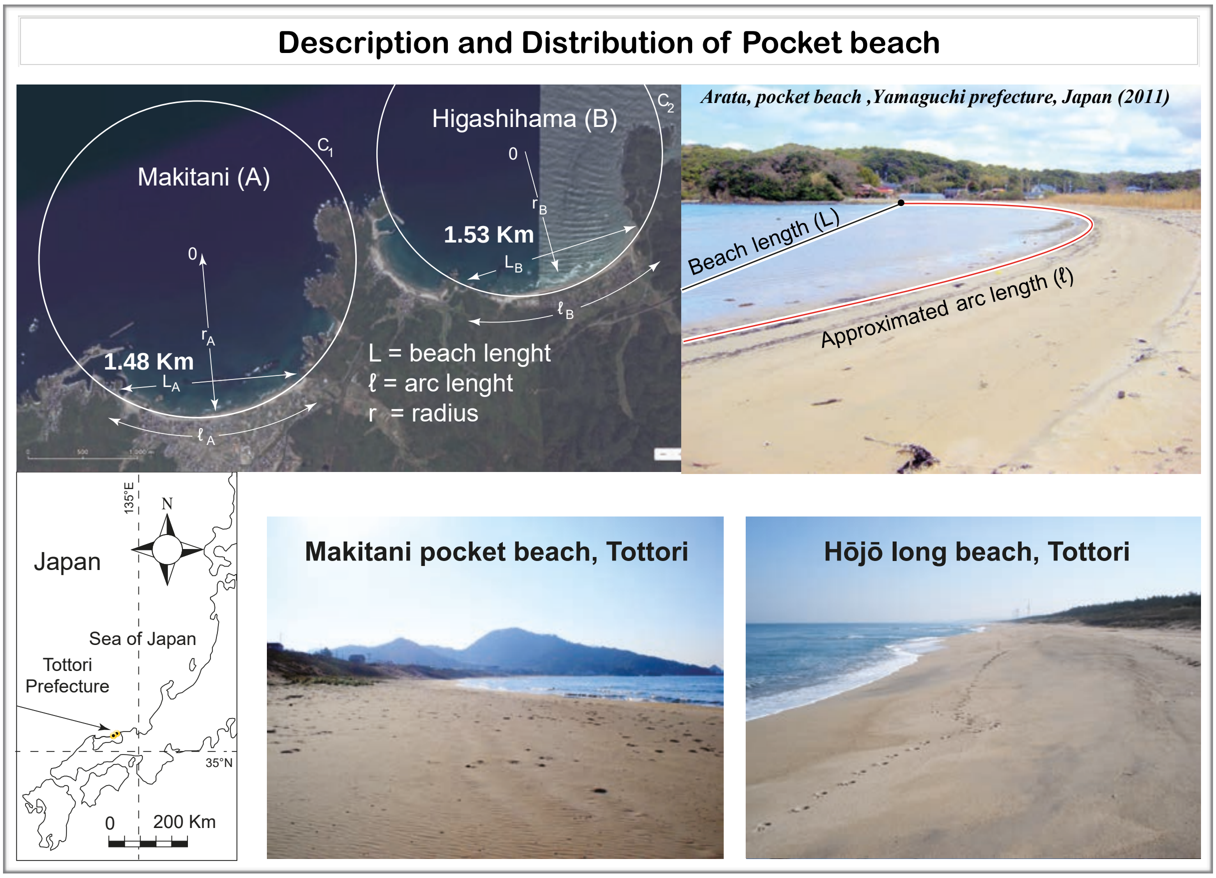

Figure 6. Shape of the Makitani and Higashihama pocket beaches in Tottori, Japan: (L) beach length, (l) arc length of the beach, and (r) radius of the approximated circle.

Table 1. Shape and characteristics of beaches on the coastline of Yamaguchi, Shimane and Tottori, South West Japan. (L= length of beach, and l = arc length of beach).

Sites	L (km)	ℓ (km)
Yamaguchi prefecture		
Ayaragi + Yasuoka	2.40	2.50
Fukue	2.20	.
Yoshimi	0.60	.
Toyoura	2.20	3.00
Yoshimo	0.95	.
Doigahama	1.00	1.20
Hinaka	0.25	0.35
Akada	0.40	0.55
Tunoshima	0.67	0.72
Agawa	0.62	0.92
Average	1.13	1.32

Sites	L (km)	ℓ (km)
Shimane prefecture		
Nakasu	0.15	0.18
Mochiishi	12.50	1.89
Araiso	0.69	0.71
Kitahama	0.28	0.30
Tanoura	0.30	0.38
Orii	0.63	0.65
Kuromatsu	0.85	0.90
Nishihamada	1.43	1.78
Shimokou	1.10	1.15
Hashi	3.80	3.98
Tunozu	4.55	4.80
Gohtsu	0.95	0.98
Asari	2.39	2.53
Iwamifukumitsu	0.74	0.78
Yusato	0.28	0.28
Kotogahama	1.25	1.45
Nima	0.50	0.53
Ohura	1.33	1.38
Isotake	1.25	1.30
Uozu	0.11	0.11
Shizuma	1.35	1.40
Average	1.73	1.31

Sites	L (km)	ℓ (km)
Tottori Prefecture		
Houzyou-1 + Houzyou-2	19.50	19.60
Tomari	2.91	2.98
Ishiwaki	0.96	0.98
Anedomari+Hamamura	5.80	6.13
Hakuto + Karo	6.75	6.80
Sakyuuhigashi	7.50	7.58
Makitani	1.44	1.48
Higashihama	1.44	1.53
Average	5.79	5.89

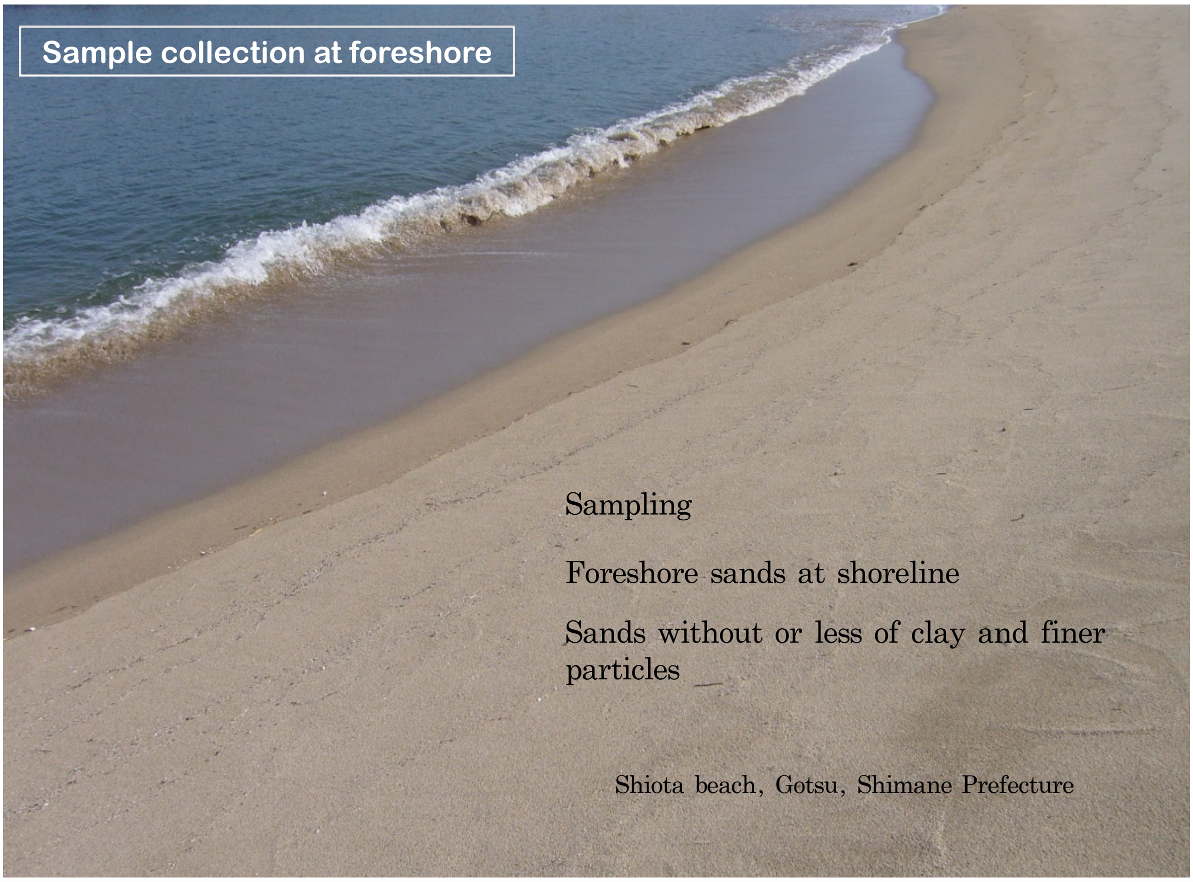

Figure 7. Foreshore sampling of beach sands at shoreline, Sands without or less of clay and finer particles.

Chapter Two

2. MATERIALS AND METHODS

2. 1. Sample collection at foreshore

Sampling sites were selected based on the accessibility and character of sites. Tidal information, obtained from the Japan Meteorological Agency, was used to ensure sampling was performed at low tide or moderate tide times. Beach sand samples were taken from the uppermost few centimetres of the beach; the location of sampling on each beach was chosen such that the clay content and fine particle content was as low as possible, and the coarse sands content was as high as possible, as illustrated in Figure 7. For each sample, approximately 200 grams of sand were collected using a stainless-steel scoop from the foreshore of selected sites along the coasts of South West Japan on the coastlines of Northern Kyushu, Yamaguchi, Shimane, Tottori, Tango Peninsula and Noto Peninsula. In some sites, the extent of sea walls of artificial structures constructed for coastline protection by reducing the rate of erosion prevented sample collection. Samples were collected from the foreshore surface and the location from which the samples were obtained recorded. Beach widths were measured using a linen tape, and beach slope measured with an inclinometer. The samples were stored in their natural state (that is, wet from seawater) in the laboratory before further processing. The experimental workflow for the sample preparation and data analysis are illustrated in Figure 8.

2. 2. Sample preparation and analysis

In the laboratory, approximately one-third of each sample was transferred to Pyrex beakers in their natural state, covered with aluminium foil to allow air circulation, and dried in an oven at 110° C for 24 hours. Once dried, sub-samples of the sediments were crushed in an automatic agate mortar and pestle grinder to produce a powder suitable for analysis. Fused glass discs and pressed powder briquettes were prepared from the crushed samples for major oxide and trace element analysis, respectively. In order to determine the Loss on Ignition (LOI), 5.000 ± 0.001 g of the dried powder sample were transferred to porcelain crucibles. The samples were ignited for at least two hours in a muffle furnace at 1050° C and the weight differential reported as a percentage loss.

The ignited material was then manually disaggregated and re-crushed in an agate pestle and mortar, and returned to a 110° C oven for at least 24 hours. The fused glass discs were prepared in an NT-2000 automatic bead sampler using the ignited material in addition to an alkali flux comprising 80% lithium tetraborate and 20% lithium metaborate, with a sample:flux ratio of 1:2. Analytical methods, instrumental conditions and calibration followed those described by Kimura and Yamada (1996). The pressed powder briquettes were prepared by pressing about 5 g of powdered sample into 40 mm diameter plastic rings, using a force of 200 kN for about 60 s in an automatic pellet press (E-30 T.M Maekawa) following the Ogasawara (1987) method. Average errors for all elements were less than ±10% relative. Analytical results for GSJ standard JSl-1 were acceptable compared to the proposed values of Imai *et al*. (1996).

Major elements expressed as oxides (SiO_2, TiO_2, Al_2O_3, Fe_2O_3*, MnO, MgO, CaO, Na_2O, K_2O, and P_2O_5) and 18 trace elements (As, Pb, Zn, Cu, TS, Ni, Cr, V, Sr, Y, Nb, Zr, Th, Sc, F, Br, I, and Cl) were obtained using an automated RIX 2000 system (Rigaku Denki Co. Ltd.) at Shimane University. The composition of the sand in terms of particle size was investigated using the Shimadzu SALD-3000S Laser Diffraction Particle Size Analyzer; microscopic observation of the sand was performed on sand holders.

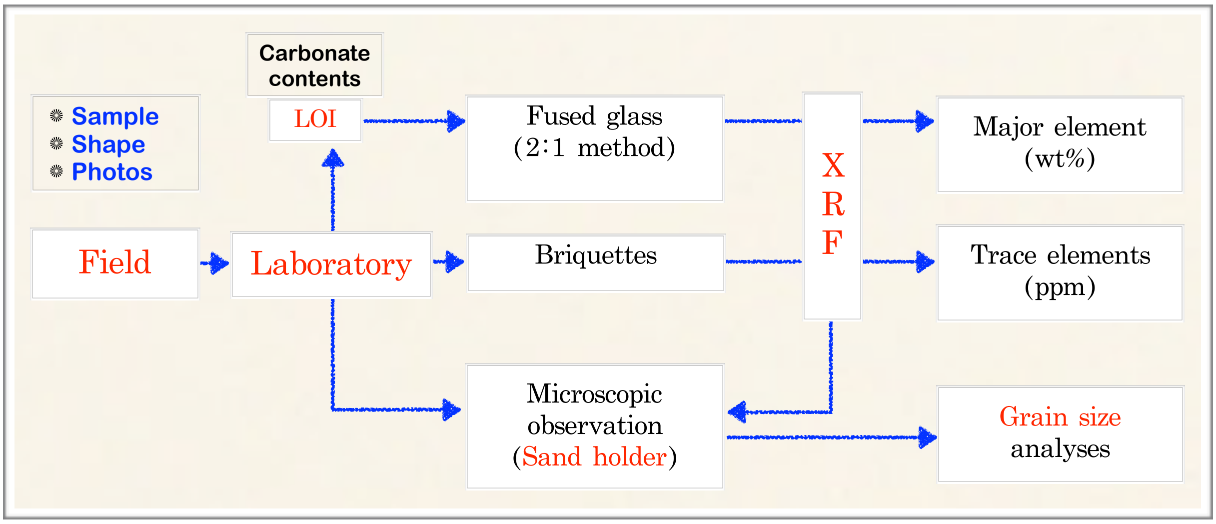

Figure 8: Experimental workflow for the sample preparation and data analysis.

Chapter Three

3. RESULTS

3. 1. Major and Trace Elements Geochemistry

Beach sand collected along the coasts of Southwest Japan, on the coastlines of Northern Kyushu, Yamaguchi, Shimane, Tottori, Tango Peninsula and Noto Peninsula comprise siliciclastic (quartz and feldspar) and biogenic deposits. The sands are representative of the characteristics of their constituent materials. These materials originate from a variety of sources and processes – some are transported to the beaches by marine currents from external sources or by rivers from nearby land, some are produced by erosion of the shoreline in the vicinity of the beach, some are created in situ by living organisms while others are related to human activity. The abundance of the major elements determined from the beach sand samples from the six coastal sites under investigation are summarized in Table 8. The corresponding LOI values are included in each Table for each location. The average geochemical composition of 15 local river sediments from AIST & GSJ (2013a), 15 near-shore marine sediments along the San' in district from AIST & GSJ (2013b), UCC (Rudnick & Gao, 2005) and UCJA (Togashi & Imai, 2000) estimated from the representative surface rocks and the means of major elements and trace elements are included in Table 8 for comparison.

3. 1. 1. Northern Kyushu

XRF major and trace element analyses of the beach sands from Northern Kyushu, Japan, are listed in Table 2 and Table 8. The beach sands had moderate to high SiO_2 contents, with abundances ranging from 54.43wt% to 91.23wt% (mean 77.24wt%); this is well above the 66.62 wt% present in the average Upper Continental Crust (UCC) reported by Rudnick and Gao (1995). The higher values in the beach sands reflected their quartz content. The next most abundant element, Al_2O_3, ranges from 4.71wt% to 18.35wt%, averaging (10.62wt%), less than in UCC (15.40wt%). In most samples, CaO contents are low (< 5wt%) and less than UCC (4.76wt%), reflecting low shell contents. Samples from Ashia and Munakata-1 are exceptions, with higher CaO contents of 13.47wt% and 28.43wt%, respectively. Among the remaining major elements K_2O (average 2.97wt%, range 1.63 - 4.64wt%), Na_2O (2.17wt%, range 0.87 - 3.63wt%) and Fe_2O_3* (1.35wt%, range 0.31 - 3.97wt%) are the next most abundant. Other major elements (MgO, TiO_2, MnO, and P_2O_5) are less abundant, and average values for all are less than in UCC.

Loss on ignition (LOI) data are presented in Table 2 to indicate variations in organic matter and calcium carbonate content of the beach sand sediment. Average LOI was low, averaging only 3.45wt%. However, the very high CaO contents at Ashiya and Munakata-1 identified in the XRF analysis was reflected in two the LOI readings for these two sites, which were significantly higher that this average figure, at 10.87wt% and 18.78wt% respectively. Table 2 also shows the concentration of trace elements in the beach sands. The two elements with the highest contents were chlorine (average concentration 2920ppm (range 44 to 10660ppm)) and sulphur (average concentration 871ppm (range 405 to 2260ppm)). The strontium content was significant, averaging 382ppm (range 76ppm to 989ppm), whereas iodine content varied from 3ppm to 3630ppm, averaging 145ppm. Fluorine content ranged from 11ppm to 340ppm, and zirconium from 8ppm to 67ppm. With average concentrations of 27ppm and 20ppm respectively, the vanadium and chromium contents were considerably lower than those seen in the UCC (97ppm and 92ppm respectively). Concentrations of other trace elements such as As, Pb, Zn, Cu, Ni, Y, Th, Sc, and Br were less than 20ppm on average, and below the abundances in UCC.

3. 1. 2. Yamaguchi Prefecture

Yamaguchi coastal beach sand samples had low to high SiO_2 contents, with abundances ranging from 4.72wt% to 92.16wt%, and averaging 61.20wt%, the high values reflecting their quartz content (Table 3 and Table 8). CaO was the next most abundant, the average value being 28.18wt% with a range of 0.77wt% to 87.37wt% (low values corresponding to high SiO_2 content and vice versa). The wide range of these values represented two situations – those samples with higher values were indicative of a significant biogenic $CaCO_3$ presence, but a low shell content was suggested by those with lower CaO values. Al_2O_3 was the next abundant element with (4.63wt%) average and ranges from 0.65wt% to 9.50wt%. Among the remaining major elements, K_2O (average 1.76wt%, range 0.34 - 4.40wt%), MgO (average 1.46wt%, range 0.10 - 4.93wt%), Na_2O (average 1.31wt%, range 0.30-1.99wt%), and Fe_2O_3*

(1.18wt%, range 0.01-2.66wt%) were the next most abundant. Other major elements (TiO_2, P_2O_5, and MnO) were less abundant.

The Yamaguchi coastal beach sand samples demonstrated relatively low to high LOI contents with CaO contents (averaging 28.18wt%, ranging from 0.77 to 87.37wt%). Among the analysed trace elements, Cl had the highest content as a result of contaminations from seawater, averaging 12602ppm, and ranging from 40ppm to 54231ppm, followed by total sulphur (TS) averaging 2263ppm, with a range from 30ppm to 5557ppm. Sr contents were significant, averaging 695ppm and ranging from 44ppm to 1358ppm, whereas F contents varied from 11ppm to 274ppm, averaging 11ppm. Zr contents ranged from 41ppm to 144ppm and V from 3ppm to 43ppm. The average contents of I and Sc were 28ppm and 20ppm, respectively. Concentrations of other trace elements were less than 20ppm on average. The Yamaguchi beach sands contained small amounts of SiO_2, Al_2O_3, and Fe_2O_3*, whereas CaO and LOI accounted for over 65% and 35% respectively and were relatively rich in organic matter. Of particular note were the samples from three beaches – Doigahama, Hinaka and Akada. These beaches' samples comprise carbonate or biogenic sands, composed primarily of foraminifera, ostracod, shells and sea urchins, the primary constituent of which is $CaCO_3$. The high LOI results were demonstrated by XRF analysis, confirming the high $CaCO_3$ content of the sands.

3. 1. 3. Shimane Prefecture

As expected, SiO_2 was the most abundant from the Shimane coastal beach sand samples, averaging 82.27wt%, with a range of 54.38-89.50wt%, followed by

Al_2O_3 (average 8.77wt%, range 4.54-16.46wt%) (Table 4 and Table 8). Among the remainder, CaO (2.70wt%, range 0.45-35.35wt%), K_2O (2.16wt%, range 0.88-4.44wt%), Fe_2O_3* (1.66wt%, range 0.42-3.14wt%) and Na_2O (1.65wt%, range 0.87-2.97wt%), were the next most abundant on average. MgO (average 0.49wt%) and TiO_2 (average 0.24wt%) were present in small amounts, whereas MnO and P_2O_5 (both averaging 0.48 and 0.03wt%) were present only in trace amounts. In these samples, overall, LOI contents ranged from 0.42-22.59wt%, averaging 2.18wt%. Cl was the most abundant trace element (again a result of seawater contamination), with an average value of 2995ppm, and a maximum of 9959ppm. The TS values were significant, ranging from 275ppm to 3398ppm, with a mean value of 621ppm. Sr was the next most abundant, with a maximum of 1126ppm, a minimum of 77ppm, and an average value of 209ppm. Among the remaining trace elements, only F, Zr, Zn, Cr, V, As, and I contents were present in moderate concentrations, other trace elements, Pb, Cu, Ni, Y, Nb, Th, Sc and Br showing very low concentrations.

3. 1. 4. Tottori Prefecture

The samples from the Tottori coastal beach sands generally comprised silicate materials (for example, feldspar and quartz), the high quartz content being reflected in their high SiO_2 content (mean value 72.05wt%, range 66.30-82.23wt%). (See Tables 5 and 8.) There were also relatively high levels of Al_2O_3 present, albeit only in the order of one-fifth the level of SiO_2 (average 14.71wt%, range 10.05-17.35wt%). A relatively wide range of values about the average of 3.86wt% was seen for CaO content (0.84-7.49wt%), with a significant shell material content being indicated by similar values from the LOI analysis (a range of 0.05-5.50wt%, average 1.81wt%). Na_2O and K_2O, also likely to be contained within feldspar, was less abundant, averaging 2.91wt% and 2.62wt%, respectively. Three major elements (Fe_2O_3*, MgO and TiO_2), were present only in minor amounts (averages 2.48wt%, 1.02wt%, and 0.26wt% respectively), and P_2O_5 and MnO were present only in trace amounts (both averaging 0.05wt%). Iodine (I) was the most abundant trace element averaging 3698ppm, with a maximum of 7394ppm. It was followed by total Chlorine (Cl), which averaged 578ppm (range 342-1007ppm), and Sr (average 384ppm, range 131-598ppm). Average concentrations of all other trace elements except TS (152ppm) were less than 100ppm, reflecting the high SiO_2 content and marked quartz dilution in this suite of sediments.

3. 1. 5. Tango Peninsula

Results showed that SiO_2, dominated the analysed sand samples averaging 78.02wt% (Eastern San' in coast sands), 81.02wt% (Tango Peninsula sands) and 84.83wt% (Wakasa Bay sands) (Tables 6 and 8). The other sites' samples showed relatively high SiO_2 content, with three exceptions. These three sites were Kirihama (average 69.06wt%), Shibayama (66.82wt%) and Takeno (41.89wt%) and, as would be expected given their high SiO_2 content, they exhibited high CaO contents of 13.77wt%, 11.21wt% and 43.35wt% respectively, as shown in Table 6. The high SiO_2 concentrations resulted in low contents of other elements, with Al_2O_3 contents of between 5.30 and 11.86wt% in the Eastern San' in coast sands, 7.60 to 12.44wt% in the Tango Peninsula and 5.55 to 10.27wt% Wakasa Bay sands (Table 6). Average Al_2O_3 contents were 8.45wt% in the Eastern San' in coast sands, 9.92wt% for the Tango Peninsula sands and 7.95wt% in the Wakasa Bay sands (Table 8). Seven other elements were present in significant quantities; these were TiO_2, Fe_2O_3*, MnO, MgO, Na_2O, K_2O and P_2O_5. As shown in Table 6, their concentrations were, in the most part, less than 5wt% and, in some cases, less than 1wt%. Among the trace elements, the contents of ferromagnesian elements (Ni, Cr, V and Sc) and large cations (Y, Nb, Zr, Th and Sr) tended to be less abundant than they were in the UCC and the JAUC (Table 8).

3. 1. 6. Noto peninsula

Generally, beach sands from the Noto Peninsula were characterized by moderate contents of SiO_2 (75.44-83.43wt%, average 79.00wt%) and Al_2O_3 (8.13-13.02wt%, 11.39%). Furthermore, the Fe_2O_3* content was low (1.79-5.27wt%), as were those both of MgO (0.37-1.85wt%) and of TiO_2 (0.20-0.66wt%, 0.31wt%). These can be accounted for by the presence of a high level of quartz and a low level of mafic components (see Tables 7 and 8). The low CaO contents (0.57-1.83wt%, 1.27wt%) indicated that all the beach sand samples had very low carbonate components. The contents of Cr, Ni and Sc showed a wide range from 3 to 45ppm, detection limits to 9ppm, and 1 to 9ppm respectively, suggesting a contribution from more mafic components. Contents of the high field strength elements Th, Y, Nb, showed similarly wide ranges from 6 to 9ppm, 15 to 22ppm, and 5 to 8ppm respectively.

Table 2. XRF major (wt%) and trace (ppm) element analyses of beach sands from northern Kyushu, Japan. LOI, oven-dried loss on ignition; and indices of Chemical Index of Alteration (CIA), Plagioclase Index of Alteration (PIA) and Chemical Index of Weathering (CIW).

SAMPLE	SiO_2	TiO_2	Al_2O_3	Fe_2O_3*	MnO	MgO	CaO	Na_2O	K_2O	P_2O_5	LOI	CIA	PIA	CIW	As	Pb	Zn	Cu	Ni	Cr	V	Sr	Y	Nb	Zr	Th	Sc	TS	F	Br	I	Cl
Fukuoka Prefecture (n=26)																																
Ashiya	67.12	0.29	9.64	3.11	0.08	1.45	13.47	2.09	2.70	0.06	10.87	24	19	26	23	14	26	3	.	11	41	556	16	3	37	1	30	1724	101	11	11	6197
Namitsu 1	88.25	0.10	6.21	0.99	0.02	0.36	1.50	0.94	1.63	0.01	5.58	51	51	59	20	13	21	4	.	31	36	423	14	2	46	2	21	1535	49	12	23	10660
Namitsu 2	75.17	0.18	9.98	2.21	0.04	0.91	6.49	2.20	2.77	0.04	1.87	35	31	39	15	12	14	2	.	23	14	181	11	2	46	2	6	674	35	5	36	1007
Munakata 1	54.43	0.19	8.28	1.73	0.04	1.84	28.43	1.96	3.00	0.08	18.78	13	8	13	11	11	18	6	.	5	17	989	14	.	.	2	46	2260	.	9	3	5232
Munakata 2	85.39	0.09	5.76	0.92	0.01	0.32	4.62	1.03	1.81	0.03	3.58	32	27	36	17	12	13	2	.	7	8	337	9	1	46	2	13	724	206	3	26	.
Katsuurahama	89.25	0.10	5.81	0.72	0.01	0.25	0.61	1.16	2.07	0.01	0.98	53	54	66	8	12	13	2	.	21	.	115	10	3	53	3	.	742	11	30	3630	.
Tsuyazaki	80.87	0.13	9.34	1.13	0.02	0.39	3.53	1.96	2.61	0.02	2.58	43	40	49	12	13	16	2	.	.	16	365	13	2	54	3	11	665	227	4	24	.
Miyaji	77.56	0.16	9.25	1.46	0.03	0.65	6.13	2.01	2.70	0.04	5.02	35	31	39	13	12	19	6	.	7	24	433	13	2	47	3	18	1017	172	7	19	2239
Koga	84.03	0.13	9.11	0.98	0.02	0.37	1.02	1.64	2.67	0.02	0.93	55	58	67	10	15	18	5	1	30	26	241	15	4	55	2	6	569	89	5	36	.
Singu 1	81.41	0.16	9.67	1.18	0.02	0.52	1.59	1.82	3.61	0.02	1.22	50	50	62	10	16	17	3	.	25	15	247	15	3	54	2	5	530	61	5	27	.
Singu 2	82.32	0.09	10.98	0.72	0.01	0.31	0.96	1.81	2.79	0.01	1.25	59	63	70	11	16	17	6	1	25	17	300	16	2	45	2	8	802	131	9	32	3962
Wajiro	91.23	0.09	4.71	0.50	0.01	0.26	0.29	0.87	2.05	0.00	0.82	53	56	71	8	12	12	2	2	21	.	79	9	3	46	1	.	763	60	11	33	4021
Ikinomatsubara	86.74	0.03	7.40	0.41	0.01	0.11	0.68	1.17	3.44	0.01	0.55	52	54	70	3	18	12	0	.	2	.	183	13	2	56	1	.	405	131	3	28	.
Imajuku 1	82.40	0.04	10.67	0.31	0.01	0.13	0.60	1.97	3.86	0.01	0.58	56	60	71	3	19	15	1	.	11	.	231	16	2	53	1	.	564	21	7	34	1984
Imajuku 2	76.67	0.09	13.38	0.76	0.02	0.31	1.15	2.97	4.64	0.02	0.91	53	55	66	3	21	20	2	.	2	.	274	17	3	60	1	3	598	104	9	27	1895
Nagahama 1	68.12	0.17	13.65	1.33	0.03	0.90	8.99	3.14	3.64	0.05	5.92	35	31	39	6	13	18	8	.	13	19	654	14	1	25	2	22	955	143	6	18	44
Nagahama 2	74.48	0.16	12.92	1.30	0.03	0.91	4.04	2.88	3.26	0.04	2.45	45	44	52	6	13	17	6	15	38	26	464	14	2	39	1	13	704	34	8	23	2730
Itoshima 1	72.93	0.15	10.19	1.33	0.03	0.76	9.04	2.15	3.39	0.04	6.49	30	25	34	7	13	16	6	.	19	19	557	14	2	38	2	27	1182	48	6	25	1817
Itoshima 2	79.66	0.11	10.56	0.85	0.02	0.44	3.70	1.79	2.85	0.02	3.92	45	44	52	9	15	16	5	.	33	23	434	16	3	45	2	18	1151	89	8	29	4777
Itoshima 3	77.84	0.10	10.10	0.81	0.02	0.48	4.79	1.85	3.97	0.03	3.70	39	33	46	9	16	13	4	.	9	2	410	15	2	45	3	12	805	.	8	22	2397
Nijo 1	75.72	0.27	12.47	2.29	0.05	1.14	2.90	2.65	2.46	0.04	1.13	51	51	57	4	13	23	7	15	42	62	316	14	5	58	2	13	687	340	9	23	2812
Nijo 2	71.23	0.29	15.39	2.34	0.04	1.19	3.36	3.19	2.94	0.02	1.28	52	52	58	4	15	24	9	14	43	62	386	14	4	48	2	12	586	34	8	21	288
Nijo 3	81.01	0.11	11.05	0.91	0.02	0.47	1.47	2.26	2.67	0.02	0.84	54	56	64	4	17	15	5	4	14	10	223	13	3	55	2	6	652	.	10	29	3005
Nijo 4	75.72	0.16	13.21	1.28	0.02	0.61	2.92	2.55	3.49	0.04	1.34	50	50	58	8	15	16	6	3	20	13	354	14	3	49	1	6	503	.	5	28	.
Nijo 5	79.20	0.09	11.58	0.73	0.01	0.32	2.64	2.23	3.17	0.02	2.26	49	49	58	8	17	15	4	2	19	12	365	16	3	41	2	9	662	.	5	30	693
Shikaka	76.50	0.17	12.54	1.42	0.03	0.74	2.73	2.69	3.16	0.02	1.29	50	49	57	4	15	20	7	9	26	31	359	15	4	44	2	8	568	31	6	23	380
Saga Prefecture (n=4)																																
Karatsu 1	64.77	0.52	18.35	3.97	0.06	1.63	4.03	3.54	3.09	0.03	2.73	53	53	58	5	15	45	20	7	24	109	419	15	6	54	2	14	788	59	8	14	2737
Karatsu 2	73.96	0.23	14.31	1.70	0.04	0.69	2.71	3.08	3.25	0.02	1.40	52	52	59	8	16	22	6	3	21	38	369	13	4	49	2	9	561	103	6	26	.
Karatsu West 1	74.69	0.14	14.10	1.14	0.02	0.46	2.51	3.68	3.24	0.03	1.50	50	50	57	8	15	19	2	.	17	14	382	13	3	56	2	8	665	.	7	35	1685
Karatsu West 2	68.46	0.22	8.00	2.02	0.03	1.30	15.91	1.70	2.29	0.07	11.77	19	15	20	13	11	20	2	.	20	34	816	12	1	8	3	43	2081	.	8	15	3674

Table 3. XRF major (wt%) and trace (ppm) element analyses of beach sands from Yamaguchi Prefecture, Japan. LOI, oven-dried loss on ignition; and indices of CIA, PIA and CIW.

SAMPLE	SiO_2	TiO_2	Al_2O_3	Fe_2O_3*	MnO	MgO	CaO	Na_2O	K_2O	P_2O_5	LOI	CIA	PIA	CIW	As	Pb	Zn	Cu	Ni	Cr	V	Sr	Y	Nb	Zr	Th	Sc	TS	F	Br	I	Cl
Toyoura 1	84.52	0.05	6.84	0.52	0.01	0.21	3.04	1.51	3.27	0.02	2.80	37	29	46	7	17	12	2	6	18	.	155	18	1	55	3	1	745	.	11	32	3480
Toyoura 2	84.00	0.03	7.79	0.36	0.01	0.13	2.27	1.11	4.29	0.02	2.15	42	35	57	7	18	5	1	5	10	.	110	24	0	50	3	1	499	235	5	30	.
Kawatana	73.73	0.09	9.50	0.77	0.02	0.46	9.02	1.97	4.40	0.03	7.18	28	19	33	5	18	16	3	1	11	.	386	23	2	73	5	8	1113	.	11	21	4804
Kogushi	84.42	0.09	7.14	0.01	0.20	0.20	3.14	1.39	3.39	0.01	2.75	38	30	47	4	17	15	1	3	18	.	150	20	1	63	5	3	735	.	11	26	10049
Doigahama	4.72	0.06	0.65	0.45	0.03	4.93	87.37	1.31	0.35	0.12	41.12	.	.	.	1	7	1	4	.	5	.	1348	7	.	.	.	39	5557	62	15	.	18114
Arata	57.40	0.23	5.73	1.64	0.03	1.47	29.85	1.77	1.81	0.09	19.35	.	.	.	7	11	23	3	.	10	.	954	12	.	.	1	24	2517	78	14	.	11784
Kanda	31.39	0.14	2.73	0.99	0.02	2.76	59.35	1.40	1.05	0.16	23.66	.	.	.	4	8	8	3	.	10	.	1354	8	.	.	.	37	4106	145	14	.	13222
Tunoshima 1	46.62	0.11	2.01	0.67	0.02	1.23	47.69	0.86	0.65	0.12	26.44	.	.	.	2	8	5	4	.	8	.	1254	5	.	.	1	33	3817	24	9	.	8941
Tunoshima 2	37.30	0.24	3.03	1.35	0.03	1.46	54.86	0.97	0.63	0.13	28.82	.	.	.	2	7	8	5	.	13	.	1316	5	.	.	1	35	3645	181	9	.	6715
Agawa	48.29	0.19	5.01	1.77	0.03	1.83	39.92	1.33	1.51	0.12	24.08	.	.	.	9	9	19	6	.	9	.	1143	11	.	.	2	30	2789	.	10	.	5094
Hinaka	18.90	0.18	3.43	1.79	0.05	4.11	68.69	1.89	0.83	0.14	35.49	.	.	.	5	7	16	5	.	8	.	1336	10	.	.	1	35	4023	89	13	.	54231
Akada	21.36	0.11	2.62	0.98	0.03	3.50	68.71	1.69	0.85	0.14	35.01	.	.	.	4	8	6	4	.	16	.	1358	8	.	.	.	38	4693	96	15	.	180
Ushirohama A	84.68	0.04	7.25	0.38	0.01	0.17	2.43	1.24	3.79	0.01	2.68	41	33	53	5	17	8	1	5	18	.	120	21	1	53	3	1	980	115	14	30	6568
Ushirohama B	89.28	0.03	5.63	0.33	0.01	0.11	0.77	0.94	2.88	0.01	1.56	48	46	66	5	14	7	1	5	15	.	85	19	1	51	3	.	422	114	4	31	.
Narabimatsu	87.89	0.05	5.94	0.36	0.01	0.10	1.74	0.83	3.07	0.01	1.30	43	37	57	3	16	8	13	8	13	.	44	18	.	41	4	.	744	116	12	35	40
Yasuoka	81.64	0.22	4.85	1.25	0.02	0.60	8.16	1.44	1.78	0.05	6.52	20	15	22	7	14	32	5	5	32	.	335	12	1	77	2	10	1414	.	9	22	26640
Ayaragi	88.90	0.11	4.28	0.79	0.02	0.29	2.95	0.90	1.73	0.02	2.93	33	26	39	6	12	18	2	9	19	.	142	11	1	55	2	4	1010	.	14	36	7541
Yoshimi A	87.24	0.32	3.41	1.42	0.03	0.44	5.62	0.86	0.62	0.04	4.67	22	19	23	4	12	27	4	8	40	3	255	7	2	79	2	6	1061	76	12	27	6361
Yoshimi B	87.07	0.31	3.72	1.39	0.03	0.45	5.38	0.97	0.64	0.04	4.59	24	21	25	5	11	26	2	9	37	3	258	8	2	78	2	8	1031	137	11	28	5297
Yoshimi C	80.54	0.90	4.49	2.66	0.04	0.66	8.86	0.94	0.85	0.05	6.79	.	.	.	.	11	34	5	6	59	43	383	9	5	144	3	13	1212	124	8	16	3748
Yoshimi D	76.95	0.76	4.90	2.51	0.04	0.83	11.87	1.14	0.93	0.06	8.96	.	.	.	.	12	34	4	7	50	28	477	10	4	103	2	14	1577	11	11	19	6211
Yoshimo	42.39	0.20	3.83	1.40	0.04	2.31	47.17	1.51	1.01	0.13	26.23	.	.	.	.	9	20	3	6	16	.	1213	9	.	.	1	33	3652	55	8	.	8016
Arata A	32.29	0.18	3.90	1.66	0.04	3.14	55.41	1.94	1.33	0.13	29.15	.	.	.	.	10	20	6	.	20	.	1197	13	.	.	2	37	4735	274	12	.	9163
Arata B	43.88	0.18	4.39	1.53	0.04	2.47	44.25	1.69	1.45	0.11	26.21	.	.	.	.	9	20	5	.	12	.	1083	12	.	.	2	33	3917	.	18	.	17912
Arata C	28.29	0.16	3.71	1.69	0.04	3.59	59.23	1.99	1.16	0.14	32.35	.	.	.	.	9	20	6	.	7	.	1238	12	.	.	2	37	4518	89	20	.	46472
Arata D	56.58	0.19	5.94	1.68	0.03	1.55	30.47	1.63	1.83	0.10	19.39	.	.	.	.	10	24	4	.	16	.	970	12	.	.	2	26	30	14	16	.	21873
Fukue	92.16	0.38	2.27	1.61	0.03	0.29	2.60	0.30	0.34	0.02	1.86	29	27	31	4	11	15	3	5	32	14	97	6	2	73	2	1	561	128	5	34	.

Table 4. XRF major (wt%) and trace (ppm) element analyses of beach sands from Shimane Prefecture, Japan. LOI, oven-dried loss on ignition; and CIA, PIA and CIW.

SAMPLE	SiO_2	TiO_2	Al_2O_3	Fe_2O_3*	MnO	MgO	CaO	Na_2O	K_2O	P_2O_5	LOI	CIA	PIA	CIW	As	Pb	Zn	Cu	Ni	Cr	V	Sr	Y	Nb	Zr	Th	Sc	TS	F	Br	I	Cl
Shizuma	77.71	0.35	11.29	3.10	0.13	0.90	2.43	2.14	1.90	0.05	0.64	53	54	59	14	54	85	6	9	28	38	327	13	4	87	3	5	373	.	6	17	.
Uozu	76.95	0.19	12.52	1.85	0.06	0.63	3.09	2.42	2.24	0.05	1.28	51	52	57	16	33	55	5	6	20	9	395	13	2	78	3	4	510	194	5	29	11
Isotake	81.51	0.15	10.75	1.30	0.04	0.47	1.70	2.05	1.97	0.04	1.24	56	57	63	14	25	51	5	7	18	7	303	14	2	80	3	1	688	50	10	24	4234
Ohura	75.56	0.17	13.42	1.59	0.05	0.52	3.05	2.63	2.96	0.05	1.46	51	51	58	20	26	45	4	7	15	.	402	15	2	79	2	2	502	164	9	22	492
Nima	76.63	0.30	12.16	2.68	0.09	0.77	2.99	2.37	1.96	0.05	1.01	52	52	57	13	43	60	6	4	22	27	401	13	3	81	3	8	407	240	6	17	.
Kotogahama 1	83.49	0.07	9.22	0.70	0.01	0.16	1.77	1.71	2.84	0.02	1.35	50	51	61	20	13	12	2	5	11	.	225	14	.	64	.	1	439	271	6	18	.
Kotogahama 2	89.50	0.05	6.44	0.42	0.01	0.10	0.74	1.20	1.54	0.01	0.75	57	59	66	16	13	8	2	6	15	.	157	11	.	56	2	1	421	102	6	31	.
Kotogahama 3	84.23	0.21	8.32	1.91	0.05	0.44	1.16	1.63	2.00	0.05	1.08	55	57	64	19	13	10	2	4	21	.	150	12	.	55	1	1	482	.	7	31	785
Yusato	81.05	0.18	10.74	1.62	0.03	0.39	2.21	2.40	1.32	0.05	0.99	54	54	58	7	15	43	5	5	20	9	555	8	.	68	3	1	508	4	9	25	2018
Iwamifukumitsu	71.07	0.26	16.46	2.13	0.04	0.64	1.95	2.97	4.44	0.04	2.35	56	58	66	17	20	59	5	5	14	12	231	22	3	81	4	6	521	116	10	15	789
Kuromatsu 1	80.02	0.17	11.84	1.26	0.03	0.34	1.01	2.17	3.13	0.02	1.12	58	61	69	12	19	43	3	6	17	14	157	19	2	77	2	2	480	168	9	28	898
Kuromatsu 2	82.63	0.16	9.89	1.24	0.03	0.32	1.02	1.91	2.78	0.02	0.86	55	58	67	10	16	34	3	5	19	.	139	16	2	76	4	2	428	116	7	29	648
Kuromatsu 3	80.46	0.53	9.61	2.93	0.08	0.52	1.37	1.80	2.66	0.03	0.80	54	56	64	8	17	47	6	5	29	69	143	18	4	93	5	4	376	26	5	23	.
Asari 1	84.08	0.31	8.54	1.80	0.05	0.39	1.10	1.53	2.18	0.02	0.64	56	58	66	8	16	39	3	6	32	29	127	16	3	83	4	4	329	185	4	31	.
Asari 2	83.58	0.20	9.11	1.31	0.04	0.26	0.95	1.70	2.83	0.02	0.51	55	57	67	6	16	28	3	6	24	.	120	16	2	71	3	1	275	142	3	29	.
Asari 3	82.70	0.12	9.91	0.92	0.03	0.21	0.86	1.95	3.27	0.02	0.71	54	57	68	6	16	24	3	5	19	.	124	17	1	65	3	.	409	62	8	24	119
Gohtsu	87.11	0.08	8.01	0.58	0.02	0.16	0.45	1.50	2.08	0.01	0.97	59	64	71	3	14	16	3	7	25	.	87	14	1	57	3	.	799	22	13	37	7591
Tunozu	88.82	0.27	6.38	1.25	0.04	0.26	0.56	1.11	1.31	0.01	0.73	60	64	69	5	15	29	4	7	23	40	101	14	3	75	3	5	581	89	8	31	3236
Okinohama	87.74	0.70	5.80	2.64	0.08	0.29	0.69	0.87	1.17	0.02	0.42	60	63	69	5	13	31	4	5	33	103	80	13	5	97	4	3	349	168	4	24	.
Hashi 1	86.87	0.12	7.62	0.85	0.03	0.24	0.77	1.56	1.94	0.02	0.89	56	58	66	6	14	26	6	8	22	.	117	13	1	66	3	1	588	3	10	32	3841
Hashi 2	86.86	0.11	7.54	0.84	0.03	0.21	0.77	1.47	2.16	0.02	0.57	55	58	67	7	13	23	3	4	16	.	119	14	1	64	3	3	374	146	6	29	.
Hashi 3	84.25	0.09	9.22	0.74	0.02	0.18	0.77	1.81	2.89	0.02	1.02	55	58	68	6	15	19	2	6	15	.	124	16	1	65	2	.	370	9	6	26	.
Hashi 4	80.60	0.15	11.14	1.05	0.03	0.34	1.06	2.42	3.19	0.02	1.27	54	57	65	8	18	31	4	6	18	1	162	18	2	72	3	2	831	36	14	30	7493
Shimokou	77.59	0.17	12.73	1.36	0.04	0.43	1.53	2.52	3.61	0.03	1.27	54	56	65	10	17	36	3	7	15	.	216	19	2	77	3	2	588	168	11	27	2984
Nishihamada	70.66	0.40	7.40	2.87	0.05	1.24	14.36	1.68	1.22	0.11	11.44	20	18	21	14	10	55	5	6	25	19	642	13	2	56	2	20	1162	31	9	5	2512
Orii 1	80.17	0.41	8.11	3.14	0.07	1.28	3.65	1.53	1.60	0.05	2.03	43	41	47	11	16	33	12	10	25	18	226	14	.	98	4	15	620	76	7	23	241
Orii 2	76.49	0.25	9.72	2.16	0.05	0.97	6.23	1.91	2.18	0.05	4.65	37	34	40	10	15	33	10	8	25	26	328	15	.	97	5	11	1088	166	12	21	6208
Tanoura 1	86.55	0.64	5.26	3.06	0.07	0.75	1.73	0.88	1.02	0.03	1.43	48	48	54	8	13	41	9	14	46	95	103	12	4	73	4	12	438	38	4	22	.
Tanoura 2	84.96	0.39	5.88	2.57	0.07	0.83	3.02	1.08	1.19	0.04	2.45	41	39	45	8	13	35	8	15	38	49	168	12	2	78	3	9	582	283	6	27	980
Kitahama	87.29	0.21	4.54	1.16	0.03	0.33	4.61	0.92	0.88	0.03	5.05	30	27	32	10	10	20	2	3	25	9	309	9	.	82	2	8	1179	.	9	29	5371
Araiso	54.38	0.15	4.80	1.41	0.04	1.57	35.35	1.21	1.00	0.10	22.59	7	5	7	11	8	15	3	.	11	.	1126	8	.	.	2	19	3398	159	11	.	9959
Iwamitsuda 1	82.07	0.20	9.46	1.83	0.04	0.45	1.60	1.52	2.79	0.04	2.08	53	55	64	22	15	43	4	8	25	6	125	22	3	68	5	4	484	62	7	23	.
Iwamitsuda 2	82.52	0.18	8.62	1.72	0.03	0.45	2.29	1.58	2.58	0.04	2.84	48	47	56	21	14	39	7	8	21	5	156	20	2	69	6	4	702	75	11	21	3124
Mochiishi 1	83.87	0.20	8.68	1.83	0.04	0.45	0.96	1.63	2.28	0.05	1.49	56	59	67	23	14	34	5	10	27	5	96	21	3	73	7	2	603	274	7	29	1599
Mochiishi 2	85.01	0.19	8.03	1.68	0.04	0.40	0.87	1.45	2.27	0.04	1.45	56	59	67	21	14	30	5	11	26	12	86	20	3	69	7	1	599	113	7	35	2028
Mochiishi 3	85.37	0.11	7.77	1.21	0.02	0.29	1.20	1.32	2.67	0.02	1.72	52	53	64	18	14	23	4	7	25	.	101	21	2	59	5	2	510	155	7	30	583
Mochiishi 4	85.06	0.19	7.96	1.82	0.04	0.40	0.96	1.48	2.04	0.05	1.25	56	59	66	23	14	29	5	11	28	7	95	19	3	75	7	.	426	89	4	35	.
Mochiishi 5	85.55	0.19	7.63	1.79	0.04	0.40	1.06	1.40	1.90	0.05	1.36	55	58	65	23	15	26	4	10	24	8	90	19	3	72	7	.	500	.	6	33	921
Mochiishi 6	86.30	0.15	7.06	1.50	0.03	0.34	1.09	1.42	2.06	0.04	1.62	52	53	63	22	13	23	4	9	22	.	91	18	2	67	5	1	628	.	10	35	3642
Mochiishi 7	87.45	0.06	7.01	0.64	0.01	0.14	1.21	1.34	2.12	0.02	1.45	51	52	62	23	14	32	5	13	29	4	106	19	3	79	7	1	427	140	5	30	.
Nakasu 1	87.05	0.26	6.93	1.64	0.04	0.39	0.87	1.22	1.58	0.03	1.64	57	60	66	15	14	40	6	10	41	30	85	19	5	81	6	2	809	.	9	35	6416
Nakasu 2	87.04	0.29	7.38	1.67	0.04	0.37	0.80	0.93	1.45	0.03	1.53	62	67	72	18	14	51	6	10	44	51	85	20	6	74	5	4	372	89	3	34	.
Nakasu	85.07	0.41	7.63	2.24	0.06	0.49	0.98	1.17	1.92	0.04	1.31	57	61	68	18	13	43	6	11	45	28	77	19	6	72	7	3	415	.	6	27	.
Kohama	85.91	0.18	7.45	1.20	0.03	0.27	1.75	1.16	2.03	0.02	2.60	51	51	60	18	14	27	2	5	23	5	141	20	4	77	5	2	754	30	9	29	5145

Table 5. XRF major (wt%) and trace (ppm) element analyses of beach sands from Tottori Prefecture, Japan. LOI, oven-dried loss on ignition; and CIA, PIA and CIW.

SAMPLE	SiO_2	TiO_2	Al_2O_3	Fe_2O_3*	MnO	MgO	CaO	Na_2O	K_2O	P_2O_5	LOI	CIA	PIA	CIW	As	Pb	Zn	Cu	Ni	Cr	V	Sr	Y	Nb	Zr	Th	Sc	TS	F	Br	I	Cl
Houzyou 1	66.20	0.38	17.31	3.77	0.08	1.98	5.32	3.28	1.60	0.07	0.90	51	51	54	7	15	15	4	7	24	.	239	19	2	73	3	4	198	6	31	293	447
Houzyou 2	82.23	0.11	10.05	0.89	0.02	0.24	0.84	1.83	3.77	0.02	0.50	54	57	69	6	13	9	1	4	23	.	131	20	1	59	3	.	162	5	25	.	355
Tomari	73.57	0.20	14.62	1.87	0.04	0.66	2.78	3.07	3.15	0.04	0.90	52	53	59	14	13	22	3	7	19	5	371	17	2	79	3	7	62	10	26	4064	621
Ishiwaki	68.52	0.36	16.69	3.21	0.06	1.15	3.68	3.39	2.89	0.06	1.20	52	53	58	14	14	32	5	8	23	32	455	17	3	80	4	10	350	9	22	3404	613
Anedomari	68.61	0.23	17.35	2.28	0.04	0.87	4.30	3.50	2.77	0.05	1.80	51	52	56	16	14	30	4	8	22	9	506	14	2	73	3	7	157	10	20	2753	580
Anedomari	66.20	0.38	17.31	3.77	0.08	1.98	5.32	3.28	1.60	0.07	0.90	51	51	54	11	11	40	5	12	24	43	598	12	3	61	3	15	115	3	15	.	355
Hamamura	78.03	0.14	12.39	1.46	0.03	0.42	2.22	2.61	2.68	0.03	1.30	53	53	60	17	13	19	4	6	18	.	287	15	1	75	2	2	156	10	28	4505	679
Hamamura	76.56	0.16	13.43	1.70	0.03	0.58	2.52	2.58	2.39	0.03	0.80	54	55	61	16	12	22	2	7	24	3	342	14	2	78	2	4	131	3	26	.	342
Hakuto	77.43	0.28	11.12	2.84	0.06	1.26	2.52	2.34	2.11	0.03	1.30	51	51	57	15	11	29	5	12	34	24	277	15	3	77	3	5	200	10	23	3766	598
Karo	70.72	0.48	14.46	3.91	0.08	1.67	3.59	2.90	2.15	0.05	1.50	52	52	56	15	12	41	4	14	36	49	396	16	4	89	3	10	.	9	10	2951	576
Sakyuuhigashi	77.17	0.25	12.36	2.30	0.05	0.86	1.84	2.44	2.69	0.04	1.40	55	57	63	16	14	29	3	13	36	18	227	17	3	78	4	6	.	10	24	2651	549
Makitani	68.58	0.22	14.79	2.09	0.04	0.86	7.49	2.91	2.96	0.05	5.50	41	39	45	16	13	30	4	9	23	9	526	17	2	69	3	11	170	12	17	5198	996
Makitani	69.88	0.25	16.43	2.45	0.05	1.00	4.40	3.04	2.45	0.05	1.90	51	52	56	17	13	36	6	11	31	22	486	16	3	73	3	11	102	3	22	.	432
Higashihama	68.16	0.25	16.03	2.40	0.04	0.90	5.71	3.31	3.14	0.06	4.10	46	45	51	21	14	37	6	8	24	17	480	16	3	76	4	10	140	14	18	7394	1007
Higashihama	68.89	0.24	16.26	2.29	0.04	0.80	5.34	3.12	2.96	0.05	3.20	48	47	52	21	14	37	4	9	22	9	480	16	2	75	3	7	37	4	18	.	517

Table 6. XRF major (wt%) and trace (ppm) element analyses of beach sands from the Eastern San'in coast, Tango Peninsula and Wakasa Bay, Japan. LOI, oven-dried loss on ignition; and indices of Chemical Index of Alteration (CIA), Plagioclase Index of Alteration (PIA) and Chemical Index of Weathering (CIW).

SAMPLE	SiO_2	TiO_2	Al_2O_3	Fe_2O_3*	MnO	MgO	CaO	Na_2O	K_2O	P_2O_5	LOI	CIA	PIA	CIW	As	Pb	Zn	Cu	Ni	Cr	V	Sr	Y	Nb	Zr	Th	Sc	TS	F	Br	I	Cl
East San'in coasts (n=17)																																
Kasumi	84.67	0.24	7.42	1.70	0.04	0.54	2.08	1.42	1.87	0.04	48.00	48	47	55	3	15	9	5	.	2	9	172	17	2	45	1	1	530	89	7	23	1520
Shibayama	66.82	0.34	11.86	3.31	0.04	1.27	11.21	2.50	2.56	0.08	51.35	30	27	33	4	13	8	3	2	27	21	157	15	3	48	1	4	338	60	2	26	.
Sazu	87.86	0.11	6.83	0.75	0.02	0.17	0.33	1.25	2.67	0.01	55.29	55	60	72	8	14	16	4	5	90	55	181	15	4	53	2	10	567	104	6	19	1435
Yasugi	80.11	0.14	10.31	1.02	0.02	0.25	1.70	1.65	4.78	0.02	48.54	49	47	64	3	13	3	3	.	3	.	117	15	3	44	2	.	390	208	4	27	.
Kirihama	69.06	0.27	8.76	1.99	0.03	0.90	13.77	1.62	3.55	0.06	48.48	22	15	24	22	11	20	2	8	34	21	222	13	3	63	3	5	513	164	2	27	.
Takeno	41.89	0.31	5.30	2.45	0.06	2.22	43.35	1.53	2.78	0.10	39.65	6	3	6	16	12	8	3	2	20	.	142	12	2	48	3	.	514	118	5	31	.
Kumihama 1	74.35	0.24	9.74	2.22	0.05	1.00	7.45	1.63	3.27	0.04	51.73	33	28	38	12	11	12	4	1	4	5	350	12	2	51	2	13	936	16	9	20	4118
Kumihama 2	72.58	0.69	9.78	3.89	0.08	1.35	7.34	1.44	2.82	0.04	55.18	34	30	39	26	14	34	4	17	33	38	473	19	2	55	3	15	881	36	7	13	1717
Kumihama 3	83.53	0.12	7.64	1.18	0.02	0.41	2.77	1.35	2.94	0.02	49.45	42	38	51	27	15	45	6	21	139	89	472	19	5	91	4	14	765	75	5	8	
Kumihama 4	81.07	0.18	8.50	1.72	0.03	0.64	3.53	1.49	2.81	0.02	51.04	42	38	49	19	13	17	1	7	12	9	221	17	3	66	2	6	731	48	9	24	2452
Hachohama	84.24	0.09	6.35	0.85	0.02	0.31	4.79	1.14	2.19	0.02	50.31	33	27	38	22	14	28	2	14	31	28	266	17	3	66	3	7	698	.	7	20	1282
Kotobikihama	88.19	0.07	6.17	0.65	0.01	0.16	1.51	0.99	2.25	0.01	47.62	48	46	59	9	9	25	4	.	3	19	1315	16	.	.	2	46	2576	131	10	.	6414
Sunakata	83.80	0.19	7.27	1.73	0.03	0.56	3.17	1.16	2.06	0.02	53.97	42	40	49	15	12	24	5	.	2	19	826	19	1	76	4	25	1551	140	9	3	4356
Taiza	86.04	0.07	7.92	0.43	0.02	0.14	0.61	1.34	3.42	0.01	53.11	53	56	71	11	16	17	2	.	.	9	168	26	4	71	4	2	528	47	4	18	.
Hei 1	81.09	0.12	10.46	0.97	0.02	0.32	1.30	2.05	3.65	0.02	52.00	52	53	65	4	14	16	1	.	.	3	66	18	4	61	3		353	104	2	19	.
Hei 2	82.38	0.16	9.27	1.43	0.03	0.47	1.55	1.92	2.78	0.02	50.90	51	51	61	13	18	68	10	3	15	43	670	17	2	39	5	24	1186	38	6	2	1132
Hei 3	78.64	0.26	10.06	2.51	0.04	1.16	2.66	2.07	2.58	0.03	47.90	48	47	55	5	13	20	5	3	14	27	186	12	3	84	3	4	399	103	2	16	.
Tango peninsula Kyoto (n=14)																																
Iwagahana	78.13	0.12	12.44	1.04	0.02	0.34	1.23	2.89	3.78	0.02	53.00	53	55	64	4	15	21	3	1	10	15	170	19	2	67	2	2	720	131	10	32	4018
Satonami	81.01	0.06	10.85	0.54	0.01	0.20	1.17	2.45	3.70	0.01	51.70	52	53	64	3	15	8	5	11	12	.	149	18	2	47	1	.	630	175	8	31	2939
Hioki	81.19	0.09	11.54	0.78	0.02	0.28	0.87	2.54	2.67	0.01	57.20	57	60	67	4	14	17	2		19	22	151	17	3	64	3	.	793	17	11	30	6891
Ejiri	82.00	0.09	10.07	0.70	0.02	0.38	1.43	2.50	2.80	0.01	50.90	51	51	60	3	13	10	2	11	56	2	153	15	3	52	3	2	793	281	10	35	5756
Amanohashidate	80.93	0.11	11.18	0.85	0.02	0.27	1.11	2.39	3.12	0.01	54.60	55	57	65	4	15	17	3	3	29	1	153	16	3	58	2	.	378	89	2	35	.
Ryuguhama	83.21	0.03	9.06	0.36	0.01	0.17	2.21	1.78	3.17	0.01	48.60	47	45	57	6	12	7	1	.	18	.	198	18	2	45	2	5	906	.	10	32	6062
Kobashi	74.28	0.05	11.29	0.63	0.02	0.30	7.20	2.42	3.79	0.02	47.60	35	30	40	7	12	13	.	.	8	.	456	18	2	41	2	12	813	230	4	24	.
Nojiri	73.16	0.21	12.11	2.18	0.04	1.18	5.16	2.75	3.18	0.03	48.40	41	39	47	10	13	35	5	52	227	31	358	17	3	72	4	11	1019	45	10	22	5072
Tangoyura a	77.19	1.46	9.09	5.35	0.12	1.48	2.94	1.11	1.21	0.04	52.00	52	52	56	14	12	60	13	33	220	193	165	16	9	127	6	15	493	74	4	13	472
Tangoyura b	84.60	0.35	8.03	2.72	0.05	0.80	0.74	1.20	1.47	0.03	62.40	62	66	71	12	11	48	11	26	68	73	88	14	6	83	4	3	557	104	6	30	995
Kunnda a	86.61	0.12	7.65	0.78	0.02	0.29	0.64	1.44	2.45	0.01	55.40	55	59	69	3	12	16	4	3	36	8	102	15	4	65	3	1	712	.	10	32	5110
Kunnda b	84.14	0.09	9.21	0.72	0.02	0.18	0.77	1.53	3.34	0.01	55.10	55	59	70	2	15	19	8	0	22	2	117	16	3	59	3		3	117	2	37	.
Tango Kanzaki a	82.53	0.45	8.71	3.42	0.06	1.05	0.91	1.33	1.51	0.04	61.80	62	65	70	18	12	58	12	31	66	112	93	15	7	93	4	7	712	.	9	27	4544
Tango Kanzaki b	85.26	0.31	7.60	2.53	0.05	0.73	0.70	1.29	1.49	0.03	60.60	61	64	70	20	11	42	8	23	41	62	87	13	5	79	3	3	644	61	9	31	2393
Wakasa bay (n=7)																																
Matubara	84.17	0.43	7.58	3.20	0.06	0.88	0.86	1.08	1.65	0.09	60.70	61	65	71	7	12	42	14	20	44	59	61	18	5	77	5	7	365	145	3	24	.
Sakajiri	82.15	0.31	9.58	2.07	0.06	0.52	1.04	1.61	2.59	0.06	57.10	57	61	69	9	17	50	6	12	39	26	118	21	5	96	8	3	797	127	6	30	1297
Diamondo	90.31	0.02	5.55	0.25	0.01	0.04	0.12	0.63	3.06	0.00	54.90	55	64	82	.	.	.	.	.	.	.	.	.	.	.	.	.	.	.	.	.	.
Suishou	87.81	0.03	6.79	0.44	0.01	0.05	0.17	0.96	3.74	0.01	53.50	53	60	78	9	16	5	1	7	42	.	18	28	4	41	4	.	491	89	4	33	.
Sugehama	80.75	0.13	10.27	1.31	0.03	0.22	0.79	1.46	5.02	0.02	52.70	53	56	73	7	19	42	4	8	26	.	63	35	8	62	6	.	925	1	12	24	4988
Sada	83.24	0.18	7.71	1.46	0.04	0.36	2.99	1.39	2.59	0.04	50.60	42	39	50	11	16	33	3	8	32	2	185	19	3	87	5	5	849	76	8	28	2922
Kehinomatubara	85.36	0.09	8.18	0.96	0.03	0.17	0.26	1.51	3.42	0.02	55.30	55	60	74	4	17	18	3	11	28	.	39	28	4	54	8	.	549	130	8	28	1533

Table 7. XRF major (wt%) and trace (ppm) element analyses of beach sands from Noto Peninsula, Japan. LOI, oven-dried loss on ignition; and CIA, PIA and CIW.

SAMPLE	SiO_2	TiO_2	Al_2O_3	Fe_2O_3*	MnO	MgO	CaO	Na_2O	K_2O	P_2O_5	LOI	CIA	PIA	CIW	As	Pb	Zn	Cu	Ni	Cr	V	Sr	Y	Nb	Zr	Th	Sc	TS	F	Br	I	Cl
Sanrihama-A	75.44	0.49	12.59	3.84	0.07	1.06	1.70	2.20	2.51	0.10	2.23	58	60	66	20	15	56	10	9	29	96	281	19	6	117	8	8	628	89	9	19	3727
Sanrihama-B	76.12	0.47	12.52	3.63	0.07	0.94	1.57	2.12	2.45	0.10	1.76	59	62	67	19	16	52	9	7	26	97	282	20	6	118	9	9	446	131	4	24	.
Awara-A	80.36	0.26	11.11	2.30	0.05	0.39	0.68	1.88	2.93	0.04	1.30	60	65	72	23	12	32	5	.	3	33	177	22	7	151	9	1	430	.	2	21	.
Awara-B	81.79	0.24	10.22	2.16	0.06	0.38	0.62	1.90	2.60	0.04	1.23	59	64	71	24	13	29	4	.	.	33	168	19	6	133	8	1	413	173	3	24	.
Awara-C	83.00	0.22	9.43	2.11	0.05	0.37	0.66	1.75	2.37	0.03	1.19	59	63	70	24	13	26	1	.	9	36	162	18	6	132	8	2	430	74	3	24	.
Kaga-A	81.52	0.24	10.49	2.11	0.05	0.41	0.61	1.89	2.64	0.04	1.47	60	65	72	28	14	31	4	.	13	34	176	19	5	125	7	2	466	13	4	28	.
Kaga-B	82.08	0.22	10.16	2.04	0.05	0.39	0.57	1.84	2.59	0.04	1.40	60	65	72	28	14	28	3	.	10	33	172	18	5	124	8	1	451	.	3	27	.
Katayamada	82.78	0.30	8.13	3.19	0.07	1.04	1.25	1.38	1.80	0.05	1.02	56	58	65	16	12	39	4	.	26	48	166	15	6	120	7	3	417	118	2	27	.
Komatsu-A	83.43	0.20	9.03	1.79	0.03	0.50	1.05	1.86	2.07	0.04	1.45	56	58	65	12	11	27	2	.	8	24	186	16	5	107	8	2	1083	118	10	27	5078
Komatsu-B	78.17	0.66	8.78	5.27	0.11	1.85	1.83	1.58	1.66	0.07	1.11	54	55	60	10	11	55	5	2	45	114	203	16	8	161	6	9	647	175	5	14	1476
Komatsu-C	80.57	0.39	9.16	3.41	0.07	1.12	1.47	1.77	1.98	0.06	1.17	55	56	63	10	11	41	6	2	14	59	204	16	6	125	7	6	612	32	6	20	510
Komatsu-D	80.48	0.27	10.94	2.06	0.03	0.58	1.28	2.07	2.22	0.05	1.58	58	60	66	10	12	40	5	1	18	47	231	17	5	101	6	5	793	275	9	33	4227
Komatsu-E	80.30	0.27	11.13	2.09	0.03	0.58	1.24	2.01	2.27	0.06	1.49	59	61	67	9	13	40	3	1	16	53	233	17	6	107	8	5	760	147	8	27	2047
Komaiko	79.14	0.32	11.36	2.51	0.04	0.74	1.46	2.02	2.34	0.06	1.82	58	60	66	11	14	43	5	2	18	52	232	18	6	109	8	6	726	61	9	29	3093
Mikawa-A	79.58	0.29	11.42	2.15	0.04	0.59	1.21	2.13	2.53	0.06	1.41	58	61	67	10	13	38	5	.	8	40	227	19	6	113	7	4	623	.	7	19	1414
Mikawa-B	79.17	0.30	11.49	2.39	0.04	0.68	1.40	2.11	2.35	0.06	1.78	58	60	66	11	16	43	7	5	21	55	239	18	6	103	7	5	813	.	11	27	5392
Hakusan-A	78.40	0.32	11.86	2.54	0.04	0.69	1.37	2.16	2.55	0.07	1.63	58	61	67	15	15	46	6	.	12	56	238	19	6	120	9	5	757	149	8	27	2823
Hakusan-B	77.95	0.33	12.11	2.60	0.04	0.76	1.48	2.18	2.49	0.07	1.81	58	61	66	13	15	47	5	1	23	65	248	19	6	106	8	7	889	131	10	26	6019
Kanazawa	77.29	0.33	12.65	2.59	0.04	0.73	1.45	2.17	2.68	0.07	1.83	59	62	68	13	16	54	5	2	15	66	255	19	6	110	8	7	746	180	8	20	3110
Hahoku	76.37	0.33	13.02	2.74	0.05	0.64	1.36	2.36	3.05	0.08	1.41	58	61	68	23	15	38	3	.	14	50	261	21	6	123	9	5	499	89	3	23	39
Shiroo-B	77.71	0.27	12.61	2.34	0.04	0.60	1.23	2.38	2.78	0.06	1.85	58	61	68	19	16	40	4	.	21	52	257	18	5	106	7	4	814	59	10	27	5187
Shiroo-A	78.00	0.29	12.29	2.46	0.04	0.65	1.29	2.29	2.65	0.06	1.85	58	61	67	19	15	40	4	.	25	49	255	18	5	107	8	5	849	160	10	27	5808
Takamatsu-C	78.85	0.28	11.75	2.45	0.04	0.66	1.35	2.16	2.41	0.06	1.83	58	61	67	20	13	39	4	2	24	58	245	18	5	101	6	8	881	.	10	27	6273
Takamatsu-B	77.05	0.28	12.93	2.34	0.04	0.60	1.25	2.51	2.95	0.06	1.87	58	61	67	20	15	39	3	3	18	55	264	19	5	108	7	5	832	130	11	24	5998
Takamatsu-A	77.55	0.29	12.56	2.50	0.04	0.66	1.31	2.35	2.68	0.06	1.93	58	61	67	20	16	42	4	1	19	52	257	18	5	102	7	5	882	60	12	28	6730
Imahama	77.99	0.29	12.17	2.60	0.04	0.68	1.41	2.24	2.52	0.06	1.95	58	61	67	22	15	39	3	2	13	55	258	18	6	100	7	6	743	34	10	24	3734
Senrihama-A	77.21	0.30	12.60	2.63	0.04	0.70	1.44	2.35	2.67	0.07	2.07	58	61	67	22	14	39	3	.	14	51	264	18	5	100	8	6	780	30	12	21	5081
Senrihama-B	77.62	0.32	12.16	2.80	0.04	0.79	1.50	2.22	2.49	0.07	2.07	58	60	66	21	15	41	5	.	17	60	256	18	6	100	7	7	832	.	11	23	6044
Senrihama-C	77.41	0.32	12.27	2.81	0.04	0.80	1.52	2.28	2.48	0.06	2.01	58	60	66	22	14	43	7	2	19	61	260	18	6	101	7	7	804	89	12	23	5078
Hakui	76.64	0.32	12.77	2.87	0.04	0.75	1.51	2.27	2.75	0.07	2.02	58	61	67	23	15	44	4	1	18	61	259	19	5	104	8	5	774	47	9	20	3994

Table 8. Summary statistics of major element abundances in beach sands from the coasts of South West Japan, on the coastline of Northern Kyushu Yamaguchi, Shimane, Tottori, Tango Peninsula, Wakasa Bay, and Noto Peninsula. LOI, oven-dried loss on ignition; and CIA, PIA and CIW. Average geochemical compositions of local river sediments from the Geological Survey of Japan and National Institute of Advanced Industrial Science and Technology (AIST 2013a), near-shore marine sediments around Yamaguchi (AIST 2013b), average Upper Crust of the Japanese Archipelago (UCJA), according to (Togashi et al. 2000), and average Upper Continental Crust (UCC) (Rudnick & Gao, 2005).

SAMPLE	SiO_2	TiO_2	Al_2O_3	Fe_2O_3*	MnO	MgO	CaO	Na_2O	K_2O	P_2O_5	LOI	CIA	PIA	CIW	As	Pb	Zn	Cu	Ni	Cr	V	Sr	Y	Nb	Zr	Th	Sc	TS	F	Br	I	Cl
Northern Kyushu (n=30)																																
Average	77.24	0.16	10.62	1.35	0.03	0.67	4.76	2.17	2.97	0.03	3.45	45	44	53	9	14	18	5	6	20	27	382	14	3	47	2	15	871	99	8	145	2920
Minimum	54.43	0.03	4.71	0.31	0.01	0.11	0.29	0.87	1.63	0.00	0.55	23	8	13	3	11	12	0	1	2	2	79	9	1	8	1	3	405	11	3	3	44
Maximum	91.23	0.52	18.35	3.97	0.08	1.84	28.43	3.68	4.64	0.08	18.78	59	63	71	23	21	45	20	15	43	109	989	17	6	60	3	46	2260	340	30	3630	10660
Yamaguchi coastal beach sands (N=27)																																
Average	61.20	0.21	4.63	1.18	0.03	1.46	28.18	1.31	1.72	0.08	15.70	18	15	22	5	11	17	4	6	19	18	695	12	2	71	2	20	2263	108	11	28	12602
Minimum	4.72	0.03	0.65	0.01	0.01	0.10	0.77	0.30	0.34	0.01	1.30	.	.	.	1	7	1	1	1	5	3	44	5	0	41	1	1	30	11	4	16	40
Maximum	92.16	0.90	9.50	2.66	0.20	4.93	87.37	1.99	4.40	0.16	41.12	48	46	66	9	18	34	13	9	59	43	1358	24	5	144	5	39	5557	274	20	36	54231
Shimane coastal beach sands (N=60)																																
Average	82.27	0.23	8.77	1.66	0.04	0.48	2.70	1.65	2.16	0.03	2.18	51	53	60	13	17	35	5	7	24	25	209	16	3	74	4	5	621	115	8	27	2995
Minimum	54.38	0.05	4.54	0.42	0.01	0.10	0.45	0.87	0.88	0.01	0.42	7	5	7	3	8	8	2	3	11	1	77	8	1	55	1	1	275	3	3	5	11
Maximum	89.50	0.70	16.46	3.14	0.13	1.57	35.35	2.97	4.44	0.11	22.59	62	67	72	23	54	85	12	15	46	103	1126	22	6	98	7	20	3398	283	14	37	9959
Tottori coastal beach sands (N=15)																																
Average	72.05	0.26	14.71	2.48	0.05	1.02	3.86	2.91	2.62	0.05	1.81	51	51	57	15	13	29	4	9	26	20	387	16	2	74	3	8	152	8	22	3698	578
Minimum	66.20	0.11	10.05	0.89	0.02	0.24	0.84	1.83	1.60	0.02	0.50	41	39	45	6	11	9	1	4	18	3	131	12	1	59	2	2	37	3	10	293	342
Maximum	82.23	0.48	17.35	3.91	0.08	1.98	7.49	3.50	3.77	0.07	5.50	55	57	69	21	15	41	6	14	36	49	598	20	4	89	4	15	350	14	31	7394	1007
East San'in district (n=22)																																
Average	78.02	0.21	8.45	1.69	0.03	0.70	6.42	1.56	2.88	0.03	50.27	41	39	49	13	13	22	4	8	29	26	353	16	3	60	3	13	792	93	6	19	2714
Minimum	41.89	0.07	5.30	0.43	0.01	0.14	0.33	0.99	1.87	0.01	39.65	6	3	6	3	9	3	1	1	2	3	66	12	1	39	1	1	338	16	2	2	1132
Maximum	88.19	0.69	11.86	3.89	0.08	2.22	43.35	2.50	4.78	0.10	55.29	55	60	72	27	18	68	10	21	139	89	1315	26	5	91	5	46	2576	208	10	31	6414
Tango peninsula (n=14)																																
Average	81.02	0.25	9.92	1.61	0.03	0.55	1.93	1.97	2.69	0.02	54.24	53	54	62	8	13	27	6	18	59	47	174	16	4	68	3	6	655	120	8	29	4023
Minimum	73.16	0.03	7.60	0.36	0.01	0.17	0.64	1.11	1.21	0.01	47.60	35	30	40	2	11	7	1	0	8	1	87	13	2	41	1	1	3	17	2	13	472
Maximum	86.61	1.46	12.44	5.35	0.12	1.48	7.20	2.89	3.79	0.04	62.40	62	66	71	20	15	60	13	52	227	193	456	19	9	127	6	15	1019	281	11	37	6891
Wakasa bay (n=7)																																
Average	84.83	0.17	7.95	1.38	0.03	0.32	0.89	1.24	3.15	0.03	54.97	54	58	71	8	16	32	5	11	35	29	81	25	5	70	6	5	663	95	7	28	2685
Minimum	80.75	0.02	5.55	0.25	0.01	0.04	0.12	0.63	1.65	0.00	50.60	42	39	50	4	12	5	1	7	26	2	18	18	3	41	4	3	365	1	3	24	1297
Maximum	90.31	0.43	10.27	3.20	0.06	0.88	2.99	1.61	5.02	0.09	60.70	61	65	82	11	19	50	14	20	44	59	185	35	8	96	8	7	925	145	12	33	4988
Noto peninsula (n=30)																																
Average	79.00	0.31	11.39	2.64	0.05	0.71	1.27	2.08	2.48	0.06	1.65	58	61	67	18	14	40	5	2	18	55	230	18	6	114	8	5	694	107	8	24	4038
Minimum	75.44	0.20	8.13	1.79	0.03	0.37	0.57	1.38	1.66	0.03	1.02	54	55	60	9	11	26	1	0	3	24	162	15	5	100	6	1	413	13	2	14	39
Maximum	83.43	0.66	13.02	5.27	0.11	1.85	1.83	2.51	3.05	0.10	2.23	60	65	72	28	16	56	10	9	45	114	282	22	8	161	9	9	1083	275	12	33	6730
Local river (n= 15) and marine sediment (n= 15) data (AIST 2013 a, b)																																
River sediment	74.72	0.61	11.70	4.83	0.12	1.59	1.79	2.42	2.09	0.13	.	56	58	63	20	50	172	43	17	43	89	204	14	8	52	7	9	.	.	.	.	.
Marine sediment	73.72	0.29	8.40	3.17	0.06	1.99	8.07	2.43	1.78	0.09	.	29	26	31	17	22	72	11	12	27	43	496	10	4	30	5	6	.	.	.	.	.
Average Upper crust of the Japanese archipelago, according to (Togashi et al. 2000), and average Upper Continental Crust (UCC) (Rudnick & Gao, 2005).																																
JUC	67.53	0.62	14.67	5.39	0.11	2.53	3.90	2.72	2.42	0.12	.	51	52	57	7	17	74	25	38	84	110	225	26	9	135	8	16	.	.	.	.	.
UCC	66.62	0.64	15.40	5.04	0.10	2.48	3.59	3.27	2.80	0.15	.	51	52	57	5	17	67	28	47	92	97	320	21	12	193	10	10	.	.	.	.	.

3. 2. UCJA and UCC – Normalized compositions

As has been seen, there were many differences between the geochemical compositions of the coastal sand samples taken from the six coastal regions. These variations in composition are the result of a number of factors, including differential weathering, differences in the relative proportions of the quartz, feldspar and biogenic content of the sands in the locations and differences in the origins of the constituent substances. To compare the compositions of the beach sand in the individual sites, average values were normalized against the average UCJA, according to (Togashi *et al.* 2000), and against the average UCC (Rudnick & Gao, 2005). Both the UCJA-normalized and the UCC-normalized patterns for five of the six study regions' beach sands compositions had very similar shapes. These regions were: Northern Kyushu, Shimane, Tottori, Tango Peninsula, and Noto Peninsula. Normalization revealed that, with the exception of SiO_2, elements were depleted relative both to UCJA and UCC, as shown in Figure 9. The depletion was particularly marked for the ferromagnesian elements (MgO, Fe_2O_3*, TiO_2, Ni, Cr, V) which are typically strongly depleted in felsic volcanic rocks such as granites and for mobile elements CaO, Na_2O and Sr, all of which are liable to loss during weathering (Nesbitt & Young, 1984). In contrast, the UCJA-normalized as well the UCC-normalized diagrams for the Yamaguchi beach sand samples, for most of major and trace elements were less than 1 (Figure 9), exceptions being CaO, Sr, and Th.

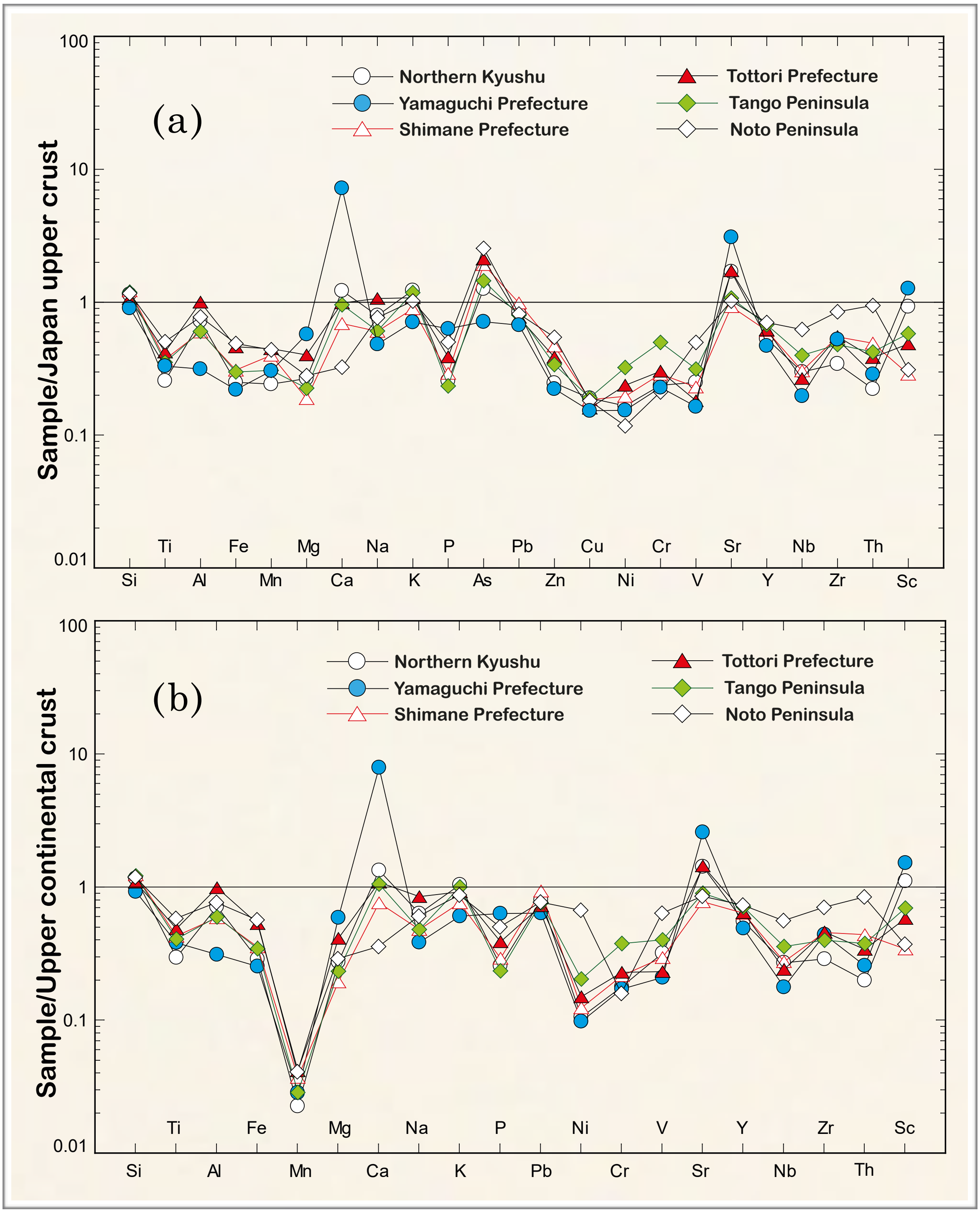

Figure 9. Average major and trace elements diagrams of beach sands collected along the coasts of South West Japan, on the coastline of Northern Kyushu, Yamaguchi, Shimane, Tottori, Tango Peninsula, and Noto Peninsula, normalised to average Upper Crust of the Japanese Archipelago (UCJA), according to (Togashi *et al*. 2000), and average Upper Continental Crust (UCC) (Rudnick & Gao, 2005).

3. 3. Inter-Element Relationship

Figure 10 illustrates Harker variation diagrams for selected elements in the beach sand samples, in each case the major element content being plotted against the SiO_2 content. The increase of SiO_2 reflects a greater geochemical maturity. All of the major elements plotted show general trends towards decreased abundance with increased silica content. The significant SiO_2, Al_2O_3 and Na_2O contents of beach sands form northern Kyushu, silica rich sands form Yamaguchi, Shimane, Tottori, Noto Peninsula and Tango Peninsula, indicate that quartz and feldspar are the main constituents. The overall depletion of CaO and MgO suggests that the carbonate content of the beach sand sediments is generally low, in the majority of samples. Silicate or siliciclastic sands – those sands comprising grains originating from clasts, or fragments of silicate rocks – generally consist of feldspars, micas, quartz and other silicate substances. While the majority of the components are quartz and plagioclase feldspar, as indicated by the high SiO_2 content and significant CaO, Na_2O and Al_2O_3 contents, relatively high K_2O contents suggested significant K-feldspar and K-bearing micas contents were also present. CaO showed a well-defined decrease with increasing SiO_2, except for higher values in a small group of Yamaguchi beach sands with lower SiO_2 contents. These samples also had higher LOI values, and hence were likely to contain a biogenic $CaCO_3$ component, such as shell material.

To better understand the major element composition, the samples were broadly subdivided as follows: silica, aluminium, and calcium (Figures 11 and 12). The geochemical compositions of these three subgroups (represented by SiO_2, Al_2O_3, and CaO) for the six study areas' coastlines were displayed on a modified map of the Geological Survey of Japan (GSJ) and National Institute of Advanced Industrial Science and Technology (AIST). As expected, SiO_2 contents were greater in samples from the silica-rich sands from the Yamaguchi and Shimane pocket beaches due to their abundance of quartz; these account over 80% of silica. The maximum SiO_2 concentration was observed in the silica-rich sands from Yamaguchi, Shimane, Kotogahama and Kotobikihama, which may be due to the input of sediments supplied through major river systems from the Chūgoku Mountains to the Japan seacoast (the Takasu, Gono Hii, Hino, Tenjin and Sendai rivers). The Al_2O_3 contents varied from approximately 5wt% to over 10wt% in some samples; this variation can be attributed to the contribution of fine grains and feldspars. The maximum Al_2O_3 contents were seen in the northern Kyushu and Tottori beach sand. Beach sand samples from Tottori typically consisted of silicate minerals with little quartz but a significant quantity of feldspar. Furthermore, the presence of considerable CaO in the Yamaguchi beach sand samples indicated a significant biogenic $CaCO_3$ component; in this case, the likely constituents were Foraminifera, shells or animal skeletons, which – like sea urchin and ostracod – primarily comprise the compound (Figure 13). Biogenic carbonate sands found in the coastal zone and shallow water consist of porous or hollow particles with a rough texture.

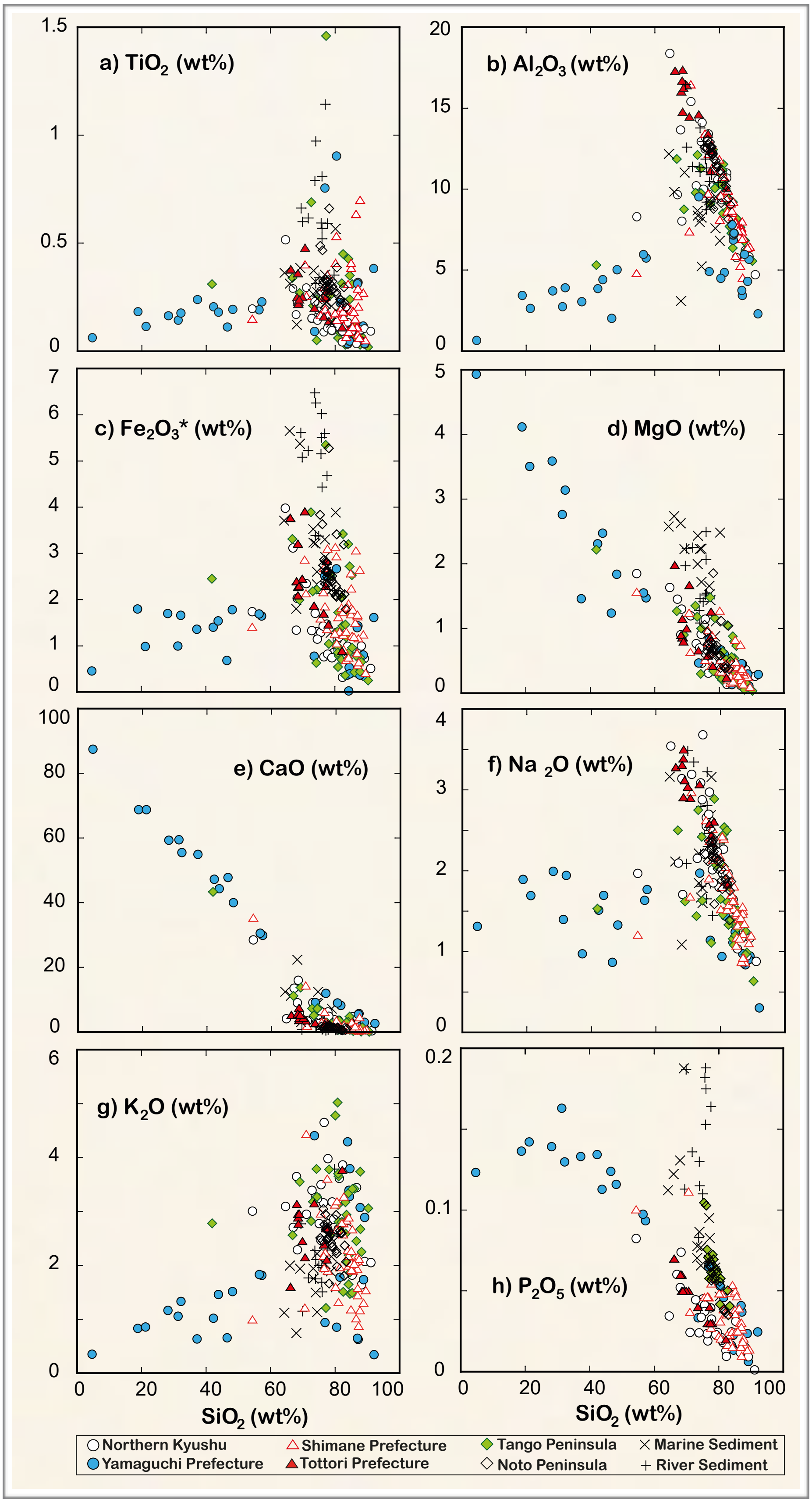

Figure 10. Harker diagrams for selected major elements of beach sands collected along the coasts of South West Japan, on the coastline of Northern Kyushu, Yamaguchi, Shimane, Tottori, Tango Peninsula, and Noto Peninsula.

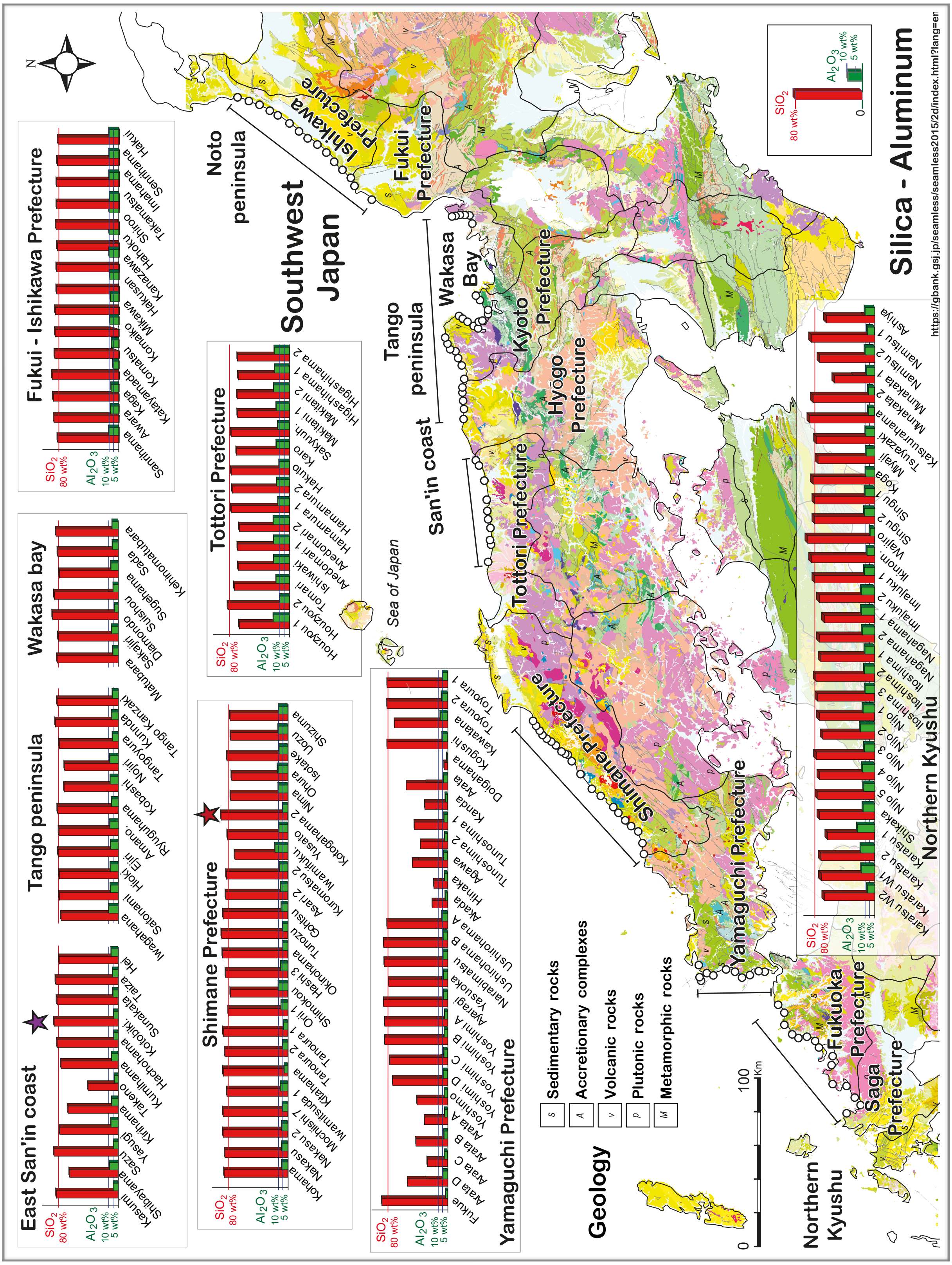

Figure 11. Geological map of South West Japan, showing the geochemical composition of SiO_2 and Al_2O_3 elements, and location of beaches sampled along the coastline of Northern Kyushu, Yamaguchi, Shimane, Tottori, Tango Peninsula, Wakasa Bay, and Noto Peninsula. Modified from the Geological Survey of Japan (GSJ) and National Institute of Advanced Industrial Science and Technology (AIST), 2016.

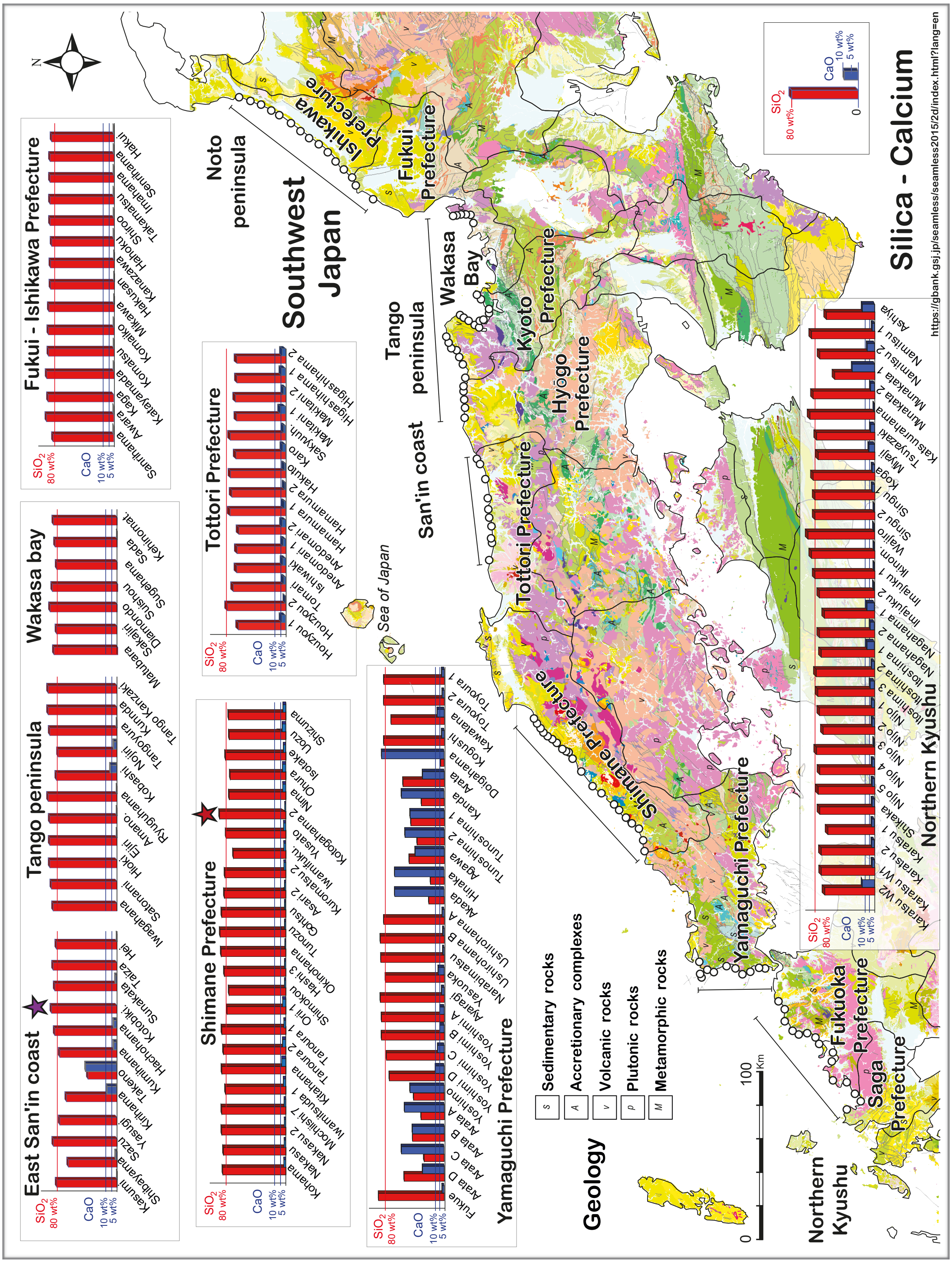

Figure 12. Geological map of South West Japan, showing the geochemical composition of SiO_2 and CaO elements, and location of beaches sampled along the coastline of Northern Kyushu, Yamaguchi, Shimane, Tottori, Tango Peninsula, Wakasa Bay, and Noto Peninsula. Modified from the Geological Survey of Japan (GSJ) and National Institute of Advanced Industrial Science and Technology (AIST), 2016.

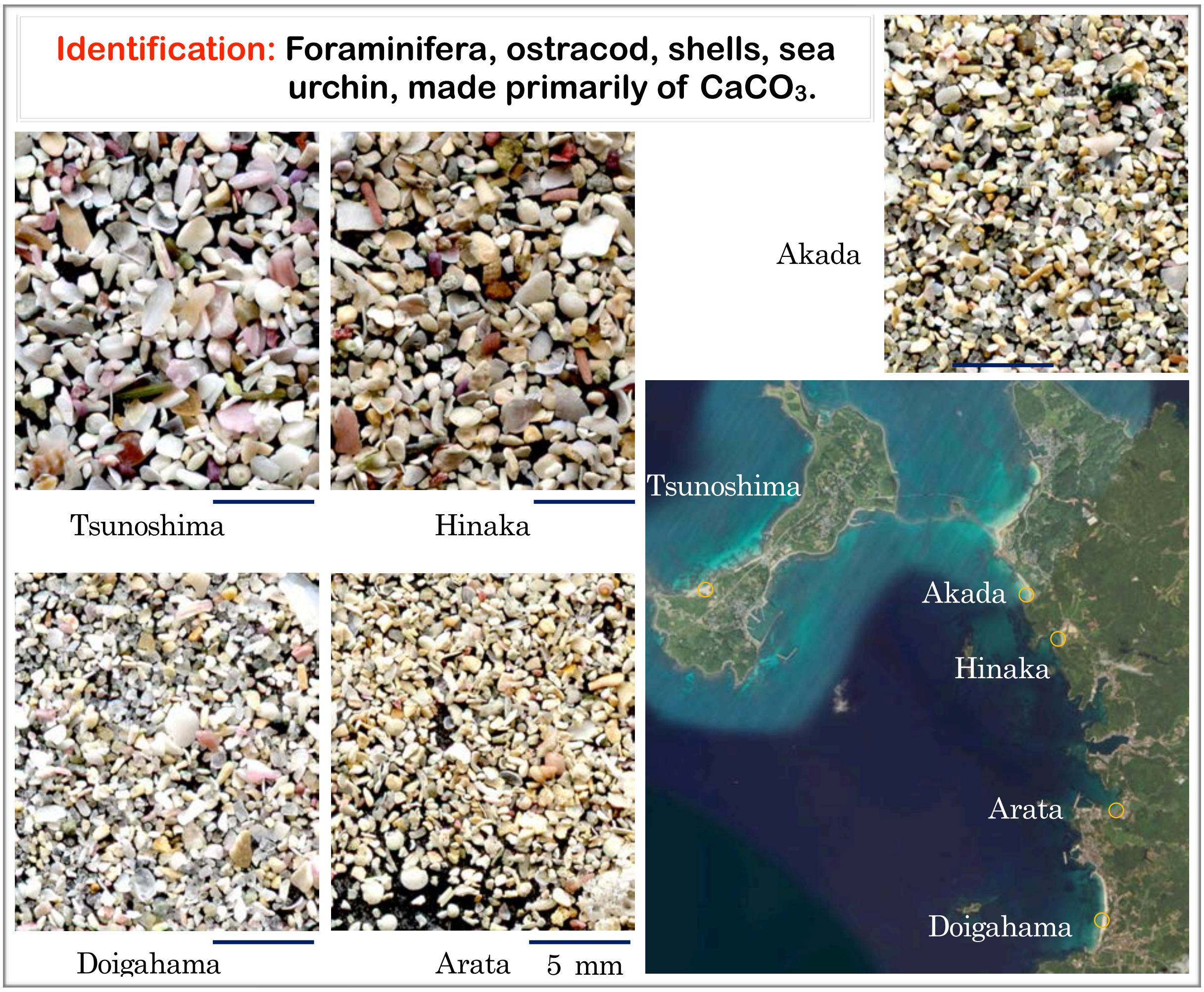

Figure 13. Selected microscopic photographs biogenic carbonate sands from the Tsunoshima, Akada, Hinaka, Arata, and Doigahama Beaches, Yamaguchi Prefecture, South West Japan. The identified species are Foraminifera, ostracod, shells, and sea urchin, made primarily of $CaCO_3$.

The variations of ecosystem and geography of marine condition in Hinaka and Arata beach are shown in figure 14. Typical small-scale pocket beach, and inlet of beach shape characteristic. Rocky points of both sides of the Hinaka beach, *Zostera marina* and other sea weed are exposed on the shore of the Hinaka beach suggesting the existence of under-water sea plant field. On the left side of the Hinaka beach, *Zostera marina* are found on the shore (Figures 15a, 15b and 15c. Doigahama beach is more strait than Arata beach (Figure 16), but sea plant habit is suggestive. Under-water structure may make a variety of geography for ecosystem.

Figure 14. The variations of ecosystem and geography of marina condition in Hinaka and Arata beaches, Yamaguchi Prefecture, South West Japan. Typical small-scale pocket beach, and inlet of beach shape characteristic.

Figure 15a. Rocky points of both sides of the Hinaka beach, *Zostera marina* and other sea weed are exposed on the shore of the Hinaka beach.

Figure 15b. Rocky points of both sides of the Hinaka beach, *Zostera marina* and other sea weed are exposed on the shore of the Hinaka beach.

Figure 15c. Rocky points of both sides of the Hinaka beach, *Zostera marina* and other sea weed are exposed on the shore of the Hinaka beach. On the left side of the Hinaka beach, *Zostera marina* are found on the shore.

Figure 16. The variations of ecosystem and geography of marine condition in Doigahama beach, Yamaguchi Prefecture, South West Japan.

Chapter Four

4. DISCUSSION

4. 1. Evaluation of biogenic productivity

To evaluate the biogenic productivity in the Yamaguchi coast, the climatic conditions and water quality were observed.

Temperature is one of the most important parameters controlling the environment. The Tsushima Warm Current (TWC) is the main surface current flowing into the Japan Sea (JS) through the Tsushima Strait and emerging through the northern Tsugaru Strait and Soya Strait. As a branch of the Kuroshio Current, the TWC is characterized by high temperature. Figure 17 shows the mean surface water mass temperature at 50 m for two periods – 11^{th} August to 20^{th} August, 2016, and 11^{th} May to 20^{th} May, 2016 May, early summer Japan Meteorological Agency (2016). The current transports a large quantity of heat and warm-water marine organisms into the Sea of Japan; it is also a major source of nutrients in the JS, contributing 55% of the phosphorous and 67% of the nitrogen in the upper 200 m of the JS (Yanagi, 2002). Primary production in the JS is relatively high among marginal seas (Yamada *et al.*, 2005). This suggests that the TWC through Tsushima strait, may be responsible for high biogenic productivity in Northern Kyushu and Yamaguchi coast, which ultimately influences contents of beach sand geochemistry. The occurrence of tidal flats is another factor in higher carbonate productivity. At Arata beach, Yamaguchi, the tidal difference exceeds 1 m (Figure 18).

Water quality types for beaches are assessed by Prefectural Government of Fukuoka in northern Kyushu and Yamaguchi for the Ministry of Environment of Japan (2016). Beach classification is based on two factors, the chemical oxygen demand (COD) and the faecal coliform content. Classification is into one of three categories – in decreasing order of quality, Type AA and Type A beaches are considered to be 'good' quality, while Type B beaches are considered to be of 'satisfactory quality. The specifications for each of the factors, as shown in Figure 19, are as follows: Type AA – COD < 2 g/l, faecal content not detected; Type A – COD < 2 mg/l, faecal content < 100 / 100 ml; Type B – COD < 5 mg/l, faecal content < 400 / 100 ml. The water quality, as designated by the Type, could affect the biogenic $CaCO_3$ productivity. The Yamaguchi beaches are classified as Type AA and A, which the northern Kyushu beaches are classified as Type B.

4. 2. Geochemical Maturity

Pettijohn *et al*. (1972) first discussed the concept of geochemical maturity in sediment, believing that maturity should be assessed using the QFL diagram, but there are more than 50 sand and sandstone classification systems. It is necessary to use laboratory analysis is required with point counting (usually considering 500 points) and petrographic thin sections; carbonates are excluded. Therefore, the QFL methods, the beach shape and grain size are not relevant in the context of this study.

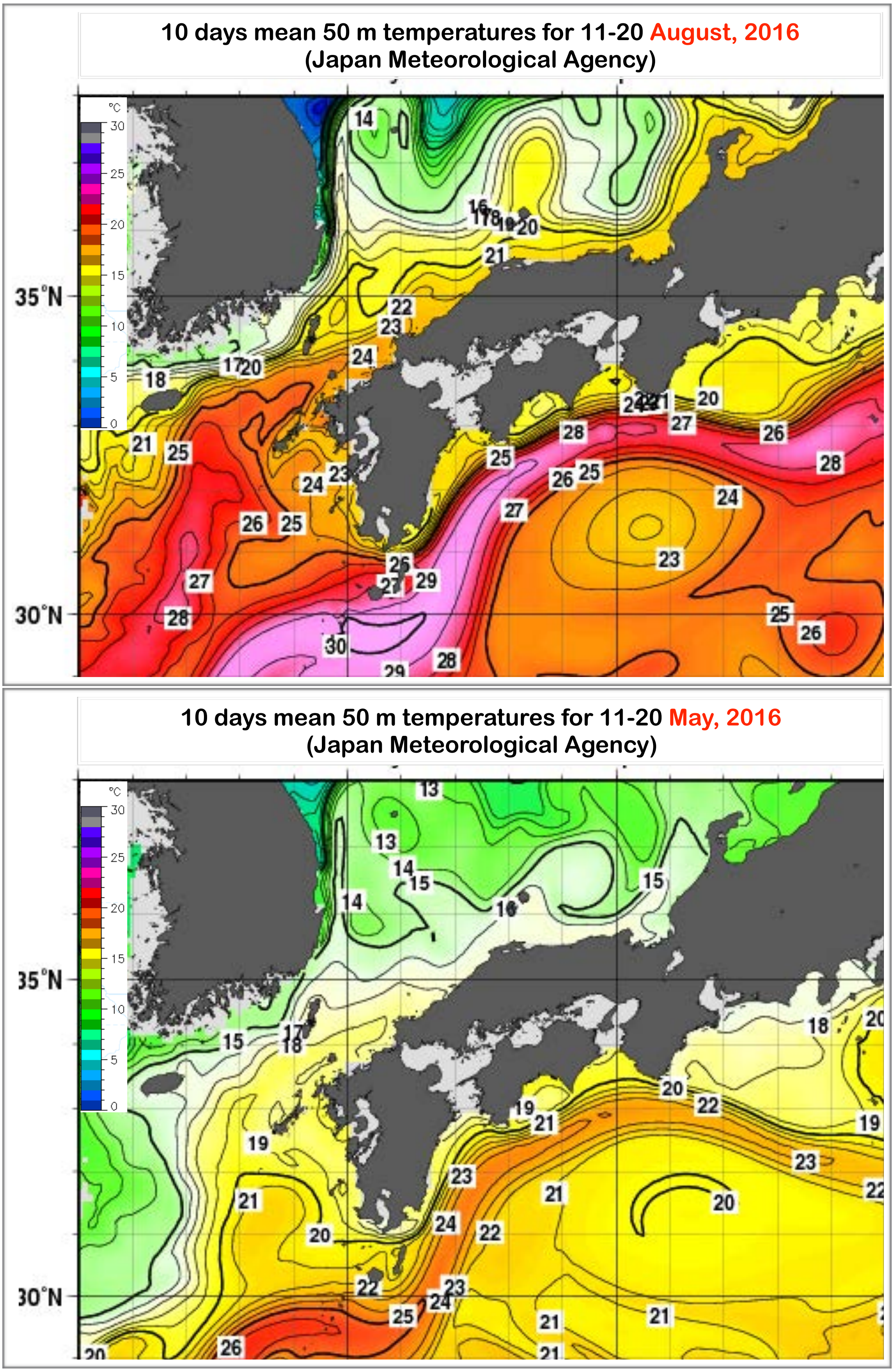

Figure 17. Surface water mass temperature; mean 50 m in western Japan for 11th-20th August 2016. In addition, for 11th-20th May, 2016 (Japan Meteorological Agency).

Geochemical maturity is a compositional state of a clastic sedimentary body in which quartz is dominant, while less-resistant particles, such as feldspars, detrital carbonates or lithic fragments, are either absent or present in much smaller quantities (Blatt *et al*., 1972; Pettijohn *et al*., 1972; Daniel, 2004). Geochemically mature sandstones are classified as quartz arenites or orthoquartzites if they comprise at least 95% quartz. Sedimentary petrologists and sedimentologists (Schwab, 1975; Potter, 1978; Suttner *et al*., 1981; Franzinelli & Potter, 1983; Suttner & Dutta, 1986; Johnsson *et al*., 1988; Potter 1994; Nesbitt & Young, 1996; Nesbitt *et al*., 1996, 1997; Potter *et al*., 2001; Daniel, 2004) have extensively used geochemical maturity as a key indicator of sediment provenance, transport history, and weathering history.

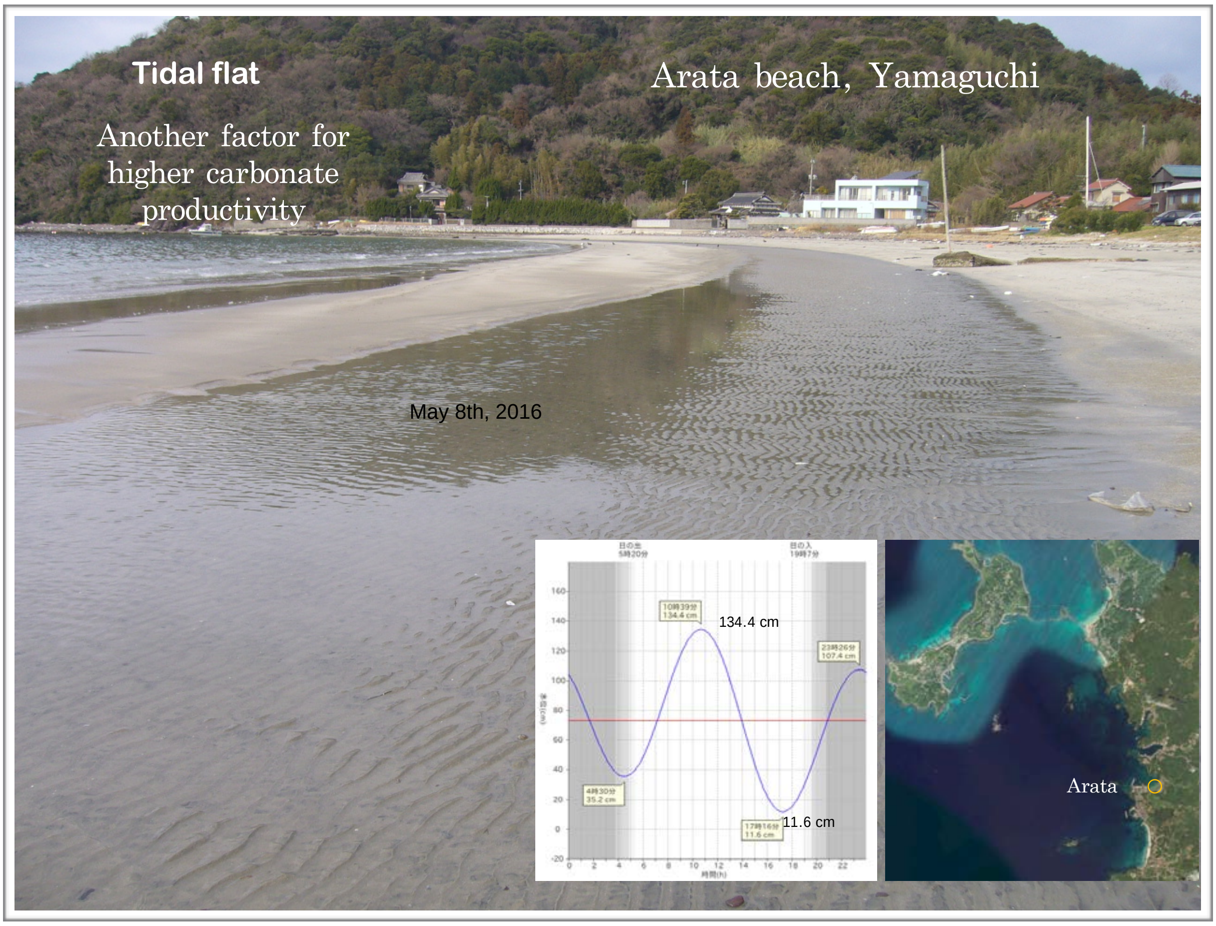

Figure 18. Tidal-flat deposits on the foreshore of Arata beach, Yamaguchi, South West Japan.

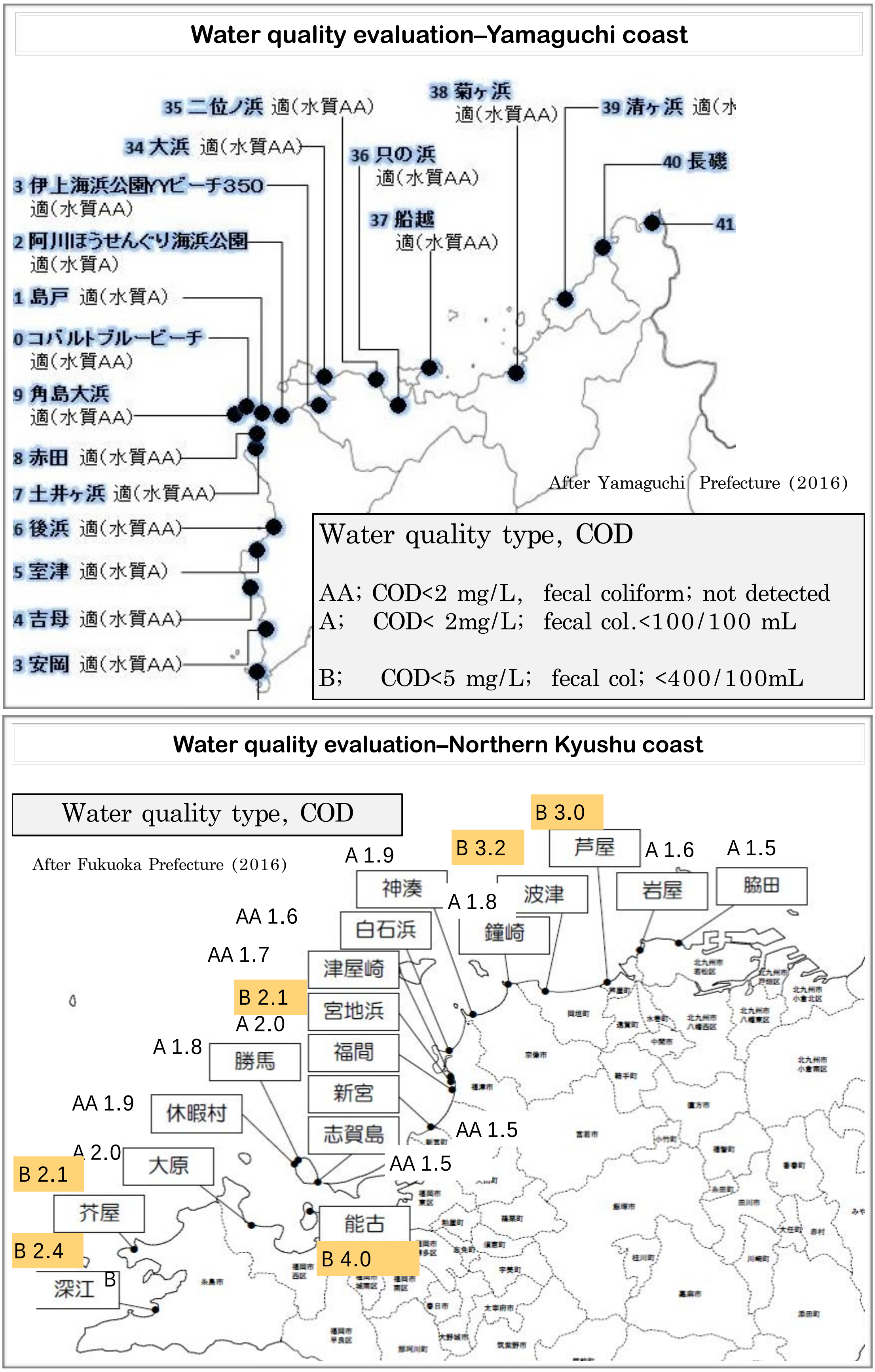

Figure 19. Classification based on the chemical oxygen demand (COD) and faecal coliform criteria of levels of water quality in Yamaguchi in contrast to level water quality in northern Kyushu, South West Japan.

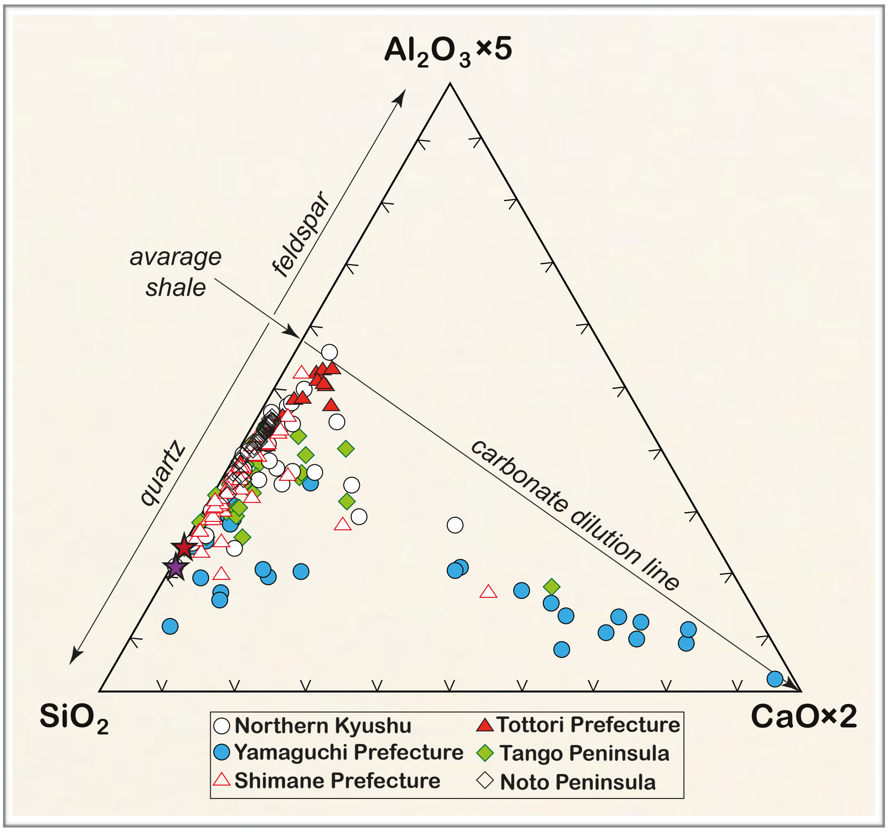

Figure 20. Ternary diagram of relative proportions of $Al_2O_3 \times 5$, SiO_2, and $CaO \times 2$ (Brumsack, 1989), of beach sand samples from Northern Kyushu, Yamaguchi, Shimane, Tottori, Tango Peninsula, Wakasa Bay, and Noto Peninsula, southwest Japan. An arbitrary multiplier of 5 and 2 are used respectively for Al_2O_3 and CaO in order to better distribute the data points within the graph.

In a very simplistic way, the investigated beach sand from the coasts of Southwest Japan, on the coastline of Northern Kyushu, Yamaguchi, Shimane, Tottori, the Tango Peninsula and the Noto Peninsula comprise variable mixtures of terrigenous detritus (represented by Al_2O_3 and SiO_2) and biogenous material (represented by CaO). To compare the relative proportions of the major components, the relative proportions of CaO (mostly calcium carbonate), SiO_2 (quartz and alumosilicates), and Al_2O_3 (alumosilicates, feldspar) were plotted in a triangle diagram (Figure 20) (Brumsack, 1989). The diagram showed that the sediments from Yamaguchi trend from the CaO to the SiO_2 poles showing a distinct distribution pattern along the carbonate dilution line, indicating that they represented a simple background sedimentation diluted by biogenic carbonates. By contrast, most northern Kyushu beach sand and the sands rich in silica from Kotogahama, Kotobikihama, Shimane, Yamaguchi and the Tango Peninsula plotted on a SiO_2-Al_2O_3 mixing line. This was consistent with these samples having a broadly lower content of carbonate and more variable distribution. The shift towards the SiO_2 edges indicated excess silica contents; this reflected an abundance of coarse-grained particles and was particularly high in those samples exhibiting a low carbonate content. It is probable that tides and rivers deposited these sands. The majority of beach sand from Noto Peninsula and Tottori plotted on a straight mixing line between quartz and feldspars components richer in Al_2O_3 and Average Shale. This suggested that more intensely weathered clays (possibly with a higher kaolinite proportion) were characteristic for these sediments.

4. 3. Geochemical classification

Maturity is reflected best in quartz, rock fragments, feldspars and grain size. As the percentage of quartz increases, the mineralogical maturity also increases. The SiO_2/Al_2O_3 ratios of clastic rocks are sensitive to sediment recycling and weathering processes and can be used as indicators of sediment maturity. With increasing sediment maturity, quartz survives preferentially to feldspars, mafic minerals and lithics (Roser & Korsch, 1986; Roser *et al.*, 1996). Average SiO_2/Al_2O_3 ratios in unaltered igneous rocks ranging from approximately 3.0 (that is, basic rocks) to approximately 5.0 (acidic rocks). Values of the SiO_2/Al_2O_3 ratio greater than 5.0 in sandstones are an indication of progressive maturity (Roser *et* *al.*, 1996). SiO_2/Al_2O_3 and Na_2O/K_2O ratios may vary depending on the maturity of the sediments. Low values of SiO_2/Al_2O_3 ratios and high values of Na_2O/K_2O indicate mineralogically immature sediments. The SiO_2/Al_2O_3 ratio was higher in the silica rich sands from Yamaguchi, Shimane and the Noto Peninsula than in northern Kyushu, the Tango Peninsula and Tottori sands (Figure 21a). Similarly, the Na_2O/K_2O ratio followed a similar inverse trend; it was high in Tottori, Tango Peninsula and northern Kyushu sands and lower in the Noto Peninsula, Shimane and the silica-rich sands from Yamaguchi (Figure 21b). The lower Na_2O/K_2O ratios in the studied sands were attributed to the enrichment of K-feldspar compared to plagioclase.

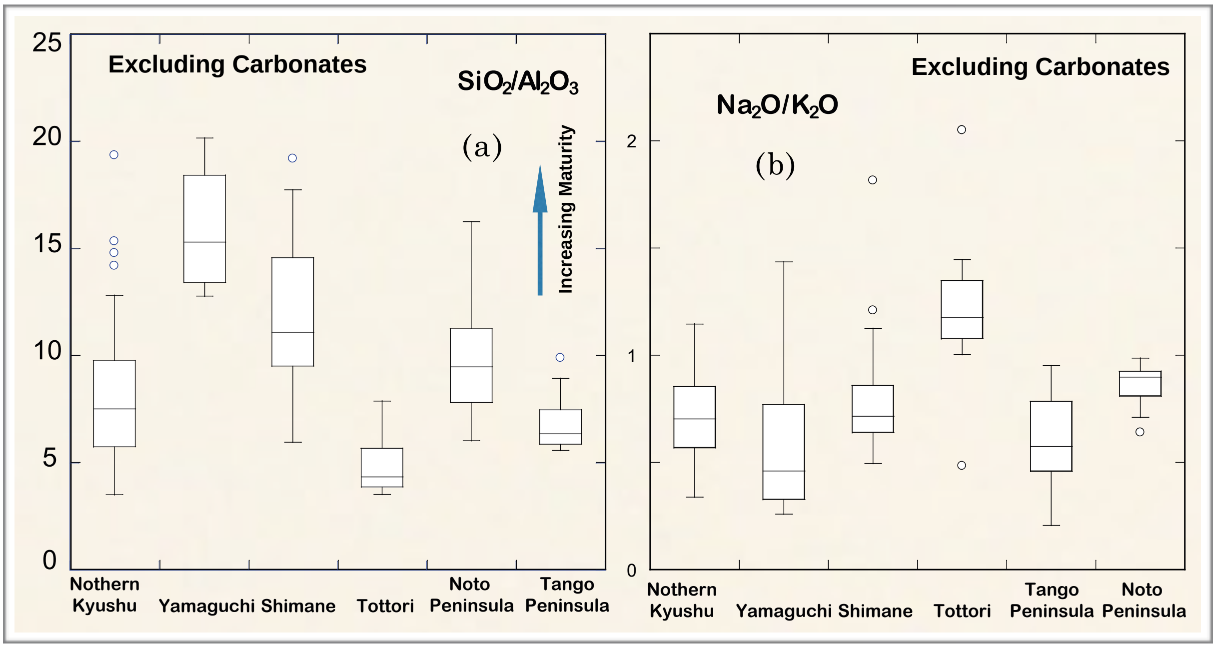

Figure 21. Box plots showing the SiO_2/Al_2O_3 and Na_2O/K_2O ratios in the investigated beach sands from the coasts of South West Japan, on the coastline of Northern Kyushu, Yamaguchi, Shimane, Tottori, Tango Peninsula, and Noto Peninsula.

The most used classification parameters are the SiO_2/Al_2O_3 ratio, primarily reflecting the abundance of quartz, clay and feldspar, the Na_2O/K_2O ratio, which defines an index of chemical maturity and the $Fe_2O_3^*/K_2O$ ratio that defines an index of mineral stability. In Figure 25, the log ratios of Na_2O/K_2O are plotted against the log ratios of SiO_2/Al_2O_3, and the log ratios of $Fe_2O_3^*/K_2O$ are plotted against the log ratios of SiO_2/Al_2O_3 (Pettijohn *et al.*, 1972; Herron, 1988).

Figures 19a and 19b show the geochemical classification diagrams of Pettijohn (1972) and Herron (1988) for the beach sand of the same coastal regions as were investigated in this study. As can be seen, they demonstrated the same petrographic results. While the sands from the Noto Peninsula can be seen in the Na_2O/K_2O vs. SiO_2/Al_2O_3 diagram of Figure 22a to have plotted in the arkose field, most of those in the Tango Peninsula, Shimane, northern Kyushu and Yamaguchi plotted in the arkose and subarkose fields. Tottori beach sands are classified as litharenites and arkoses. Figure 22b shows that the investigated beach sand from the coasts of all six investigated areas of Southwest Japan were bracketed by arkose and subarkose, with a diminishing trend towards sublitharenite, reflecting the increasing abundances of quartz and feldspar. The diagram may be used to ascertain not only the dominant mineral components, as previously considered, but also to identify trends in soil maturity and aging. That is, beach sands rich in feldspars are usually classified as young, while those in which quartz is dominant are considered more mature, the higher age indicating greater transport. By observation of sands holder of the Hashi beach, Shimane Prefecture, beach sands composed primarily of well-sorted quartz, a durable mineral that is hard and does not weather easily in Figure 23. In addition, grain size distribution of beach sand collected at the shorelines of selected beaches on the western San’ in coast is shown in Figure 24.

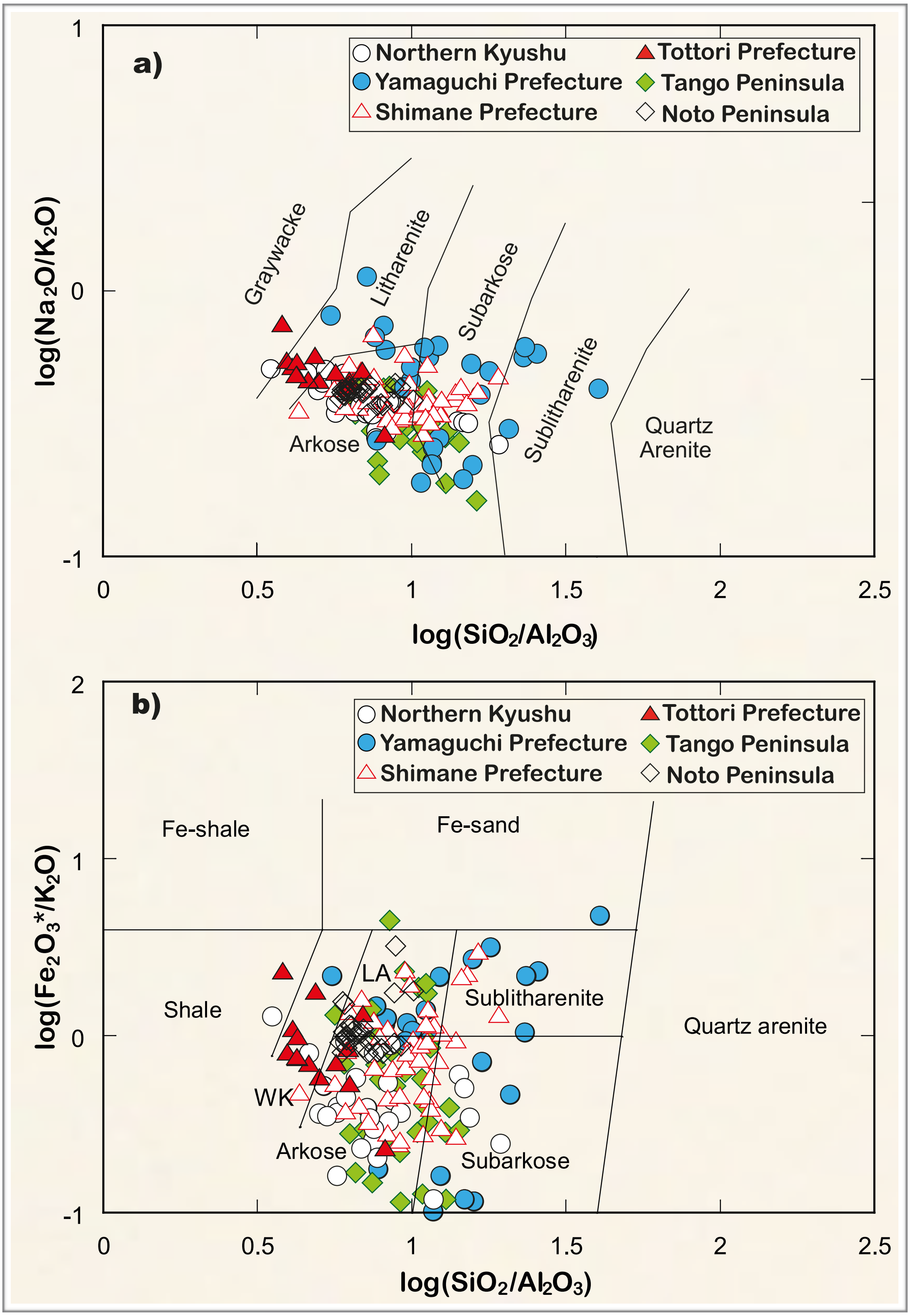

Figure 22. Geochemical classification schemes of beach sands along the coastline of Northern Kyushu, Yamaguchi, Shimane, Tottori, Tango Peninsula, Wakasa bay, and Noto Peninsula. Based on: **a)** log(SiO_2/Al_2O_3) versus log(Na_2O/K_2O) diagram of Pettijohn *et al*. (1972), and **b)** the log (SiO_2/Al_2O_3) versus log (Fe_2O_3*/K_2O) diagram of Herron (1988). LA. Litharenite and WK. Wacke.

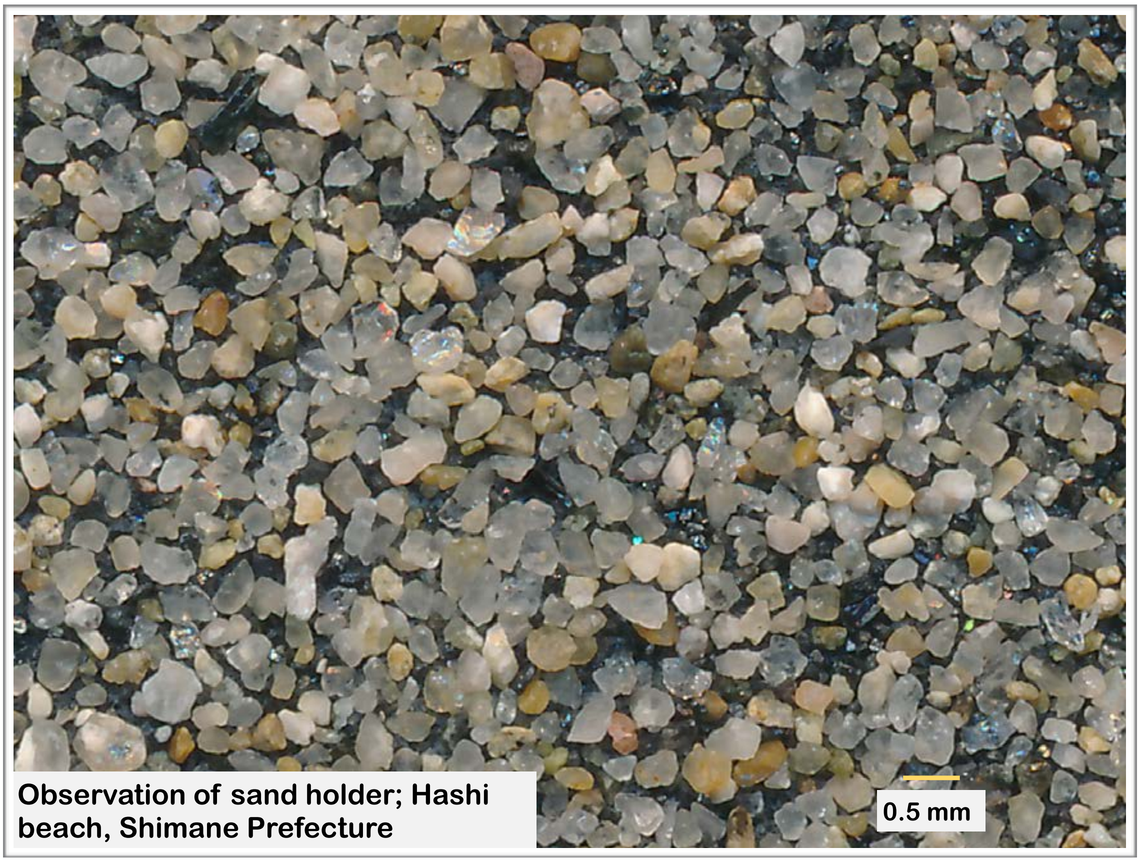

Figure 23. Observation of sands holder of the Hashi beach, Shimane Prefecture. Beach sands composed primarily of well-sorted quartz, a durable mineral that is hard and does not weather easily.

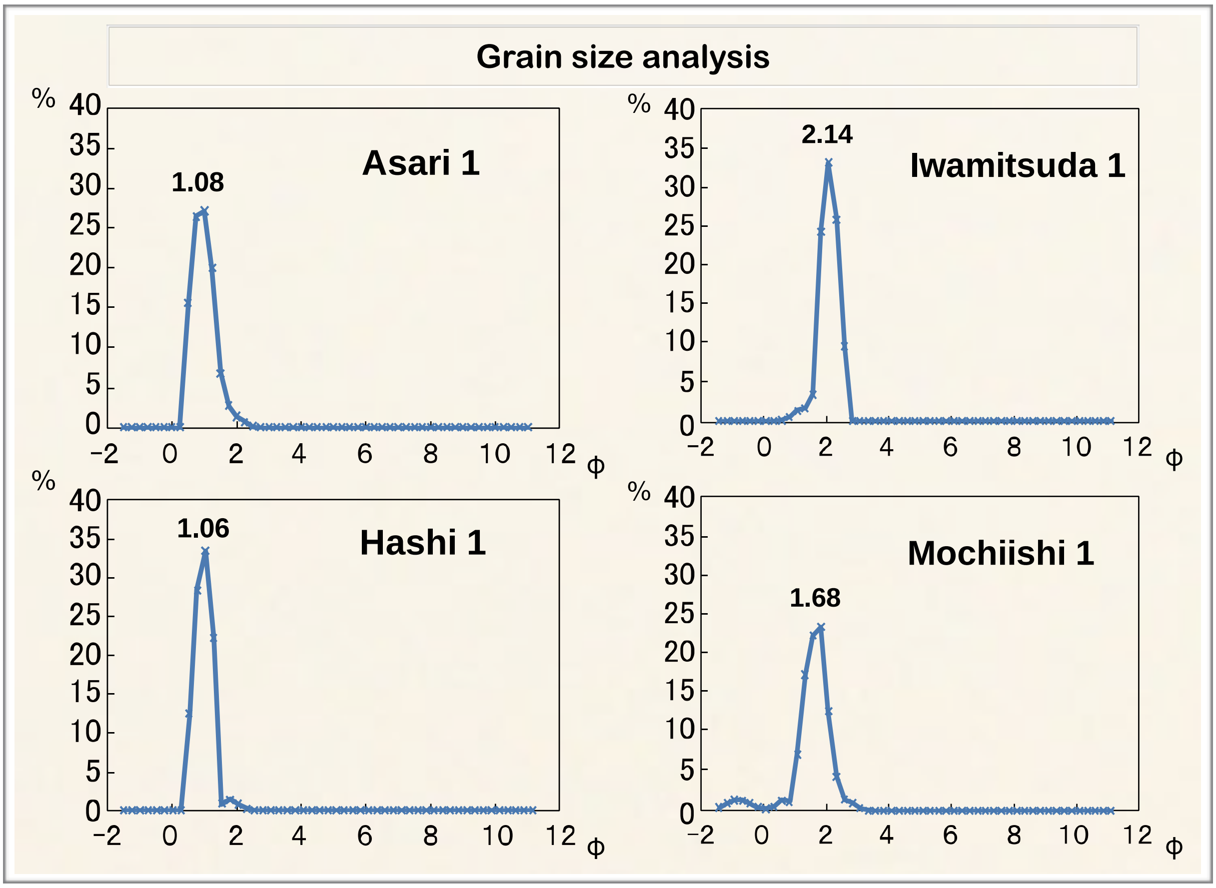

Figure 24. Grain size distributions of beach sands collected at the shorelines of selected beaches on the western San' in coast. Ishiga *et al*. (2010).

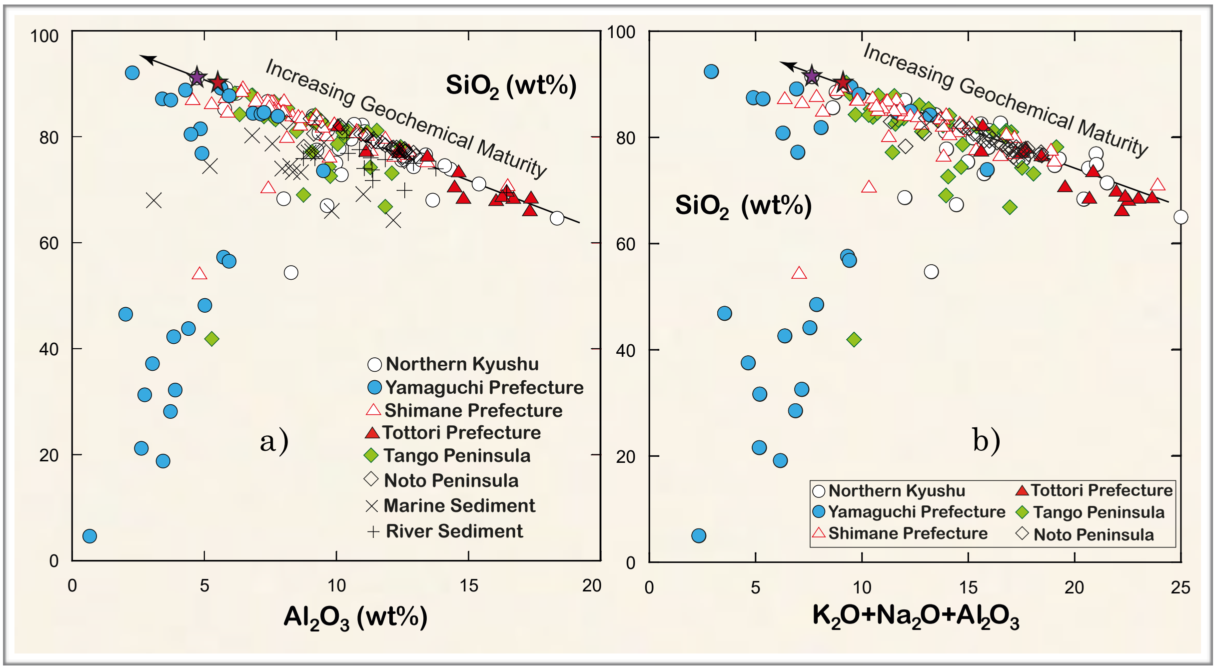

Figure 25. a) Bivariate plot of SiO_2 against Al_2O_3, and **b)** plot of SiO_2 (reflective of quartz content) versus $K_2O+Na_2O+Al_2O_3$ (reflective of feldspar content) of beach sand samples from Northern Kyushu, Yamaguchi, Shimane, Tottori, Tango Peninsula, Wakasa bay, and Noto Peninsula, South West Japan.

A bivariate plot of SiO_2 against Al_2O_3 is shown in Figure 25a; Figure 25b is a plot of SiO_2 (reflective of quartz content) against $Na_2O+K_2O+Al_2O_3$ (reflective of feldspar content). The latter plot is representative of quartz content against feldspar content and overall reflects chemical maturity as a function of climate, according to Suttner and Dutta (1986). The plotted samples revealed semi-arid to semi-humid climatic conditions in the area from various sources tending towards increasing chemical maturity. Beach sand samples from Shimane and quartz-rich sands from Yamaguchi showed high degrees of maturity, which probably indicate rich chemical weathering in the respective source areas. Overall, the investigated beach sands from the northern Kyushu, Tottori, Tango Peninsula and Noto Peninsula beaches showed variable degrees of chemical maturity, ranging from low to intermediate levels. The beach sands plotted in the semi-arid region may have experienced little or no chemical weathering and are far less mature than those plotted in the semi-humid area.

The composition of beach sand is highly variable according to the local rock sources and conditions. While the primary component of beach sand from silica-rich sands from Yamaguchi, Shimane, Kotogahama, Kotobikihama and the Tango Peninsula is quartz, or silica (SiO_2), the distributions of sand sediment along these beach areas are substantially regulated by the influence of sand the sediments derived from the Chūgoku Mountains. large quantity of sediment originates from the basin areas located upstream, as most of the river basins lie above granite, which is easily weathered (Somura *et al.*, 2012). Meanwhile, Tottori sands were largely composed of weathered feldspar particles. A number of influences on these sediments, including the fluvial systems and erosion of the older materials that underlie the inner shelf. Furthermore, it is likely that further erosion is the result of longshore currents and coastal mechanisms, including reworking of the beach and winnowing. Admitting that sediments from Tottori sand dunes are formed from sediments derived from the nearby Chugoku Mountains and transported by the Sendai River to the ocean. In contrast, the biogenic carbonate sands from Yamaguchi are primarily composed of shell fragments, which might be expected, given the influence of the warm Tsushima Strait in increasing biogenic productivity in the region.

4. 4. Weathering process

Wronkiewicz & Condie (1987) stated that climate and the rate of tectonic uplift determine the extent of chemical weathering. Reduced tectonic activity and a shift towards warmer, more humid conditions are correlated with an increase in chemical weathering (Jacobson *et al.*, 2003). Therefore, the weathering indices of sedimentary rocks can provide useful information regarding the tectonic activity and climatic conditions in the source area. Various researchers have proposed different weathering indices (Nesbitt & Young, 1982; Harnois, 1988) commonly used by many researchers across the globe. Chemical weathering strongly affects major element geochemistry of siliciclastic sediments (Nesbitt & Young, 1982; Johnsson *et al.*, 1988; McLennan, 1983).

The Chemical Index of Alteration (CIA), a quantitative measure proposed by Nesbitt and Young (1982, 1984), is a potentially useful means of evaluating the degree of chemical weathering and was used to evaluate the extent of weathering in this study. This index measures the extent to which feldspar has been converted to aluminous weathering products. CIA ratios in feldspar and fresh source rocks are typically ~50, whereas those in residual weathering products such as kaolinite and gibbsite can reach 100. This index can be calculated using molecular proportions, from the formula: CIA = 〔Al_2O_3 / (Al_2O_3+CaO*+Na_2O+K_2O)〕 × 100. CaO* was corrected using the subsequent methodology proposed by McLennan *et al.*, (1993), in which CaO values are accepted only if CaO<Na_2O; when CaO>Na_2O, it is assumed that the concentration of CaO equals that of Na_2O. High CIA values reflect the removal of mobile or unstable cations (Ca, Na, K) relative to highly immobile or stable residual constituents (Al, Ti) during weathering (Nesbitt & Young, 1982). Conversely, low CIA values indicate the near absence of chemical alteration and consequently may reflect cold and/or arid conditions (Nesbitt & Young, 1982, 1989). As defined by Nesbitt and Young (1982), a CIA of between 50 and 60 represents incipient weathering, a value between 60 and 80 represents intermediate weathering, while a value greater than 80 represents extreme weathering.

The CIA values are shown in Figure 26. As can be seen, the average CIA values were: Tottori beach sand 51 (range 41 – 55), the Tango Peninsula 53 (range 35 – 62) and the Noto Peninsula 58 (range 54 – 60). The slightly elevated CIA of beach sands from Shimane, Tottori, Tango Peninsula, and Noto Peninsula relative to average granodiorite reflected very weak alterations due to chemical weathering, suggesting that progressive weathering had occurred.

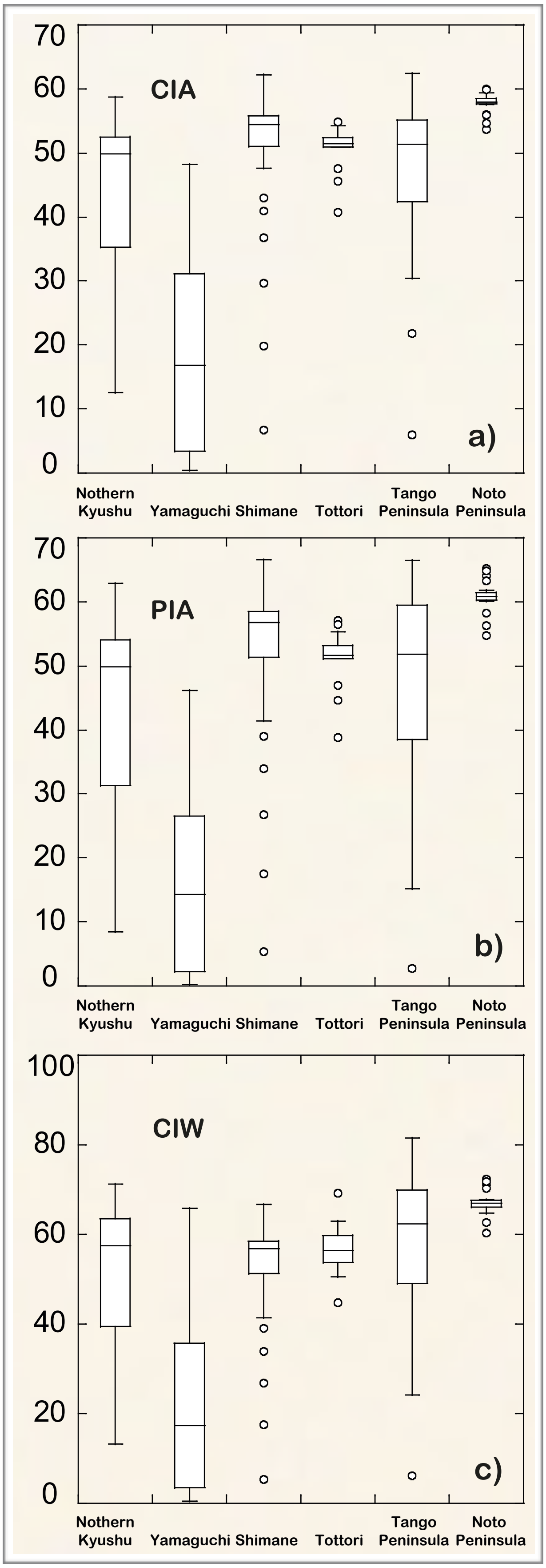

Figure 26. Box-plot diagrams of geochemical weathering indices. a) Chemical Index of Alteration (CIA), b) Plagioclase Index of Alteration (PIA), c) and Chemical Index of Weathering (CIW).

The overall range of the CIA values was similar to or slightly greater than the CIA values of the UCC. These CIA values indicate that the sediments were slightly weathered.

The degree of the chemical weathering can be estimated using the Plagioclase Index of Alteration (PIA) modified from the CIA equation to monitor plagioclase (Fedo *et al*., 1995). The plagioclase index of alteration is calculated according to the following equation in molecular proportions: PIA = $(Al_2O_3-K_2O)$ / $(Al_2O_3+CaO^*+Na_2O-K_2O)$ × 100. High PIA values (>84) indicate intense chemical weathering while lower values (~50) are characteristic of unweathered, or fresh, rock samples. Post-Archean Australian Shales (PAAS) have a PIA value of 79. The PIA values of beach sands from the northern Kyushu coast ranged from 44 to 63. The mean PIA value for the Tottori beach sand was 51 and for the Noto Peninsula was 58.

Weathering effects can also be evaluated using the Chemical Index of Weathering (CIW) in molecular proportions) identical to the CIA, from the formula: CIW = Al_2O_3 / $(Al_2O_3+CaO^*+Na_2O)$〕 × 100. This equation is more appropriate in understanding the extent of plagioclase alteration alone since K_2O is subtracted from Al_2O_3 in the numerator and denominator of the CIA equation. However, it should be noted that Fedo *et al*. (1995) argued that the CIW was, in fact, inappropriate as a means of quantifying the intensity of chemical weathering. His reasoning was that there was potential for misinterpretation of the resultant CIW values. For example, the CIW of 80 for unweathered potassic granite was similar to that of residual products of smectite, while the CIW of 100 for clay minerals (for example, gibbsite, illite and kaolinite) was similar to that of residual products of the same minerals. Interpretation of CIA and CIW is similar; a value of 50 represents unweathered UCC and a value in the order of 100 represents highly weathered materials with complete removal of alkali and alkaline-earth elements (McLennan *et al.*, 1983; McLennan, 1993; Mongelli *et al.*, 1996).

The CIW values of beach sands from the Eastern San' in coast, Tango Peninsula and Wakasa Bay ranged from 51 to 72, 56 to 71 and from 62 to 82 respectively. The average CIW values for Shimane, the Tango Peninsula and the Noto Peninsula sands (60, 62, and 67 respectively) were slightly higher that those of the northern Kyushu, Yamaguchi and Yamaguchi coasts (Table 8). The CIW index values are higher than CIA values for the analysed samples, on account of the exclusion of K_2O from the index. A low to moderate weathering of the beach sands collected from the six coastal regions of interest in South West Japan was determined from the calculated CIW values.

4. 5. Palaeoweathering indices in A-CN-K and A-C-M diagrams

Nesbitt and Young (1984) and Fedo *et al.* (1995) used the ternary diagrams Al_2O_3-(CaO+Na_2O)-K_2O (the A-CN-K diagram) and Fe_2O_3*+MgO-(CaO+Na_2O+K_2O)-Al_2O_3 (the A-CNK-FM diagram) to infer weathering profiles. These diagrams are typically plotted such that A (that is, Al_2O_3) is located at the top apex (see Figure 27), CN (CaO*+Na_2O) is located at the bottom left apex and K (K_2O) is located at the bottom right apex. Interpretation of these plots assists in the understanding of weathering patterns and mineralogical composition, as described by Nesbitt and Young (1985, 1989). Plagioclase and K-feldspar plot at 50% Al_2O_3 on the left and right boundaries, respectively to form the feldspar join. The clay mineral groups, kaolin, chlorites and gibbsite plot at the A apex (100% Al_2O_3). The initial weathering trends of igneous rocks are sub-parallel to CN-A. Calcite plots at the CN apex. Illite and smectites plot on the diagram at 70% and 85% Al_2O_3. As weathering progresses, clay minerals are produced at the expense of feldspars and bulk composition of soil/sediments samples evolve up the diagram towards the A apex, along the weathering trend. Therefore, the samples that have been weathered most heavily will be dominated by aluminous clay minerals, which will be reflected in the A-CNK-FM diagram by positions closest to the A apex. The weathering trend intersects the A-K boundary once all plagioclase is weathered and then is redirected towards the A apex because K is extracted from the residues in preference to Al (Nesbitt *et al.*, 1996).

As shown in the ternary A−CN−K plot in Figure 24a, the CIA ratios of the investigated beach sands from Shimane, Tottori and the Tango and Noto Peninsulas were generally low (less than 60), indicating minimal weathering. In the A-CN-K ternary plot (Figure 24a), the majority of the investigated beach sand from northern Kyushu, Shimane and the Tango and Noto Peninsulas occupied the central part of the triangle, generally closer the A-CN line and plotted close to the plagioclase and K-feldspar lines, suggesting poor weathering conditions. Most of the beach sands from this group were around the weathering trends of granites and felsic volcanic rock near the plagioclase-K-feldspar line. Some beach sand samples from northern Kyushu, Yamaguchi, and the Tango

Peninsula scattered below the feldspar line, but close to the A-CN side of the diagram, confirming that due to their high CaO content they possess low CIA values.

Weathering trends may, as described by Nesbitt and Young (1984, 1989) also be observed in the molar proportions of Al_2O_3 (A), $CaO^*+Na_2O+K_2O$ (CNK) and FeO^*+MgO (FM). In these diagrams, the upper (A) apex represents Al_2O_3, the lower left (CNK) apex CaO*, Na_2O and K_2O and the lower right (FM) apex FeO* (total iron as FeO*) and MgO (Figure 24b). Plagioclase plus K-feldspar (Fel) plot on the left-hand boundary at 50% Al_2O_3, illite plots on the left boundary at approximately 75% and greater, while Al_2O_3, kaolin and gibbsite plot at the A apex. Biotite plots three-quarters of the way along the line between feldspars and the FM apex and chlorite plots on the right-hand boundary as a solid solution ranging from approximately 15% to 25% Al_2O_3.

In this study, the majority of the beach sands investigated were positioned on a line connecting the FM apex with the Fel point on the A-CNK boundary of the A-CN-K diagram. Moreover, these sands were located close to the feldspar composition (that is, close to the Fel point). The average UCC and UCJA also plotted in a similar position. The exceptions to this were the sands from Yamaguchi and the tango Peninsula. Overall, on both the A-CN-K diagram (Figure 24a), and the A-CNK-FM diagram (Figure 24b), all investigated beach sands from the coasts of South West Japan, on the coastlines of Northern Kyushu, Yamaguchi, Shimane, Tottori and the Tango and Noto Peninsulas displayed an incipient weathering history.

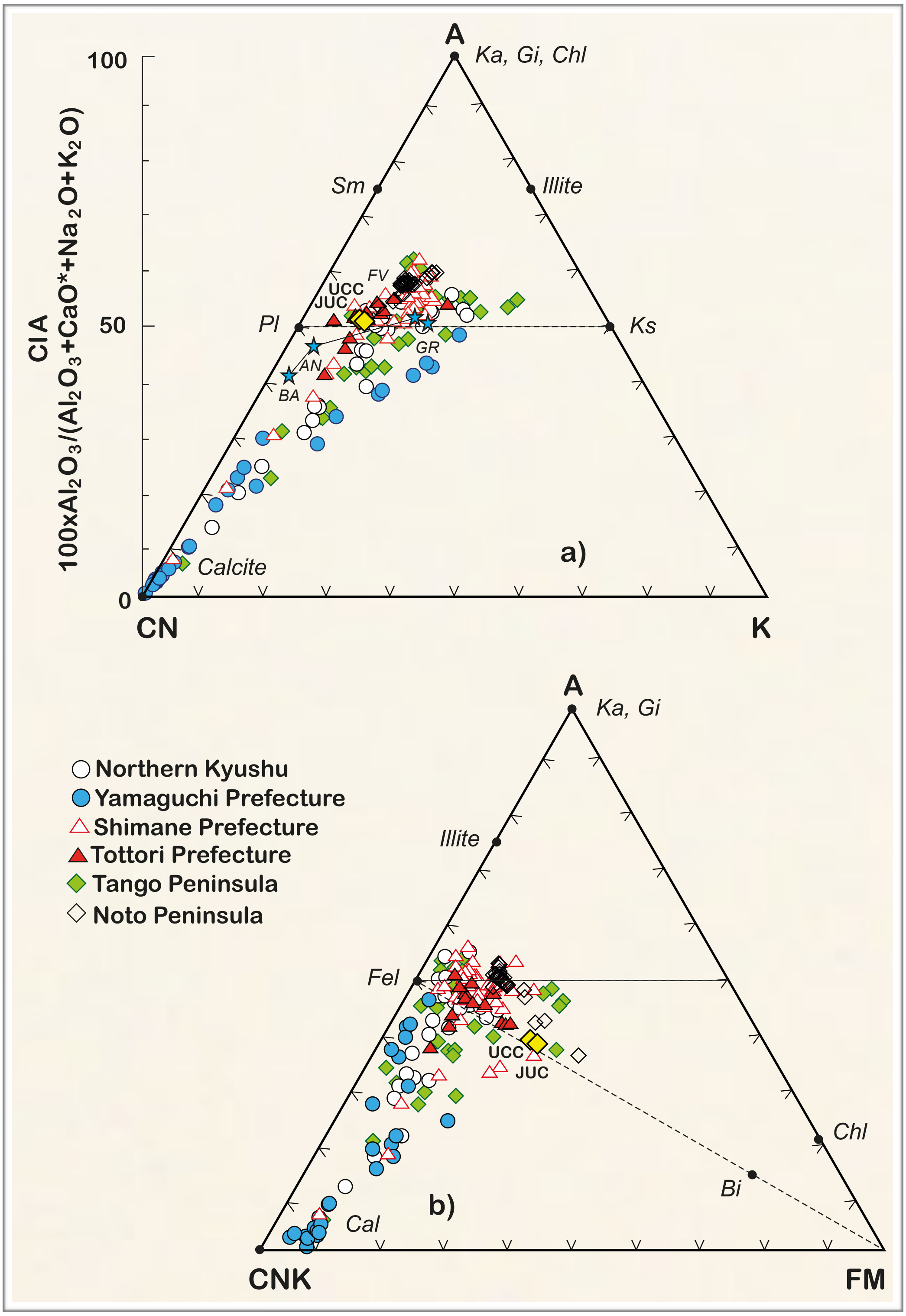

Figure 27. (a) A-CN-K and **(b)** A-CNK-FM (after Nesbitt and Young, 1984; Fedo *et al.*, 1995) and CIA showing weathering trends for investigated beach sands from the coasts of South West Japan, on the coastline of Northern Kyushu, Yamaguchi, Shimane, Tottori, Tango Peninsula, and Noto Peninsula. Ka= kaolinite; Chl= chlorite; Gi= gibbsite; Sm= smectite; Pl= plagioclase; Ks= K-feldspar; Fel= feldspar; Bi= biotite. Dotted line linking stars is the compositional trend in pristine average Phanerozoic-Cenozoic igneous rocks (Condie, 1993). Stars: BA= basalt, AN= andesite, FV= felsic volcanic rock, GR= granite. A= Al_2O_3; CN= CaO^*+Na_2O; K= K_2O; CNK=$CaO^*+Na_2O+K_2O$; FM= FeO^*+MgO.

Chapter Five

5. CONCLUSIONS

In this study, beach sands from the coastlines of the northern Kyushu, Yamaguchi, Shimane, Tottori and the Tango and Noto Peninsulas regions of South West Japan were investigated. Geochemical classification schemes of log(Na_2O/K_2O) versus log(SiO_2/Al_2O_3), and log($Fe_2O_3^*/K_2O$) against log(SiO_2/Al_2O_3) showed the sands to be bracketed by arkose and subarkose. Furthermore, diminishing trends towards sublitharenite were seen, reflecting increasing abundances of both quartz and feldspar. Sands from Yamaguchi, Shimane, Kotogahama and Kotobikihama, which are rich in silica, were found to be highly mature geochemically, with SiO_2 content over 85wt%, diluting all other components. Sands from Tango Peninsula as well as Wakasa Bay were very similar showing moderate geochemical maturation. Beach sands from Tottori and the Noto Peninsula have lower SiO_2/Al_2O_3 values, reflecting the abundance of feldspar, suggesting geochemical immaturity. Those beach sands are derived from the local granite bedrock so is composed primarily of quartz, feldspar, plagioclase and trace iron-rich minerals.

After normalization to both the UCC and the UCJA, the compositions of the sands from northern Kyushu, Shimane, Tottori and the Tango and Noto Peninsulas demonstrated very similar shapes. A moderate degree of geochemical maturation was suggested for these five sites by the relative depletion of all elements other than SiO_2 in comparison with respect to the UCC and UCJA. The majority of the sediments formed under arid or semi-arid conditions tended towards increasing chemical maturity, suggesting that the beach sands are from multiple sources. The Chemical Index of Alteration, Plagioclase Index of Alteration and Chemical Index of Weathering suggested below average to moderate weathering conditions in the source area as well as immature to moderately mature beach sand sediment. This may reflect cold and/or arid climate conditions, encouraging an increase in chemical maturity in the source area.

Sands of northern Kyushu displayed lower carbonate contents than might have been expected given the warm-water currents there. This was attributed to the low water quality (Type B), which would reduce biogenic $CaCO_3$ productivity. By contrast, the Yamaguchi sands exhibited high to moderately low carbonate contents due to the abundance of warm-water species and good water quality (Type AA). The contents of local river and near-shore marine sediments differed significantly from those at Yamaguchi, suggesting that the inputs of existing river or marine sediment to the beach from currents or storm events were minimal.

Silica is not only maturity, if less derivation of clastics, carbonate productivity dominated, therefore, carbonate sand maturity could be one new word. In relation to Global warming, carbonate productivity could be accelerated, so the data of Yamaguchi beach will be a background for evaluation of the climate change.

REFERENCES

Bhatia, M. R. (1983). Plate Tectonics and Geochemical composition of Sandstones. *The Journal of Geology,* **91(6)**, 611–627. doi:10.1086/628815

Blatt, H., Middleton, G., Murray, R. (1972). Origin of Sedimentary Rocks. Prentice-Hall, Englewood Cliffs, NJ. 634.

Brown, M. (1998). Unpairing metamorphic belts: P-T paths and a tectonic model for the Ryoke belt, southwest Japan. *Journal of Metamorphic Geology,* **16(1)**, 3–22. doi:10.1111/j.1525-1314.1998.00061.x

Brumsack, H. J. (1989). Geochemistry of recent TOC-rich sediments from the gulf of California and the black sea. *Geologische Rundschau,* **78(3)**, 851–882. doi: 10.1007/bf01829327

Carranza-Edwards, A., Kasper-Zubillaga, J. J., Rosales-Hoz, L., Alfredo-Morales, E., & Santa-Cruz, R. L. (2009). Beach sand composition and provenance in a sector of the southwestern Mexican Pacific. *Revista Mexicana de Ciencias Geológicas,* **26(2)**, 433-447.

Condie, K.C. (1993). Chemical composition and evolution of the upper continental crust: Contrasting results from surface samples and shales. *Chemical Geology,* **104**, 1–37. doi: 10.1016/0009-2541(93)90140-e.

Condie, K.C., Noll, P.D. & Conway, C.M. (1992). Geochemical and detrital mode evidence for two sources of early Proterozoic sedimentary rocks from the Tonto basin Supergroup, central Arizona. *Sedimentary Geology,* **77(1-2)**, 51–76. doi: 10.1016/0037-0738(92)90103-x.

Danchenkov, M., Lobanov, V., Riser, S., Kim, K., Takematsu, M., & Yoon, J.-H. (2006). A history of physical oceanographic research in the Japan/east sea. *Oceanography,* **19(3)**, 18–31. doi:10.5670/oceanog.2006.41

Daniel, M.R. (2004). Mineralogical maturity in dune fields of North America, Africa and Australia. USGS Sta. Pub. Research. Paper 155.

De-Jong, K., Kurimoto, C., & Ruffet, G. (2008). Triassic 40Ar/39Ar ages from the Sakaigawa unit, Kii peninsula, Japan: Implications for possible merger of the central Asian Orogenic belt with large-scale tectonic systems of the east Asian margin. *International Journal of Earth Sciences,* **98(6)**, 1529–1556. doi:10.1007/s00531-008-0340-1

Fedo, C.M., Wayne Nesbitt, H. & Young, G.M. (1995). Unraveling the effects of potassium metasomatism in sedimentary rocks and paleosols, with implications for paleoweathering conditions and provenance. *Geology*, **23(10)**, 921. doi: 10.1130/0091-7613(1995)023<0921:uteopm>2.3.co;2.

Franzinelli, E., & Potter, P. E. (1983). Petrology, chemistry, and texture of modern river sands, Amazon river system. *The Journal of Geology,* **91(1)**, 23－39. doi:10.1086/628742

Gamo, T., & Horibe, Y. (1983). Abyssal circulation in the Japan sea. *Journal of the Oceanographical Society of Japan,* **39(5)**, 220－230. doi:10.1007/bf02070392

Geological Survey of Japan (GSJ) and National Institute of Advanced Industrial Science and Technology (AIST), 2016.

Geological Survey of Japan and National Institute of Advanced Industrial Science and Technology GSJ & AIST (2013a). Stream sediment database. Geochemical map of Japan. A database of maps showing geochemical element distribution in Japan. Retrieved April 26, 2013, from https://gbank.gsj.jp/geochemmap/shosai.htm

Geological Survey of Japan and National Institute of Advanced Industrial Science and Technology GSJ & AIST (2013b). Marine sediment database. Geochemical map of Sea and Land of Japan. Retrieved April 26, 2013, from https://gbank.gsj.jp/geochemmap/ocean/shosai/kitakyusyusanin.html

Harnois, L. (1988). The CIW index: A new chemical index of weathering. *Sedimentary Geology,* **55(3-4)**, 319－322. doi: 10.1016/0037-0738(88)90137-6.

Herron, M.M., 1988. Geochemical classification of terrigenous sands and shales from core or log data. *Journal of Sedimentary Petrology,* **58**, 820-829.

Imai, N., Terashima, S., Itoh, S. & Ando, A. (1996). Compilation Of Analytical Data On Nine Gsj Geochemical Reference Samples, "Sedimentary Rock Series". *Geostandards and Geoanalytical Research,* **20(2),** 165－216. doi: 10.1111/j.1751-908x.1996.tb00184.x.

Inoue, M., Tanaka, K., Kofuji, H., Nakano, Y. & Komura, K. (2007). Seasonal variation in the 228Ra/226Ra ratio of coastal water within the sea of Japan: Implications for the origin and circulation patterns of the Tsushima coastal branch current. *Marine Chemistry,* **107(4)**, 559－568. doi: 10.1016/j.marchem.2007.08.003.

Ishiga, H., Koakutsu, K., & Sano, E. (2010). Characteristics of pocket beaches in the western San' in coast, southwest Japan, and evaluation of geochemical maturity of beach sand. *Geoscience Rept. Shimane Univ.,* **29**, 21 – 31.

Ishihara, S. (1977). The magnetite-series and ilmenite-series granitic rocks. *Mining Geology,* **27**, 293-305.

Jacobson, A.D., Blum, J.D., Chamberlain, C.P., Craw, D. & Koons, P.O. (2003). Climatic and tectonic controls on chemical weathering in the New Zealand southern Alps. *Geochimica et Cosmochimica Acta,* **67(1)**, 29 – 46. doi: 10.1016/s0016-7037(02)01053-0.

Japan Meteorological Agency (2016). Retrieved January 8, 2016, from http://www.jma.go.jp/jma/indexe.htm

Johnsson, M. J., Stallard, R. F., & Meade, R. H. (1988). First-Cycle quartz Arenites in the Orinoco river basin, Venezuela and Colombia. *The Journal of Geology,* **96(3)**, 263 – 277. doi:10.1086/629219

Kimura, J., & Yamada, Y. (1996). Evaluation of major and trace element XRF analyses using a flux to sample ratio of two to one glass beads. *Journal of Mineralogy, Petrology and Economic Geology,* **91(2)**, 62 – 72. doi:10.2465/ganko.91.62

Kitamura, A., Kimoto, K., & Takayama, T. (1997). Reconstruction of the thickness of the Tsushima current in the sea of Japan during the Quaternary from molluscan fossils. *Palaeogeography, Palaeoclimatology, Palaeoecology,* **135(1-4)**, 51 – 69. doi:10.1016/s0031-0182(97)00029-1

McLennan, S.M., Hemming, S., McDaniel, D.K. & Hanson, G.N. (1993). Geochemical approaches to sedimentation, provenance, and tectonics, in Processes Controlling the Composition of Clastic Sediments. *Geological Society of America,* 21 – 40.

McLennan, S.M., Taylor, S.R. & Eriksson, K.A. (1983). Geochemistry of Archean shales from the Pilbara Supergroup, western Australia. *Geochimica et Cosmochimica Acta,* **47(7)**, 1211 – 1222. doi: 10.1016/0016-7037(83)90063-7.

Mongelli, G, Cullers, R.L & Muelheisen, S. (1996). Geochemistry of late Cretaceous- Oligocenic shales from Varicolori formation, Southern Apennines, Italy: implication formineralogical,grain-size control and provenance. *European journal of mineral,* **8**, 733 – 754.

Nakajima, T. (1997). Regional metamorphic belts of the Japanese islands. *The Island Arc,* **6(1)**, 69–90. doi:10.1111/j.1440-1738.1997.tb00041.x

Nakajima, T., Kamiyama, H., Williams, I. S., & Tani, K. (2004). Mafic rocks from the Ryoke belt, southwest Japan: Implications for Cretaceous Ryoke/San-yo granitic magma genesis. *Transactions of the Royal Society of Edinburgh: Earth Sciences,* **95(1-2)**, 249–263. doi:10.1017/s026359330000105x

Nesbitt, H. W., Fedo, C. M., & Young, G. M. (1997). Quartz and Feldspar stability, steady and Non-Steady-State weathering, and Petrogenesis of Siliciclastic sands and Muds. *The Journal of Geology,* **105(2)**, 173–192. doi:10.1086/515908

Nesbitt, H. W., Young, G. M., McLennan, S. M., & Keays, R. R. (1996). Effects of chemical weathering and sorting on the Petrogenesis of Siliciclastic sediments, with implications for provenance studies. *The Journal of Geology,* **104(5)**, 525–542. doi:10.1086/629850

Nesbitt, H., & Young, G. (1996). Petrogenesis of sediments in the absence of chemical weathering: Effects of abrasion and sorting on bulk composition and mineralogy. *Sedimentology,* **43(2)**, 341–358. doi:10.1046/j.1365-3091.1996.d01-12.x

Nesbitt, H.W. & Young, G.M. (1989). Formation and Diagenesis of weathering profiles. *The Journal of Geology,* **97(2)**, 129–147. doi: 10.1086/629290.

Nesbitt, H.W. & Young, G.M. (1984). Prediction of some weathering trends of plutonic and volcanic rocks based on thermodynamic and kinetic considerations. *Geochimica et Cosmochimica Acta,* **48(7)**, 1523–1534. doi: 10.1016/0016-7037(84)90408-3.

Nesbitt, H.W. & Young, G.M. (1982). Early Proterozoic climates and plate motions inferred from major element chemistry of lutites. *Nature,* **299(5885)**, 715–717. doi: 10.1038/299715a0.

Ogasawara, M. (1987). Trace element analysis of rock samples by X-ray fluorescence spectrometry, using Rh tube. *Bulletin of the Geological Survey of Japan,* **38**, 57-68.

Pettijohn, F. J., Potter, P. E., & Siever, R. (1987). Sand and Sandstone. doi10.1007/978-1-4612-1066-5

Pettijohn, F.J., Potter, P.E. & Siever, R. (1972). Sand and Sandstone. *Springer-Verlag, New York.* 618.

Potter, P. E. (1978). Petrology and chemistry of modern big river sands. *The Journal of Geology,* **86(4)**, 423–449. doi:10.1086/649711

Potter, P. E. (1994). Modern sands of south America: Composition, provenance and global significance. *Geologische Rundschau,* **83(1)**, 212–232. doi:10.1007/bf00211904

Potter, P. E., Huh, Y., & Edmond, J. M. (2001). Deep-freeze petrology of Lena River sand, Siberia. *Geology,* **29(11)**, 999. doi:10.1130/0091-7613(2001)029<0999:dfpolr>2.0.co;2

Roser, B. P., & Korsch, R. J. (1986). Determination of Tectonic setting of Sandstone-Mudstone suites using SiO_2 content and K_2O/Na_2O ratio. *The Journal of Geology,* **94(5)**, 635–650. doi:10.1086/629071

Roser, B. P., & Korsch, R. J. (1988). Provenance signatures of sandstone-mudstone suites determined using discriminant function analysis of major-element data. *Chemical Geology,* **67(1-2)**, 119–139. doi:10.1016/0009-2541(88)90010-1

Roser, B. P., Cooper, R. A., Nathan, S., & Tulloch, A. J. (1996). Reconnaissance sandstone geochemistry, provenance, and tectonic setting of the lower Paleozoic terranes of the west coast and Nelson, New Zealand. *New Zealand Journal of Geology and Geophysics,* **39(1)**, 1–16. doi:10.1080/00288306.1996.9514690

Rudnick, R. L. & Gao, S. (2005). Composition of the Continental Crust, In: The Crust (ed. R.L. Rudnick). *Treatise on Geochemistry (eds. H.D. Holland & K.K. Turekian), Elsevier–Pergamon, Oxford,* **3,** 1–64.

Schwab, F. L. (1975). Framework mineralogy and chemical composition of continental margin-type sandstone. *Geology,* **3(9)**, 487. doi:10.1130/0091-7613(1975)3<487:fmacco>2.0.co;2

Somura, H., Takeda, I., Arnold, J. G., Mori, Y., Jeong, J., Kannan, N., & Hoffman, D. (2012). Impact of suspended sediment and nutrient loading from land uses against water quality in the Hii river basin, Japan. *Journal of Hydrology,* **450**, 25–35. doi:10.1016/j.jhydrol.2012.05.032

Suttner, L.J. & Dutta, P.K. (1986). Alluvial sandstone composition and paleoclimate: I. Framework mineralogy. *Journal of Sedimentary Petrology,* **56,** 329–345.

Suttner, L.J., Basu, A., & Mack, G.H. (1981). Climate and the origin of quartz arenites. *Journal of Sedimentary Petrology,* **51,** 1235–1246.

Takagi, H. (2003). Restoration of exotic Terranes along the median Tectonic line, Japanese islands: Overview. *Gondwana Research,* **6(4)**, 657–668. doi:10.1016/s1342-937x(05)71015-7

Talley, L., Min, D.-H., Lobanov, V., Luchin, V., Ponomarev, V., Salyuk, A., … Zhabin, I. (2006). Japan/east sea water masses and their relation to the sea's circulation. *Oceanography,* **19(3)**, 32–49. doi:10.5670/oceanog.2006.42

Togashi, S., Imai, N., Okuyama-Kusunose, Y., Tanaka, T., Okai, T., Koma, T., & Murata, Y. (2000). Young upper crustal chemical composition of the orogenic Japan arc. *Geochemistry, Geophysics, Geosystems,* **1(11),** n/a–n/a. doi: 10.1029/2000gc000083

Wronkiewicz, D.J. & Condie, K.C. (1987). Geochemistry of Archean shales from the Witwatersrand Supergroup, South Africa: Source-area weathering and provenance. *Geochimica et Cosmochimica Acta,* **51(9)**, 2401–2416. doi: 10.1016/0016-7037(87)90293-6.

Yamada, K., Ishizaka, J., & Nagata, H. (2005). Spatial and temporal variability of satellite primary production in the Japan sea from 1998 to 2002. *Journal of Oceanography,* **61(5)**, 857–869. doi:10.1007/s10872-006-0005-2

Yanagi, T. (2002). Water, salt, phosphorus and nitrogen budgets of the Japan Sea. *Journal of Oceanography,* **58(6)**, 797–804. doi:10.1023/a:1022815027968